# THE ASEAN JOURNAL OF RADIOLOGY

JANUARY - APRIL 2010
Volume XVI Number I
ISSN 0859 144X

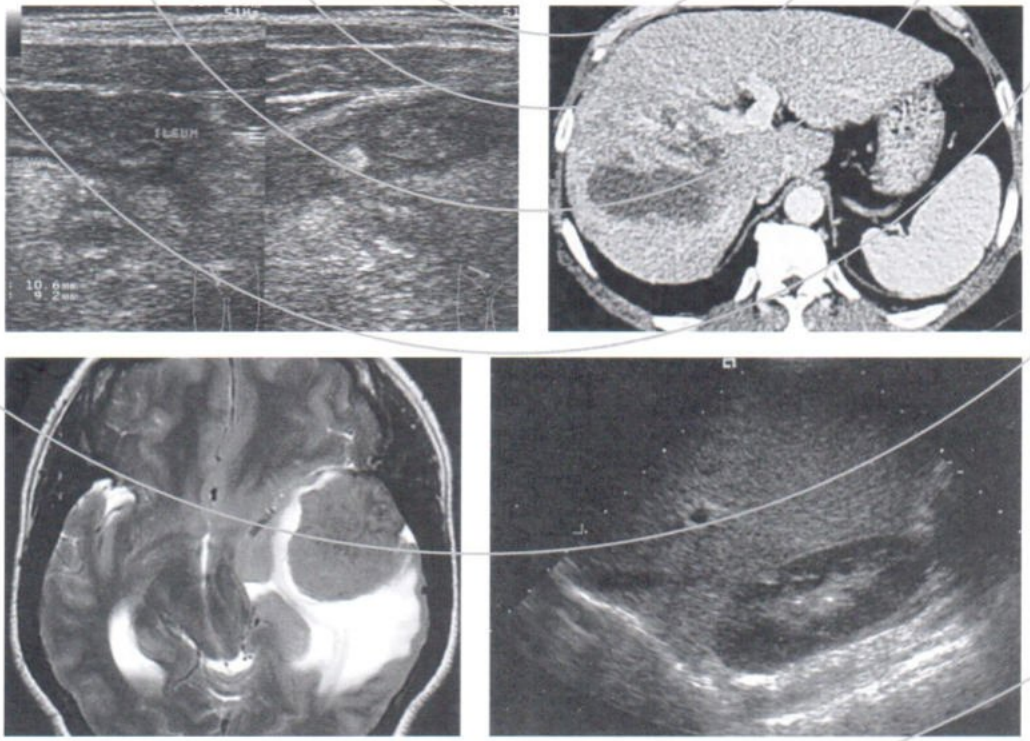

*Published by*

**Royal College of Radiologists of Thailand**

*and*

**Radiological Society of Thailand**

Bangkok, Thailand.

THE ASEAN JOURNAL OF RADIOLOGY
Jan.-Apr. 2010, Volume XVI No.I

# The Committee of Royal College of Radiologists of Thailand

*Apr 2009- Mar 2011*

| | | |
|---|---|---|
| *President:* | Permyot | Kosolbhand |
| *Vice-president:* | Yongyut | Kongthanarat |
| *Secretariat General:* | Poonsook | Jitnuson |
| *Vice-secretary General:* | Pongdej | Pongsuwan |
| *Treasurer:* | Krisdee | Prabhasavat |
| *Academic president:* | Sirintara | Singhara Na Ayudya |
| *House Master&Social Programme:* | Chutakiat | Kruatrachue |
| *Secretary:* | Piyaporn | Apisarnthanarak |
| *Registrar:* | Alongkorn | Kiatdilokrath |
| *Committee:* | Chorfa | Kaewjinda |
| | Pimjai | Siriwongpairat |
| | Chamaree | Chuapatcharasopon |
| | Pisit | Wattanaruangkowit |

# The Committee of Radiological Society of Thailand

*Apr 2009- Mar 2011*

| | | |
|---|---|---|
| *President:* | Permyot | Kosolbhand |
| *Vice-president:* | Yongyut | Kongthanarat |
| *Secretariat General:* | Poonsook | Jitnuson |
| *Treasurer:* | Krisdee | Prabhasavat |
| *Academic president:* | Amphai | Uraiverotchanakorn |
| *House Master&Social Programme:* | Chutakiat | Kruatrachue |
| *Secretary:* | Piyaporn | Apisarnthanarak |
| *Committee:* | Chorfa | Kaewjinda |
| | Chamaree | Chuapatcharasopon |
| | Alongkorn | Kiatdilokrath |
| | Pisit | Wattanaruangkowit |
| | Surat | Vinijsorn |

# The Journal of the Royal College of Radiologists & Radiological Society of Thailand

*(2009 - 2011)*



*Office:*

1. Department of Radiology, Faculty of medicine, Ramathibodi hospital 270, Rama VI Road, Toong Phayathai, Ratchathewi, Bangkok, 10400.
   Tel 02-201-1259 #110, Fax 02-201-1297, E-mail Sirintarapongpech2@hotmail.com
2. The Royal college of Radiologists & Radiological society of Thailand. 9th Floor, Royal Golden Jubilee Building, 2 Soi Soonvijai, Petchburi Road, Bankok, 10320
   Tel 02-716-5963, Fax 02-716-5964, E-mail rcrtthailand@gmail.com

# Contents

## Original Article

Original Article

# Diagnosis of Gastroesophageal Reflux Disease in Children: Comparing Barium Studies with 24-hour Esophageal pH Monitoring

**Ratanaporn Pornkul, MD.[1], Warattha Wachirapanone, MD.[1], Kaimuk Petsrikun, RN[2], Suporn Treepongkaruna, MD.[3]**

*[1] Department of Radiology, [2] Department of Nursing, [3] Department of Pediatrics, Faculty of Medicine, Ramathibodi Hospital, Mahidol University, Bangkok, Thailand*

## Abstract

**Background:** Twenty-four-hour esophageal pH monitoring is a useful investigation for diagnosis of gastroesophageal reflux disease (GERD), however, it is not widely available in developing countries including Thailand. Barium studies are widely available in our country. The objective of this study was to compare the sensitivity and specificity of the modified barium studies in our hospital with the 24-h esophageal pH monitoring for diagnosis of GERD in children.

**Subjects and methods:** All children suspected of GERD who underwent barium studies and 24-h esophageal pH monitoring within 14 days, during the 7 consecutive-years period, were retrospectively reviewed. Criteria for diagnosis of GERD by 24-h pH monitoring were having fraction time with pH below 4.0 more than 10% in infants and 5% in older children.

**Results:** Total 159 children met the criteria; 7 cases were excluded due to incomplete data. Comparing to 24-h pH monitoring, barium studies showed a sensitivity, specificity and accuracy of 61.2%, 37.7% and 47.4%, respectively.

**Conclusion:** Comparing with 24-h esophageal pH monitoring, modified barium examination still has a rather low sensitivity, specificity and accuracy for diagnosis of pediatric GERD. Barium studies may be useful for evaluation of children with clinical suspected of GERD but a limitation for diagnosis of GERD should be aware.

**Key words:** gastroesophageal reflux disease, 24-hour esophageal pH monitoring, barium studies

## Introduction

Gastroesophageal reflux (GER) is defined as regurgitation of gastric contents backwardly into the esophagus and is considered a physiologic condition.[1,2] In contrast to physiologic GER, gastroesophageal reflux disease (GERD) is a condition in which reflux is pathologic, causing troublesome symptoms and/or complications which include erosive esophagitis, esophageal stricture, Barrett's esophagus and respiratory disorders (chronic cough, recurrent pneumonia, recurrent wheezing) and apparent life threatening event.[1-5] Complications of GERD can be severe, early diagnosis and treatment of GERD is therefore essential to prevent potential serious complications.[2,6] There are many diagnostic modalities to diagnose GERD which include upper endoscopy, 24-h esophageal pH monitoring (epHm), combined multichannel intraluminal impedance (MII)-pH monitoring, barium studies, and gastroesophageal scintigraphy (milk scan).[7,8] Each modality has advantages and limitations and there is no absolute gold standard for diagnosing GERD.[9,10] Single diagnostic test is insufficiently accurate, and therefore the diagnosis and evaluation of GERD may require two or more studies.

Among these investigations, only barium studies are widely available in Thailand since they are easy to perform, tolerable, less invasive and inexpensive. Moreover, they can demonstrate the anatomic details of esophagus and upper gastrointestinal (GI) tract as well as the anatomic level of the refluxate. Some studies suggested that the sensitivity and specificity of barium studies can be improved with additional techniques.[11-13] In our hospital, barium study techniques are modified for improvement of diagnostic yield for GERD. The purpose of this study was to compare the sensitivity and specificity of modified barium studies with 24-hr esophageal pH monitoring for diagnosis of GERD in pediatric patients.

## Subjects and Methods

The study was approved by the Ethic Committee of Ramathibodi Hospital. All pediatric patients with suspected of GERD who underwent 24-h epHm and barium studies (barium swallow study or upper gastrointestinal series) within 14 days at Ramathibodi Hospital, during the 7 consecutive-years period, were retrospectively reviewed. The patients who underwent 24-h epHm but no barium examinations were excluded from this study. The results of barium studies were compared with 24-h epHm.

### Barium Studies

All patients were fasting for 3-4 hours before studies. The patients were fed with a mixture of one part of 58 percent wt/wt barium sulfate to four part of milk (100-180 ml for infants, 190-250 ml for children over 1 year of age) by feeding bottle or cup according to age. Feeding via nasogastric tube was given in those who were unable to drink by mouth. Effervescent granules were not used. The barium studies were performed under the digital subtraction fluoroscopy by one of the two pediatric radiologists following the same technical instruction. The patients lied supine in order to place the esophagogastric junctions in dependent position, while the fundus and body of the stomachs filled with barium sulfate. The patients were observed for GER throughout the barium studies and at the end of the examination. Intermittent fluoroscopy was performed every 10 seconds for a maximum of 5 minutes to look for GER. Additional procedures such

as water-siphon test and provocative maneuvers such as cough, valsalva maneuver, or abdominal compression were not performed. We routinely executed spot films of the esophagus, stomach, duodenum, and duodeno-jejunal junction in several views to assess the anatomical abnormalities. Additional spot films were taken if GER was detected during the examination. Radiographs of the esophagogastric junction which includes the whole thorax while the patients in supine position were obtained in every case for interpretation of GER. The patients were diagnosed as having GER when barium sulfate moving up from the gastric fundus to the esophagus was detected, regardless the level and amount of refluxed barium. Esophagitis was diagnosed when edematous mucosal folds or irregularity of esophageal mucosa was seen.

### 24-h esophageal pH monitoring

EpHm was performed by pediatric gastroenterologists using a digitrapper MK III (Synectics Liberty System, Sweden). The antimony crystal pH catheter with electrode (Synectics Medical, Sweden) was calibrated before each study in buffer of pH 1.07 and pH 7.01. The pH catheter was placed transnasally and located above the lower esophageal sphincter (LES), at the distance about 87% of the total esophageal length, measured from the external nares. The position of LES was determined by calculating from the child length as previously described by Strobel et al.[14] The position of pH electrode was re-checked by chest radiograph.[15] Regular feedings were given during the study period but continuous feeding via nasogastric tube was not allowed. Esophageal pH was continuously recorded for 24 hour and the recorded data were transferred to the computer for analysis (EsopHogram Version 5, Gastrosoft Inc, Sweden). Criteria for diagnosis of GERD by 24-h epHm were having fraction time with pH below 4.00 more than 10% in infants and 5% in older children, respectively.[2,15]

## Results

Total 159 pediatric patients (98 males, 61 females), aged 2-60 months, met the inclusion criteria. The most common presenting symptom was recurrent pneumonia in 111 of 159 (69.8%). Seven patients were excluded because of incomplete data, resulted in 152 patients included in this study. By reviewing the reports as well as the recorded images, GER was detected by barium studies in 94 of 152 patients (61.8%) and detected as GERD by 24-h epHm in 62 of 152 (40.8%). The sensitivity, specificity and accuracy of barium studies for detection of GERD compared with 24-h epHm were 61.2%, 37.7%, and 47.3%, respectively. (Table 1). Malrotation was detected by barium studies in 3 patients without midgut volvulus. None had esophagitis detected by barium studies.

## Discussion

The manifestations of GERD in children involve both esophageal and extra-esophageal symptoms. Because of the diverse clinical manifestations, the diagnostic evaluation of GERD can be difficult. Although there are many diagnostic modalities for GERD in children, none of them is considered as a gold standard test. Barium studies are useful for evaluation of anatomical abnormality of the esophagus and upper GI tract such as hiatal hernia, esophageal stricture, gastric outlet obstruction and intestinal malrotation. It is also useful to evaluate swallowing dysfunction and detect the H-type tracheo-esophageal (TE) fistula in children who have

**Table 1** Comparison of barium studies with 24-hour pH monitoring for diagnosis of GERD in 152 patients

| Study | 24-hour pH monitoring | | Sensitivity | Specificity | Accuracy |
|---|---|---|---|---|---|
| | Positive (n=62) | Negative (n=90) | % | % | % |
| Barium GER Positive (n=94) | 38 (25%) | 56 (36%) | 61.2 | 37.7 | 47.4 |
| Barium GER Negative (n=58) | 24 (15.7%) | 34 (23.3%) | | | |

recurrent pneumonia or chronic respiratory symptoms. In addition, barium studies can demonstrate the height of refluxate and may demonstrate an aspiration of gastric contents into upper airways or lungs. However, barium studies can give a false positive result in diagnosis of GERD since a GER episode detected during the study could be physiologic reflux. In addition, the short duration of the study can give a false negative result.[2]

In the last decade, 24-h epHm was considered as a gold standard test for diagnosing GERD [15]. However, recent studies have not proven this. It is reliable for a quantitative measurement of acid reflux into the esophagus but has a limitation in detecting non-acid reflux.[2,16] This is a particular problem in the postprandial period when stomach contents are typically neutralized for up to 2 hours after meals. In pediatric patients, particularly infants, who feed every 2-3 hours, the pH probe might significantly underestimate the amount of reflux.[17] Other possible technical problems contributing to a false negative result of the 24-h epHm include a high probe location in the esophagus, insufficient contact between the probe and esophageal fluid because of adherent food or mucus, and impaction of electrode tip against the esophageal wall.

Combined MII and pH monitoring is superior to pH monitoring alone for diagnosis of GERD since it can detect both acid and non-acid reflux episodes as well as the height of refluxed material.[18] Many studies using combined MII and pH monitoring have demonstrated that non-acid refluxes are common and account for 40-50% of reflux episodes in children with persistent respiratory symptoms[16] and neurological impairment.[19] However, the use of MII in general practice has been limited due to the lack of well established normal values in children.[17]

Upper endoscopy is useful for detection of erosive esophagitis, and a normal upper endoscopic study does not exclude GERD. Endoscopy has a sensitivity of only 30-50% in adult patients who present with heartburn.[9] Gastroesophageal nuclear scintigraphy is not recommended for the routine evaluation of pediatric patients suspected of GERD since the standard of this test are poorly established and the sensitivity for diagnosis of GERD is low.[2] Proton pump inhibitor (PPI) test has been shown in adults to have a sensitivity and specificity of 74% and 54%, respectively, comparing to endoscopy or 24-h epHm[20], but the test has not been validated for pediatric patients. Improvement following treatment does not always confirm a diagnosis of GERD since symptoms may improve spontaneously or as a placebo effect.

The majority of the patients in our study presented with extra-esophageal GERD and the most

common manifestation was recurrent pneumonia because both barium studies and 24-h epHm are commonly performed if the patients had these symptoms. The patients who underwent 24-h epHm only for evaluation of GERD may have other symptoms in majority but is not in scope of this study. Upper endoscopy is performed only in patients suspected of reflux esophagitis or those who did not respond to treatment.

Detection rate of GERD by barium studies and pH monitoring were 43% and 83% by Al-Khawari et al[21], 18% and 60% by Thompson et al[13], 38% and 68% by Sellar et al[22], and 25% and 66% by Johnston et al[12]. The higher detection rate of GER by barium studies (61.8%) than pH monitoring (40.7%) in our studies is contrary to others, and could be due to the technique used in our study. In similar to ours, the study by Al-Khawari et al[21] included small children with nearly half of the patients were below one year of age. They performed intermittent fluoroscopy every 3-4 seconds for a maximum of 5 minutes for observation of GER but the position of the patients during studies was not mentioned. We let the patients lie in supine position with barium sulfate filling fundus and body of the stomach while performing intermittent fluoroscopy every 10 seconds for a maximum of 5 minutes. We believed this is the best technique to elicit barium reflux with less radiation to the patients. Barium sulfate had to fill the gastric fundus and was around the area of esophago-gastric junction to be seen moving up into the esophagus. Gastric fundus is the most posterior part of the stomach, so only supine position is suitable for barium sulfate to perfectly fill it. It was possible that our technique can increase the sensitivity for detection of barium reflux.

In comparison with 24-h epHm, Al-Khawari et al[21] reported the sensitivity, specificity and accuracy of barium studies for diagnosis of GERD as 42%, 57% and 45%, respectively. Thompson et al[13] compared barium studies with pH proved GERD and found that the sensitivity of fluoroscopic detection of GER rose from 26% to 70% when provocative maneuvers such as coughing, Valsalva maneuver, rolling from supine to right lateral position and water-siphon test, which let the patient drink water while lying supine for observing GER, were used to elicit reflux. However, the same authors reported that with increasing of sensitivity, the specificity of barium studies was decreased from 94% to 74% with provocative maneuvers. Blumhargen et al[11] addressed a high false positive result of the water-siphon test as 29%, while Johnston et al[12] experienced sensitivity of such test to be 92% but the specificity was zero. We decided not to use these provocative maneuvers because of such evidences, along with the difficulty to perform them in small pediatric patients, and to probably decrease a false positive result. In our study, we found false positive result of 36%.

In GERD related respiratory symptoms, pathophysiologic mechanisms include microaspiration and acid-induced vagal reflex.[4] The height of refluxate could be contributed in pulmonary aspiration despite of the small quantitative amount of acid refluxes. Although the sensitivity, specificity and accuracy for the diagnosis of GERD is not high when compared with 24-h epHm, barium study can provide the height of refluxate. In addition, due to the patients with GERD may present with diverse clinical manifestations, barium studies, on the other hand, will help diagnose the diseases causing symptoms resemble GERD.

The limitation of this study is that 24-h pHm is not a true gold standard test[17], although it would result in a difficulty for interpretation, it was the best standard we had at the time of study. Further study comparing barium studies with the absolute gold standard test should be performed. Combined MII-pH study is supposed to be a gold standard test for diagnosis of GERD if normal values in children can be established.[17]

## Conclusion

Comparing to 24-hour esophageal pH monitoring; the sensitivity, specificity and accuracy of barium studies is not quite promising for the diagnosis of GERD, and certain limitations are still existed. Due to the limitation of availability of the other tests for diagnosis of GERD in children in developing countries including Thailand, barium studies which are widely available may be useful for evaluation of children with clinical suspected of GERD but a limitation for diagnosis of GERD should be aware.

## References

1. Vakil N, van Zanten SV, Kahrilas P, Dent J, Jones R. The Montreal definition and classification of gastroesophageal reflux disease: a global evidence-based consensus. Am J Gastroenterol 2006;101:1900-20.
2. Rudolph CD, Mazur LJ, Liptak GS, Baker RD, Boyle JT, Colletti RB, et al. Guidelines for evaluation and treatment of gastroesophageal reflux in infants and children: recommendations of the North American Society for Pediatric Gastroenterology and Nutrition. J Pediatr Gastroenterol Nutr 2001;32 Suppl 2:S1-31.
3. Treepongkaruna S, Phuapradit P, Assadamongkol K, Chantarojanasiri T, Preutthipan A, Suwanjutha S, et al. Gastroesophageal reflux in children with recurrent pneumonia. Rama Med J 1996;19:92-8.
4. Gold BD. Asthma and gastroesophageal reflux disease in children: exploring the relationship. J Pediatr 2005;146: S13-20.
5. Gupta SK, Hassall E, Chiu YL, Amer F, Heyman MB. Presenting symptoms of nonerosive and erosive esophagitis in pediatric patients. Dig Dis Sci 2006;51:858-63.
6. Cohen S, Parkman HP. Heartburn--a serious symptom. N Engl J Med 1999;340:878-9.
7. Dranove JE. Focus on diagnosis: new technologies for the diagnosis of gastroesophageal reflux disease. Pediatr Rev 2008;29:317-20.
8. Hirano I. Review article: modern technology in the diagnosis of gastro-oesophageal reflux disease--Bilitec, intraluminal impedance and Bravo capsule pH monitoring. Aliment Pharmacol Ther 2006;23 Suppl 1:12-24.
9. Madan K, Ahuja V, Gupta SD, Bal C, Kapoor A, Sharma MP. Impact of 24-h esophageal pH monitoring on the diagnosis of gastroesophageal reflux disease: defining the gold standard. J Gastroenterol Hepatol 2005;20:30-7.
10. van Os E, De Schryver J, Houwen RH, Ten WE. Gastroesophageal reflux disease in children: how reliable is the gold standard? J Pediatr (Rio J) 2009;85:84-6.
11. Blumhagen JD, Christie DL. Gastroesophageal reflux in children: evaluation of the water siphon test. Radiology 1979;131:345-9.
12. Johnston BT, Troshinsky MB, Castell JA, Castell DO. Comparison of barium radiology with esophageal pH monitoring in the diagnosis of gastroesophageal reflux disease. Am J Gastroenterol 1996;91:1181-5.
13. Thompson JK, Koehler RE, Richter JE. Detection of gastroesophageal reflux: value of barium studies compared with 24-hr pH monitoring. AJR Am J Roentgenol 1994; 162:621-6.
14. Strobel CT, Byrne WJ, Ament ME, Euler AR. Correlation of esophageal lengths in children with height: application to the Tuttle test without prior esophageal manometry. J Pediatr 1979;94:81-4.
15. Vandenplas Y, Sacre-Smits L. Gastro-oesophageal reflux in infants. Evaluation of treatment by pH monitoring. Eur J Pediatr 1987;146:504-7.
16. Rosen R, Nurko S. The importance of multichannel intraluminal impedance in the evaluation of children with persistent respiratory symptoms. Am J Gastroenterol 2004;99:2452-8.

17. Vandenplas Y, Salvatore S, Vieira MC, Hauser B. Will esophageal impedance replace pH monitoring? Pediatrics 2007;119:118-22.
18. Wenzl TG. Investigating esophageal reflux with the intraluminal impedance technique. J Pediatr Gastroenterol Nutr 2002;34:261-8.
19. Del Buono R, Wenzl TG, Rawat D, Thomson M. Acid and nonacid gastro-oesophageal reflux in neurologically impaired children: investigation with the multiple intraluminal impedance procedure. J Pediatr Gastroenterol Nutr 2006;43:331-5.
20. Numans ME, Lau J, de Wit NJ, Bonis PA. Short-term treatment with proton-pump inhibitors as a test for gastroesophageal reflux disease: a meta-analysis of diagnostic test characteristics. Ann Internal Med 2004; 140:518-27.
21. Al-Khawari HA, Sinan TS, Seymour H. Diagnosis of gastro-oesophageal reflux in children. Comparison between oesophageal pH and barium examinations. Pediatr Radiol 2002;32:765-70.
22. Sellar RJ, De Caestecker JS, Heading RC. Barium radiology: a sensitive test for gastro-oesophageal reflux. Clin Radiol 1987;38:303-7.

THE ASEAN JOURNAL OF RADIOLOGY 2010; 16(1): 8-18

Original Article

# Intracranial Meningiomas in Udonthani Hospital and Review of the Literature

**Khomdao Boonchit, MD.**

*Department of Radiology, Udonthani hospital, Udonthani 41000 Thailand*

## Abstract

**Objective:** To report CT scan and MR image findings of symptomatic fifty patients with intracranial meningiomas and review of the literature.

**Methods:** Retrospective review CT scan and MR image findings of fifty symptomatic patients with intracranial meningiomas operated in Udonthani hospital from October 2005 to June 2008.

**Results:** Fifty patients (4:1 female to male ratio. Mean age was 44.7 years; range 15-82 years.) were studied. 73.6% of CT scans demonstrated typical features and 18.9% showed hyperostosis. Most common locations were cerebral convexity and sphenoid ridge. three patients showed multiple meningiomas. 80% of patients showed typical MR image features and 60% dural tail sign. Peritumoral edema was found in 67.3% of patients.

**Conclusion:** Meningiomas are usually benign tumors with characteristic CT and MR imaging features. However on a review of the literature, there are several important histologic variants of meningiomas that can have unusual or misleading radiologic features.

## Introduction

Hospital-based brain tumor series indicate that the incidence of meningiomas is approximately 20% of all intracranial tumors (the most common nonglial primary intracranial tumor), whereas autopsy-based studies indicate an overall incidence of 30%.[1] Symptomatic meningiomas occur two to three times more commonly in female patients, especially those in the middle age (40-60 years) group[2] and generally are benign tumor that are derived from meningoendothelial cells.[3] Because complete surgical resection is the definite treatment for meningiomas, the single most important feature regarding therapy is tumor location, as it substantly affects surgical accessibility. Unusual imaging features are also important to avoid misdiagnosis.

## Patients and Methods

The author retrospectively analyzed CT scan and MR image findings of fifty symptomatic patients with intracranial meningiomas who underwent an operation at Udonthani hospital from October 2005 to June 2008. Forty-five patients were examined with non contrast and contrast-enhanced CT scan (Elscint EXEL 2400 ELECT CT scanner). Two patients, with non contrast T1- and T2-weighted pulse sequences and Gadolinium-enhanced a 1.5 Tesla MR (Siemens Magnetom Symphony) alone, and three patients, with CT scan and MRI. All CT scans and MRI studies were reviewed. Edema in adjacent areas of the brain, when present, was graded as mild (extending less than 1 cm. from the tumor), moderate (extending 1-4 cm. from the tumor), or severe (extending more than 4 cm. from the tumor).[3]

## Result

Age of 50 patients at the time of diagnosis were 15 to 82 years (mean 44.7 years) (Table 1) and 55 meningiomas (Table 2). The most common locations of intracranial meningiomas in this study were cerebral convexity and sphenoid ridge. Three patients showed multiple meningiomas (Table 3), all the patients were female and showed no manifestations of von Recklinghausen disease. In 73.6% of meningiomas, CT scan demonstrated typical diagnostic features, including a sharply circumscribed homogeneous hyperdensity on CT scan without contrast material enhancement, and homogeneously enhanced after the administration of contrast material. In Table 4, 13 (24.5%) meningiomas showed rim, sandlike, globular and focal calcifications. Intraaxial vasogenic edema was seen around meningiomas (which are extraaxial masses) 67.3% of patients (Table 5) and there was little associated between grade of edema and location of the tumor.

14 (25.5%) meningiomas showed midline shift which there was association with tumor location. (8 in 12 patients of sphenoid ridge meningiomas showed midline shift.)

## Discussion

Brain imaging with contrast-enhanced CT or MR imaging is the most common method of diagnostic of intracranial meningioma.[1] Contrast material enhancement of meningioma is usually rapid and striking owing to their highly vascular nature. (Fig.1)

Inhomogeneous enhancement (13.2%) was found which area of non-enhancing hypodensity should be necrotic portion of meningiomas. (Fig.2)

**Table 1** Sex and age of patients with intracranial meningiomas

| Sex | Numbers of patient (%) | Age (years) | Mean age (years) |
|---|---|---|---|
| Female | 41 (82) | 15-81 | 46.2 |
| Male | 9 (18) | 23-82 | 43.0 |
| Female & Male | 50 | 15-82 | 44.7 |

**Table 2** Location of intracranial meningiomas demonstrated by CT scans and MR images

| Tumor location | Number of meningiomas (%) |
|---|---|
| Cerebral convexity | 12 (21.8) |
| Sphenoid ridge | 12 (21.8) |
| Parasagittal | 11 (20) |
| Sellar, suprasellar, parasellar | 8 (14.6) |
| Olfactory groove | 5 (9.1) |
| Cerebellopontine angle | 3 (5.5) |
| Tentorial cerebelli | 2 (3.6) |
| Intraventricular | 1 (1.8) |
| Middle cranial fossa | 1 (1.8) |
| Total | 55 |

**Table 3** Age and locations of patients with intracranial multiple meningiomas

| Age at the time of diagnosis (years) | Locations |
|---|---|
| 31 | Convexity, intraventricular, CPA |
| 40 | Olfactory groove, sphenoid ridge, convexity |
| 54 | Sphenoid ridge, CPA |

**Table 4** Computed tomographic findings in meningiomas

| CT findings | Number of meningiomas (%) |
|---|---|
| Hyperdensity | 39 (73.6) |
| Hypodensity | 2 (3.8) |
| Isodensity | 5 (9.4) |
| Inhomogeneous hyperdensity | 7 (13.2) |
| Homogeneous enhancement | 46 (86.8) |
| Inhomogeneous enhancement | 7 (13.2) |
| Calcification | 13 (24.5) |
| Hyperostosis | 10 (18.9) |
| Total | 53 |

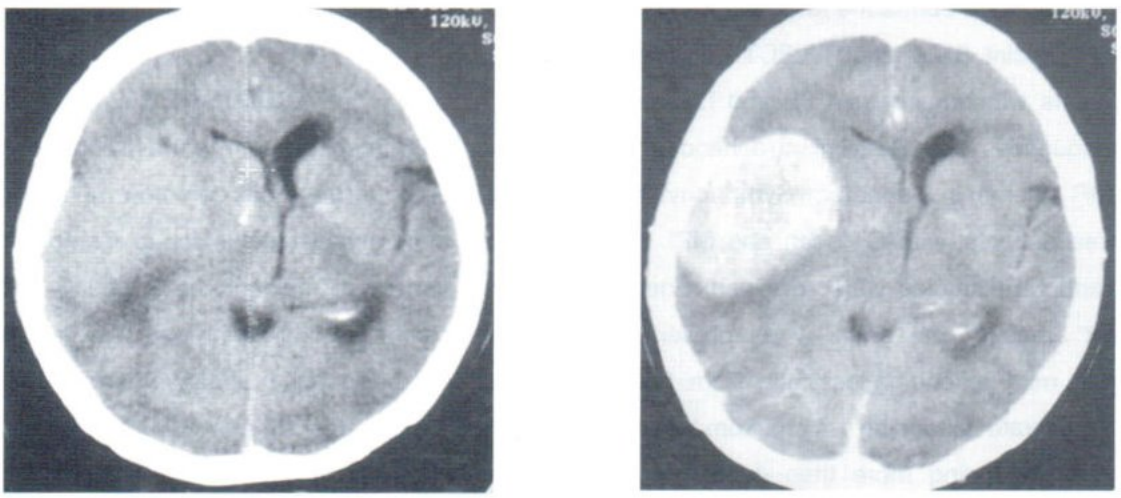

A B

**Fig.1** (A) Non contrast and (B) contrast-enhanced CT scan obtained in a 54-year-old woman showing right temporal extraaxial hyperdense mass with homogeneous enhancement, typical CT features of intracranial meningioma.

**Table 5** Intracranial meningiomas with peritumoral edema

| Peritumoral edema | Number of meningiomas (%) |
|---|---|
| No | 18 (32.7) |
| Mild | 14 (25.5) |
| Moderate | 16 (29.1) |
| Severe | 7 (12.7) |
| Total | 55 |

**Table 6** Magnetic resonance image findings in meningiomas

| MR findings | Number of meningiomas (%) |
|---|---|
| Hypointense on T1 - weighted images | - |
| Isointense on T1 - weighted images | 5 (100%) |
| Isointense on T2 - weighted images | 4 (80%) |
| Hyperintense on T2 - weighted images | 1 (20%) |
| Homogeneous enhancement | 4 (80%) |
| Inhomogeneous enhancement | 1 (20%) |
| Dural tail | 3 (60%) |

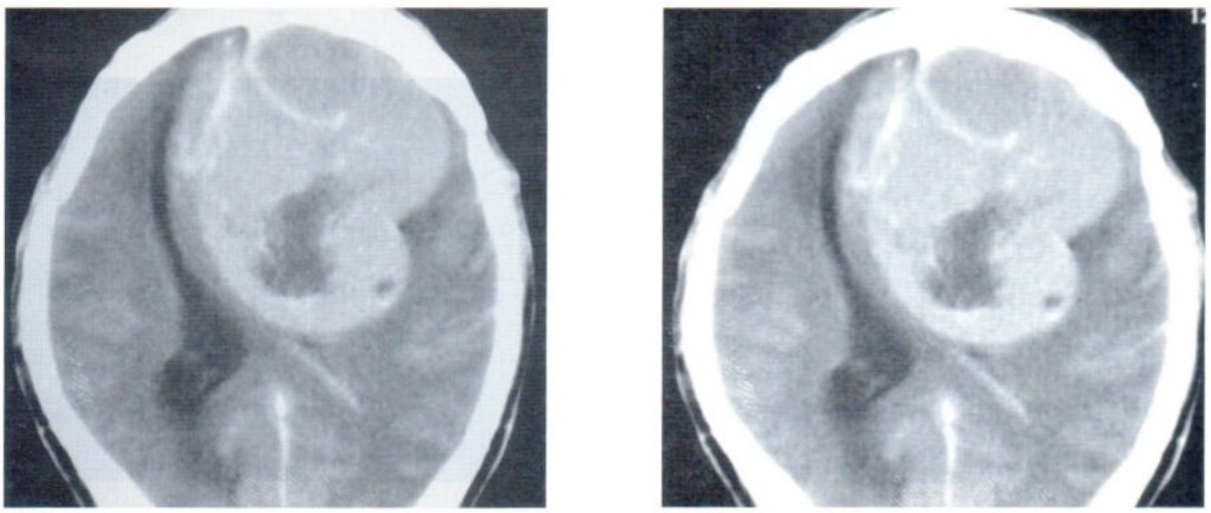

A B

**Fig.2** (A) Non contrast and (B) contrast-enhanced CT scans obtained in a 32-years-old man showing falx meningioma with inhomogeneous hyperdensity and inhomogeneous enhancement.

The CT scan best reveals the chronic effects of slowly growing mass lesions on bone remodelling. (Fig.3)

Calcification in the tumor (24.5%) (Fig.4) and hyperostosis (18.9%) (Fig.5) were features of intracranial meningioma that can easily identified on noncontrast CT scan.

The typical diagnostic features of meningiomas on magnetic resonance (MR) images, include a unilocular mass with sharply circumscribed margin and inward displacement of the cortical gray matter which on MR images obtained without contrast material enhancement, characteristically hypointense or isointense to gray matter with T1-weighted pulse sequence and isointense or hyperintense to gray matter with T2-weighted pulse sequence, and on MR images obtained with Gadolinium, there were homogeneously enhanced.[4,5] However in this report (Table 6), MR images demonstrated dural-based isointense to gray matter on T1-weighted images (100%) and isointense to gray matter on T2-weighted images (80%) with homogeneous enhancement

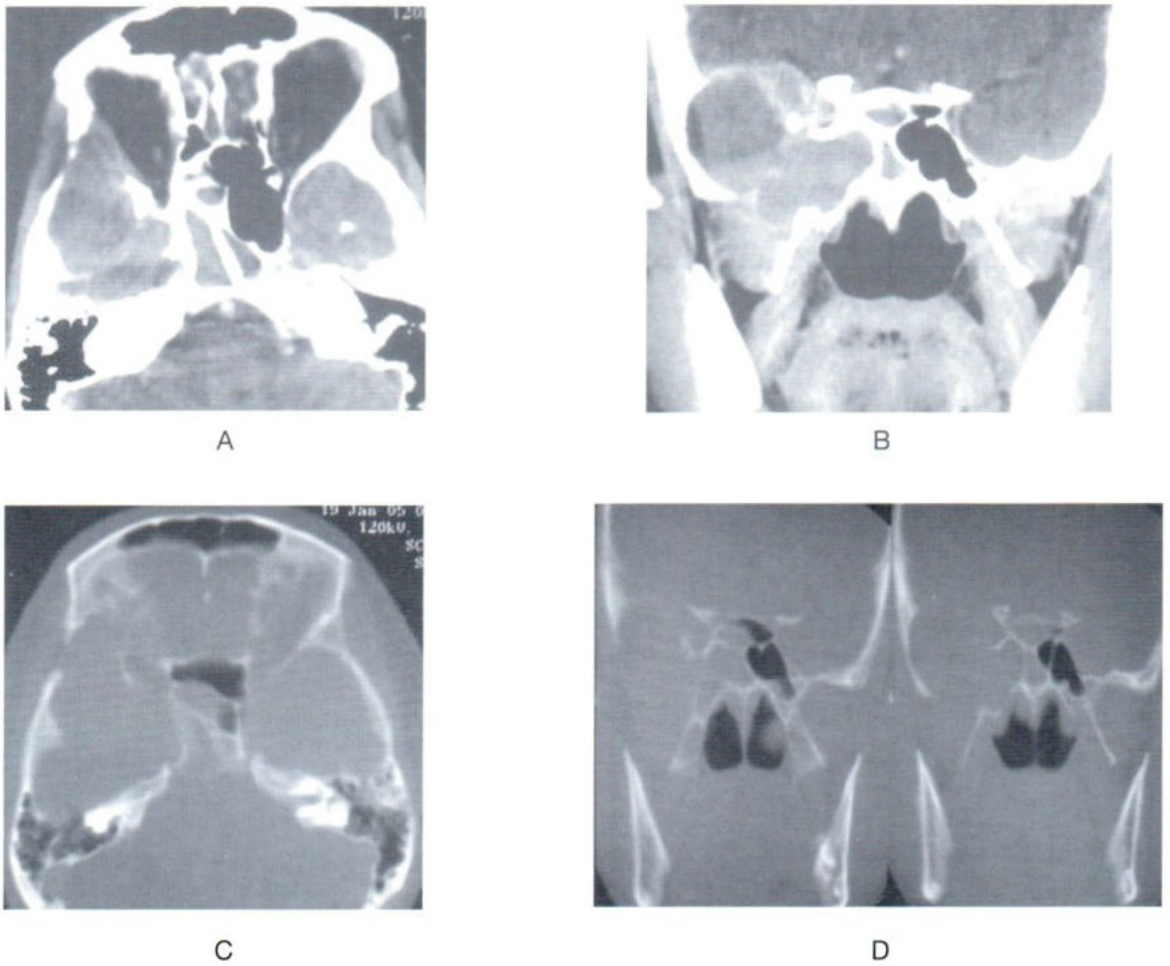


**Fig.3** (A) Axial, (B) coronal contrast-enhanced CT scans with soft tissue window and (C) axial, (D) coronal CT scans with bone window obtained in a 31-years-old man of underlying hemophilia A with sphenoid ridge meningioma and associated bone remodelling.

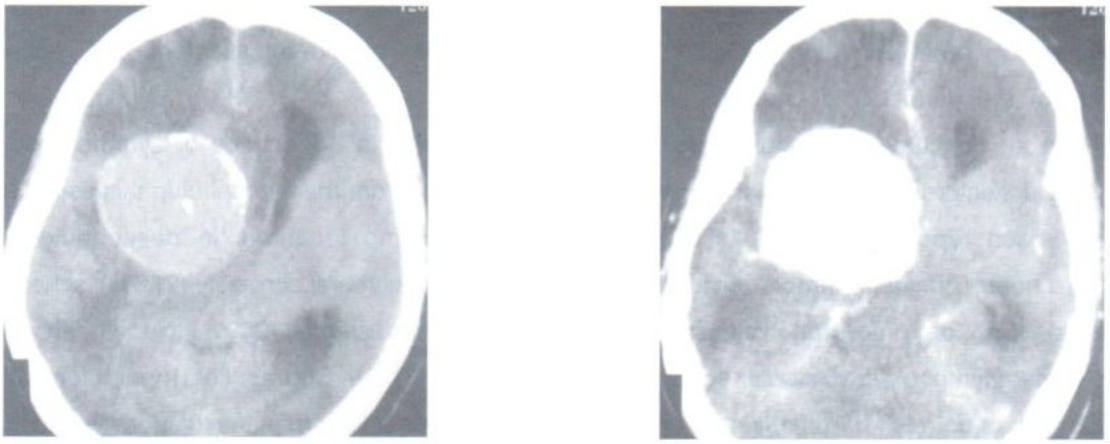

A B

**Fig.4** (A) Non contrast CT scan with soft tissue window demonstrated mass with rim and sandlike calcifications. (B) after contrast enhancement revealed rather homogeneous enhancement of meningioma in a 64-years-old woman.

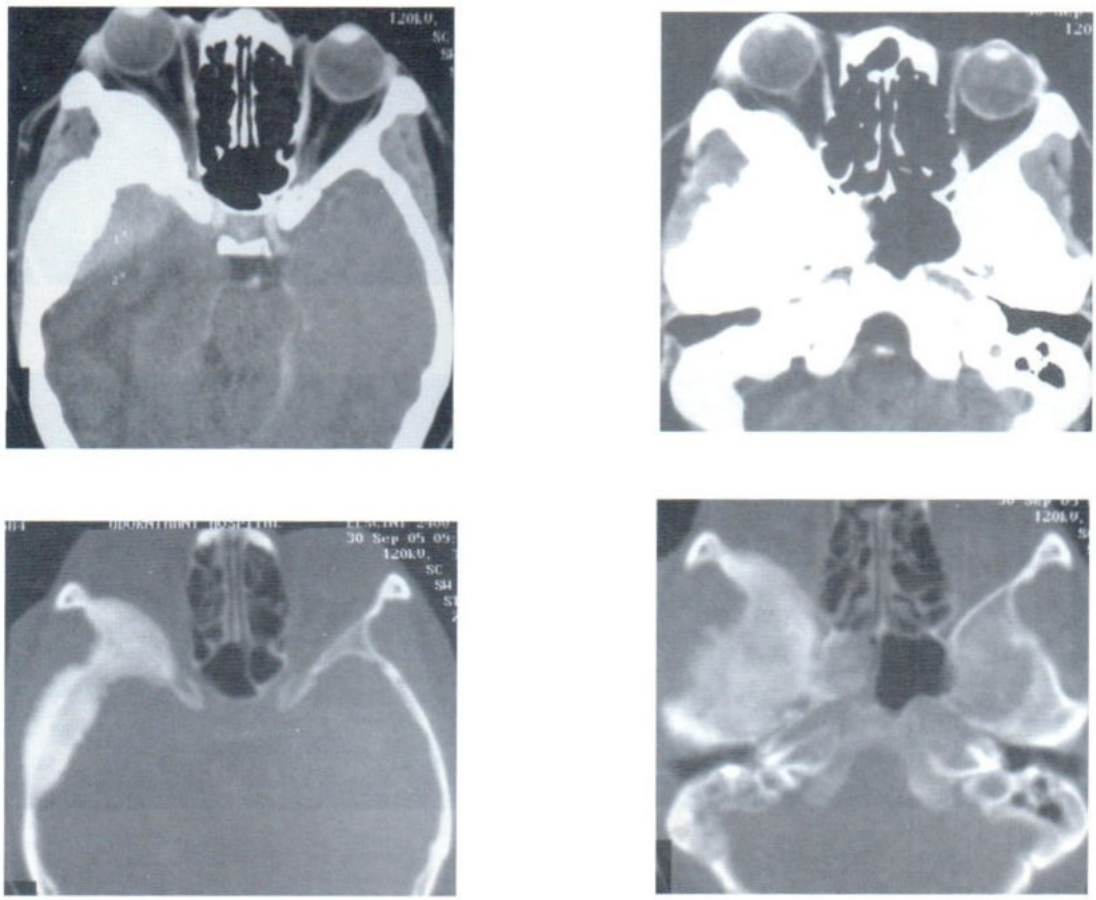

**Fig.5** CT scan with soft tissue and bone windows revealed extensive thickening of the right sphenoid and temporal bones in 42-years-old woman with sphenoid wing meningioma.

(80%)(Fig.6, 7), frequent cerebrospinal fluid cleft, and often enhancing dural tail (60%). (Fig.7e, 8) The pathology of the dural tail is unclear.[6,7] Although Goldsher et al[8] concluded that dural tails were a "highly specific feature of meningiomas" many cases have now been reported of dural tails that are attached to nonmeningioma tumors (or tumefactive processes) such as chloroma, primary central nervous system lymphoma, vestibular schwannoma and metastatic tumor etc.[6] MR imaging was superior to CT in defining extracerebral location, tumor vascularity, arterial encasement, and venous sinus invasion.[5]

Intracranial locations of symptomatic meningiomas in Udonthani hospital in this series arised in the following locations in descending order of frequency: cerebral convexity (21.8%), sphenoid ridge (21.8%), parasagittal (20%) including falcine meningioma (9.1%). Suprasellar meningioma (14.6%) commonly arise from the diaphragmatic sellae or

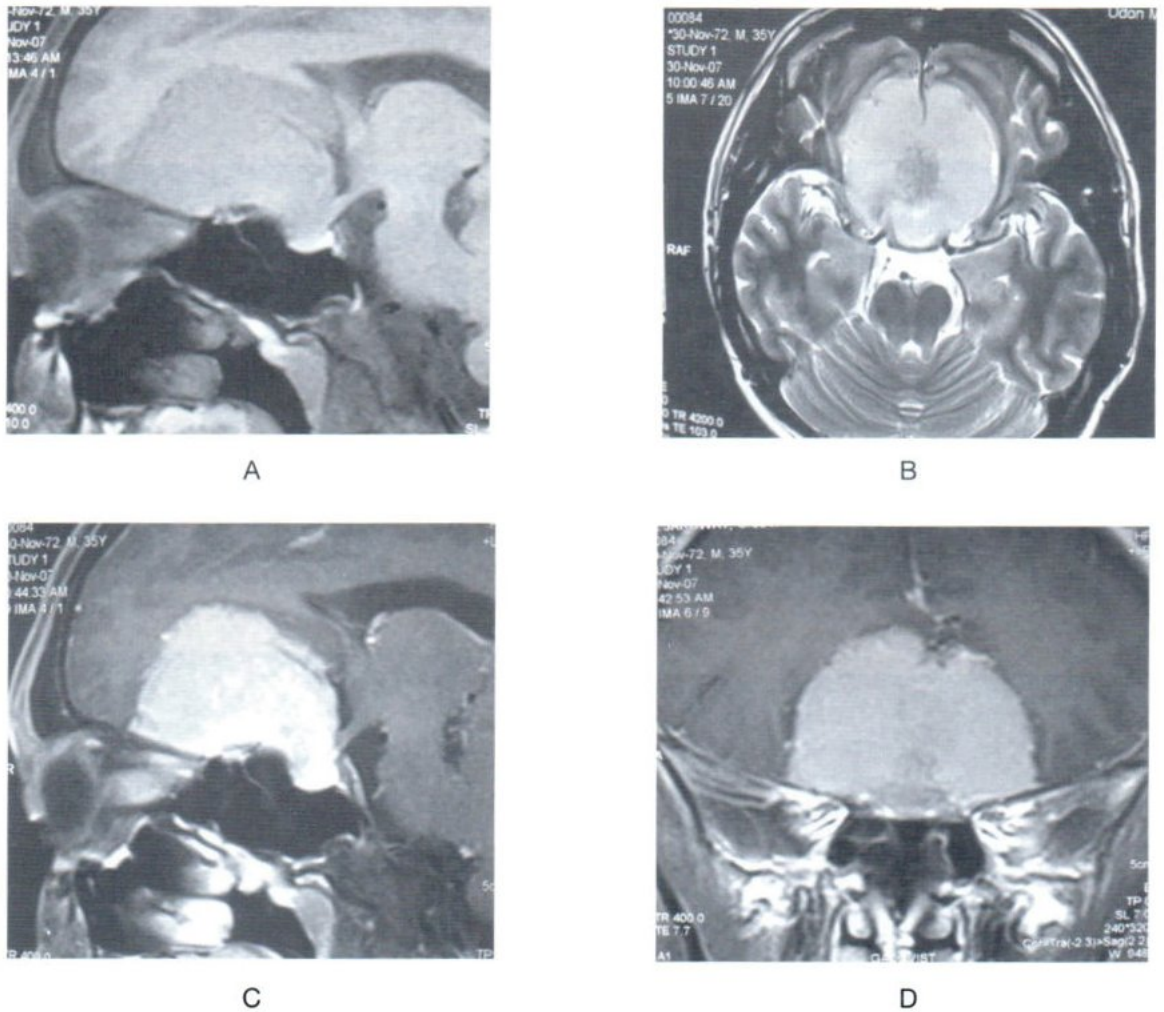

A B C D

Fig.6 (A) Sagittal T1-weighted and (B) axial T2-weighted MR images of an olfactory meningioma obtained in a 35-year-old man showing isointense to gray matter with homogeneous enhancement on (C) sagittal and (D) coronal Gadolinium-enhanced MR images.

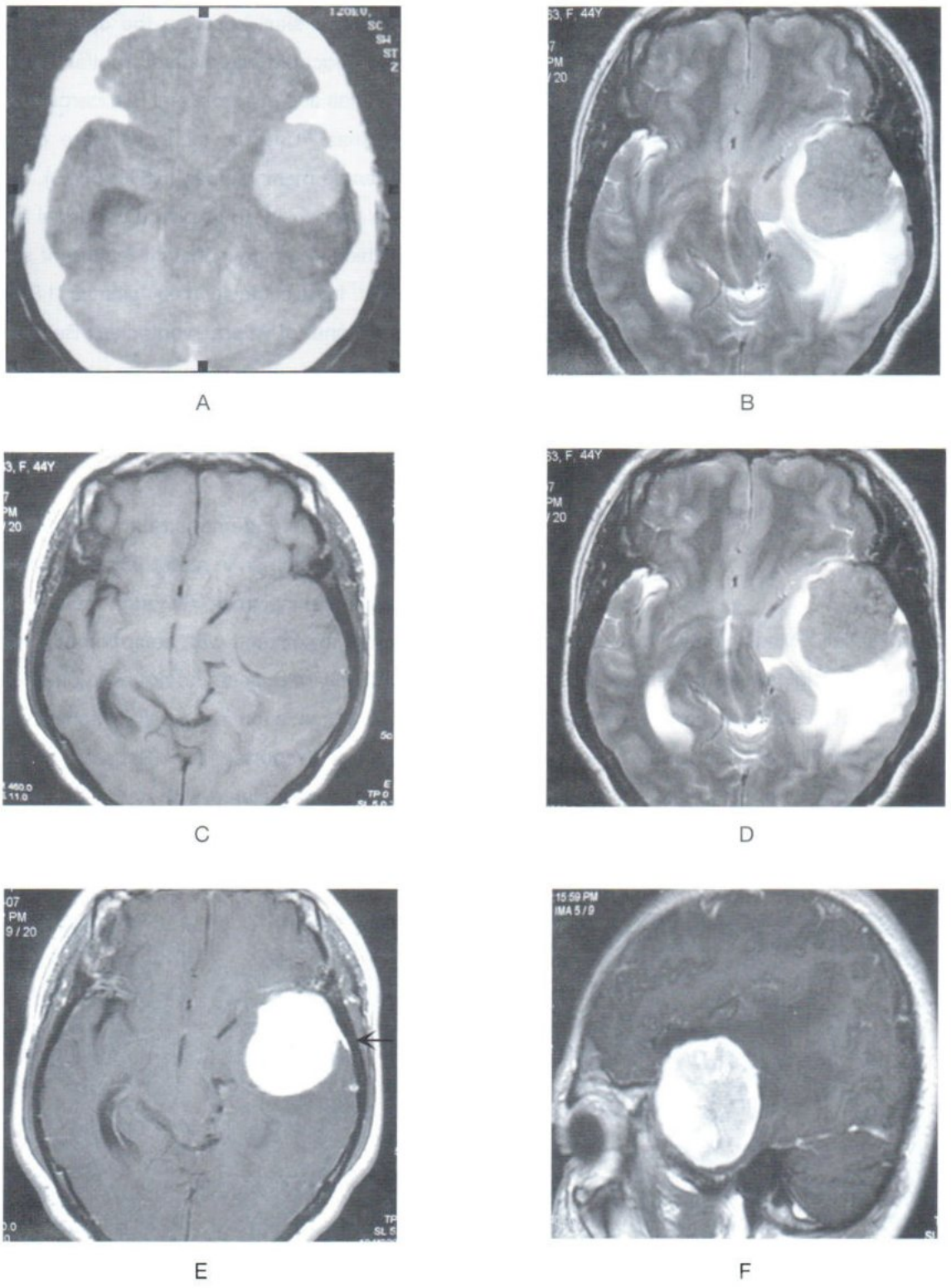

**Fig.7** (A) Non contrast and (B) contrast-enhanced CT scans in a 44-years-old woman with left temporal convexity meningioma revealed homogeneous hyperdensity and homogeneous enhancement. (C) Axial T1-weighted, (D) axial T2-wieghted, and (E) axial, (F) sagittal MR images after Gadolinium administration revealed enhancing hypointense mass. Dural tail sign is shown. (arrow in e.)

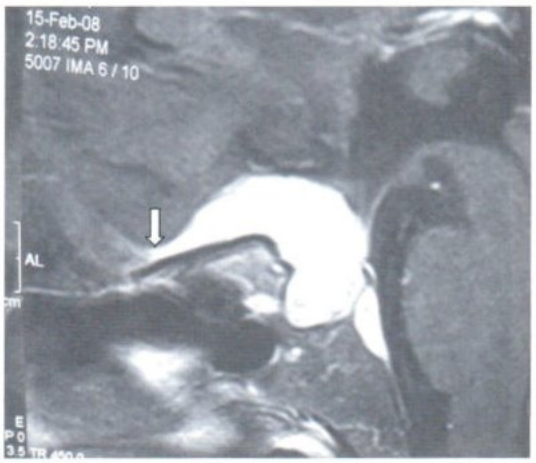


Fig.8 Sagittal T1-weighted MR image with Gadolinium enhancement in 54-years-old woman revealed an enhancing dural tail sign along planum sphenoidale (arrow).

tuberculum sellae.[7] Meningiomas may be entirely parasellar if they originate from the dural wall of the cavernous sinus. Olfactory groove meningiomas (9.1%) arise over the cribiform plate, they can be differentiated from tuberculum sellae meningiomas because olfactory groove meningiomas arise more anterior in the skull base, so the optic nerve and chiasm are located inferolateral to olfactory groove meningiomas and superolateral to tuberculum sellae meningiomas.[9] Unusual locations were cerebellopontine angle meningiomas (5.5%) (Fig.9), they did not have propensity to involve the internal auditory canal (which is a fairly constant feature of schwannomas).[10,11] Intraventricular meningiomas (1.8%) were in the trigone of lateral ventricles. Because the choroid plexus is more bulky in the lateral ventricles, incidence of lateral ventricle meningiomas is higher compared with those in the third and fourth ventricles.[12,13]

Lusin et al[14] demonstrated CT findings of multiple meningiomas in about 9% of patients with intracranial meningiomas. Although multiple meningiomas are associated with neurofibromatosis type 2, the majority of patients do not have other characteristic features such as multiple schwannomas.[2] Geuna et al[15] reported 2 of 9 cases of multiple meningiomas associated with neurofibromatosis.

Meningiomas are known to be hypervascular,

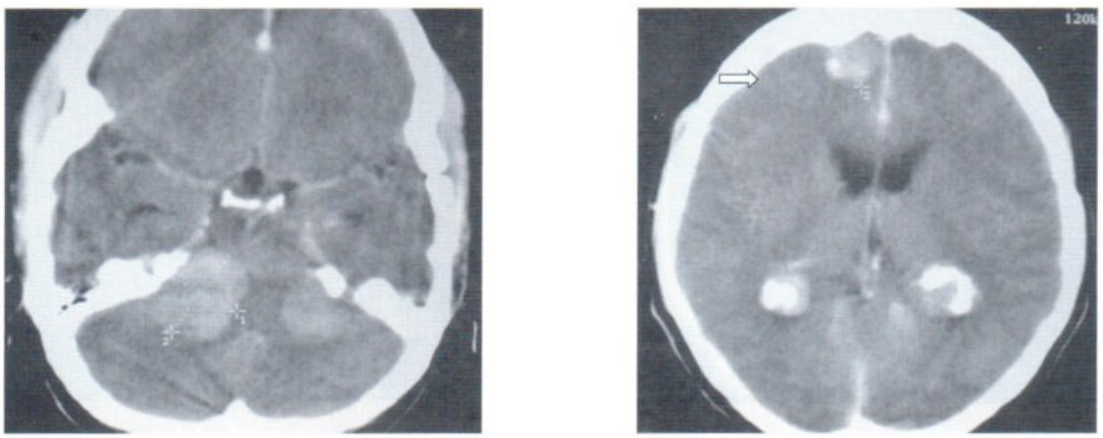

A B

Fig.9 Contrast-enhanced CT scans of a 31 years-old woman showed multiple meningiomas (A) bilateral CPA and (B) intraventricular meningiomas with globular calcifications. The right parasagittal meningioma with peripheral focal calcification was noted. (arrow in b.)

which results in additional adjacent reactive changes such as hyperostosis and sinus blistering.[16] In this study 10 (18.9%) meningiomas showed hyperostosis.

The dural tail sign is seen on contrast-enhanced MR images as a thickening of the enhanced dura mater that resembles a tail extending from a mass. Many investigators[8,17] were able to show little or no direct tumor involvement. It was therefore proposed that dural tails represented reactive changes to the dura mater, with perhaps minimal to meningothelial nodules that were adjacent to but not in contiguity with the tumor.

The cause of intraaxial peritumoral edema associated with meningiomas is controversial. However, Bradac et al[18] have found poor correlation between peritumoral edema and either the vascular supply of a meningioma or the presence of dural sinus invasion. The degree of peritumoral edema has little correlation with tumor size[18] and no correlation with location of tumor.[19]

On a review of the literature, any meningoendothelial cell whether intracranial, spinal or ectopic, can potentially result in the formation of a meningioma. These ectopic meningiomas may arise within diploic space, from the outer table of the skull, in the overlying skin, inside the paranasal sinuses,[20-22] in the parotid gland, and from the parapharyngeal space. Theories to explain these sites of origin include derivation from the arachnoid around the cranial nerve sheaths or from arachnoid cells disseminated during the formation of the skull.[2] A variety of pathological subtypes of meningioma have been defined and are outlines in table 7. Eric et al[3] reviewed 21 in 131 cases of CT and pathological findings showed atypical features of intracranial meningiomas such as necrosis, hemorrhage, scarring and cystic change. The term *cystic meningioma* has been used to described two different morphologies: intratumoral cavities and extratumoral or arachnoid cysts[2] which should be considered in the differential diagnosis of brain tumors with a cystic component. Cysts may result from direct secretion of fluid by tumor cells, from absorption of internal hemorrhage, or from loculated cerebrospinal fluid in scar tissue within or adjacent to the meningioma.[23] Lipoblastic meningioma and meningeal hemangiopericytoma are also atypical features of meningiomas.[2]

**Table 7** World Health Organization classification of tumors of meningothelial cell origin

| Grade | Tumor Types |
|---|---|
| I | Meningioma |
| | Meningothelial (syncytial) |
| | Transitional |
| | Fibrous |
| | Psammomatous |
| | Angiomatous |
| | Microcystic |
| | Secretory |
| | Clear cell |
| | Lyphoplasmocyte-rich |
| | Metaplastic variants (xanthomatous, myxoid, osseous, cartilaginous) |
| II | Atypical meningioma |
| III | Anaplastic (malignant) meningioma |

## Conclusion

Meningiomas are usually benign tumors with characteristic CT and MR imaging features, although too small group of MR image findings in this study. However on a review of the literature, there are several unusual or misleading features of meningiomas such as cysts, hemorrhage and fat. Meningio-

mas may originate in unexpected locations such as the ventricles, orbit, paranasal sinuses and meningioma en plaque. Because meningiomas are so common, the radiologists must be aware of their less frequent and uncharacteristic imaging features in order to suggest the correct diagnosis in cases that are atypical.

## References

1. Rockhill J, Mrugala M, Chamberlain MC. Intracranial meningiomas: an overview of diagnosis and treatment. Neurosurg Focus 2007;23(4):1-7.
2. Buetow MP, Buetow PC, Smimiotopoulos JG. Typical, atypical, and misleading features in meningioma. Radiographic 1991;11:1087-106.
3. Russell EJ, George AE, Kricheff II, Budzilovich G. Atypical computed tomographic features of intracranial meningioma: radiological-pathological correlation in a series of 131 consecutive cases. Radiology 1980;135:673-82.
4. Elster AD, Challa VR, Gilbert TH, Richardson DN, Contento JC. Meningiomas: MR and histopathologic features. Radiology 1989;170:857-62.
5. Spagnoli MV, Goldberg HI, Grossman RI, Bilaniuk LT, Gomori JM, Hackney DB, Zimmerman RA. Intracranial meningioma: high-field MR imaging. Radiology 1986; 161(2):369-75.
6. Wallace EW. The dural tail sign. Radiology 2004;233:56-7.
7. Johnson DE, Woodruff WW, Allen IS, Cera PJ, Funkhouser GR, Colemo LL. MR imaging of the sellar and juxtasellar regions. Radiographics 1991;11:727-58.
8. Goldsher D, Litt AW, Pinto RS, Bannon KR, Kricheff II. Dural "tail" associated with meningiomas on Gd-DTPA-enhnaced MR images: characteristics, differential diagnostic value, and possible implications for treatment. Radiology 1990;176:447-50.
9. Hentschel SJ, DeMonte F. Olfactory groove meningiomas. Neurosurg Focus 2003;14(6):1-5.
10. Derome PJ, Guiot G. Bone problems in meningiomas invading the base of the skull. Clin Neurosurg 1978;25: 435-51.
11. Wu E, Tang Y, Bai R. CT in diagnosis of acoustic neuromas. AJNR 1986;7:645-50.
12. Laird FJ, Harner SG, Laws ER Jr, Reese DF. Meningiomas of the cerebellopontine angle. Otolaryngol Head Neck Surg 1985;93(2):163-7.
13. Bhatoe HS, Singh P, Dutta V. Intraventricular meningiomas: a clinicopathological study and review of the literature. Neurosurg Focus 2006;20(3):1-6.
14. Jelinek J, Smirniotopoulos JG, Parisi JE, Kanzer M. Lateral ventricular neoplasms of the brain: differential diagnosis based on clinical CT and MR findings. AJNR 1990;11:567-74.
15. Lusin JO, Nakagawa H. Multiple meningiomas evaluated by computed tomography. Nuerosurgery 1981;9:137-41.
16. Rowbotham GF. The hyperostosis in relation with the meningioma. Br J Surg 1939;26:593-622.
17. Tokumaru A, Ouchi T, Eguchi T, et al. Prominent meningeal enhancement adjacent to meningioma on Gd-DTPA-enhanced MR images: histopathologic correlation. Radiology 1990;175:431-3.
18. Bradac GB, Ferszt R, Bender A, Schorner W. Peritumoral edema in meningioma: a radiological and histological study. Neuroradiology 1986;28:304-12.
19. Go KG, Wilmink JT, Molenaar WM. Peritumoral brain edema associated with meningiomas. Neurosurgery 1988;23(2):175-9.
20. Lee KF, Suh JH, Lee YE, Berry RG. Meningioma of the paranasal sinuses. Neuroradiology 1979;17(3):165-71.
21. Thompson LD, Gyure KA. Extracranial sinonasal tract meningiomas: a clinicopathologic study of 30 cases with a review of the literature. Am J Surg Pathol 2000;24(5): 640-50.
22. Swain RE Jr, Kingdom TT, DelGaudio JM, Muller S, Grist WJ. Meningiomas of the paranasal sinuses. Am J Rhinol 2001;15(1):27-30.
23. Worthington C, Caron J, Melanson D, Leblanc R. Meningioma cysts. Neurology 1985;35:1720-4.

THE ASEAN JOURNAL OF RADIOLOGY 2010; 16(1): 19-29 19

Original Article

# Transcatheter Arterial Chemoembolization in Patient with Hepatocellular Carcinoma in Srinagarind Hospital; Complications and Results

**Eimorn Mairiang, MD., Vallop Laopaiboon, MD. MSc., Warakorn Hachai-in, MD.**

*Department of Radiology, Faculty of Medicine, Khon Kaen University, Khon Kaen, 40002, Thailand*

## Abstract

**Background:** Transcatheter arterial chemoembolization (TACE) is known to be one of the best palliative treatment for unresectable HCC. However, its severe complications make its use controversial.

**Purpose:** To evaluate the complications and results of TACE in our treated cases.

**Materials and Methods:** Forty-seven patients underwent 88 TACE sessions during January 1, 2003 to December 31, 2004 at Srinagarind Hospital. Their clinical records, complications of TACE, tumor response, and survival outcomes, were reviewed retrospectively.

**Results:** Forty-seven patients (40 males [85%], 7 females [15%], mean age 51 years, underwent 88 chemoembolizations. Forty-two patients (89%) had documented cirrhosis, 28 (59%) had hepatitis B and 39 (83%) were chronic alcohol drinkers. Thirty-eight patients (81%), and 9 patients (19%) were categorized in Child's A and B classes, respectively. The common complications of TACE included fever (83%), abdominal pain (37%) and transient nausea/emesis (20%). Two patients with right portal vein (RPV) thrombosis developed acute liver failure within few days after TACE. One of them had sepsis syndrome. Partial and minimal tumor response was observed (33%). Overall survival rate was 61%, 48%, 27%, and 9% of patients at up to 6 months, 1, 2, and 3 years, respectively. The mean survival time was 13.1 months.

**Conclusion:** Most complications in our study can be corrected except for serious complication (acute liver failure) in 2 cases with RPV invasion. Very careful pretreatment planning should help reduce the problem. The response of treatment was found in 33%. The 2- and 3-years survival rate was 27% and 9%, respectively. We believe that we can do better in the future if the patients come to us in earlier stage.

**Keywords:** hepatocellular carcinoma (HCC), Transcatheter arterial chemoembolization (TACE), complications

## Introduction

Hepatocellular carcinoma (HCC) is a highly malignant tumor with a high morbidity and mortality rate. It represents the 5th most common cause of death from cancer worldwide. In Thailand, liver cancer had been found to be a leading cancer in men, and the 3rd in women.[1] Improvement of imaging technology has enabled to diagnosis of HCC at an early stage, making possible to treat tumors locally. Liver resection remains a curative treatment, particularly in the patient with TMN stage I which have 5 year survival rate about 70-75%.[2] Despite the availability of screening procedures for detection of early HCC (i.e. ultrasonography and serum α-fetoprotein [AFP] levels), the majority of patients are still not considered suitable for curative resection. Transcatheter arterial chemoembolization (TACE) had been recommended for treatment of unresectable HCC patients for reducing the mortality or morbidity, and prolong quality of life.[2]

The rationale for arterial embolization is progression of HCC, closely link to neo-angiogenic activity. At very early stage, the tumor is not highly vascularized. Its blood supply is from both the portal vein and the hepatic artery. When the tumor grows larger than 2 cm, the blood supply is mostly dependent on the hepatic artery. Large HCC receives blood supply almost entirely through the hepatic artery. Therefore arterial obstruction is the basis for an effective therapy. A mixture of chemotherapeutic agent and Lipiodol followed by absorbable gelatin sponge particles are generally used for embolization.[3-5]

TACE-related complications reported previously such as tumor rupture with hemoperitoneum, cerebral or pulmonary embolism, acute hepatic failure, liver abscess, severe septic complications, and bile duct injury[6-11] make its use controversial. We started to perform TACE in our institution since 1990, but before 2000 the medical records and film storage were incomplete. The aim of this study was to evaluate TACE-related complications, and the results after treatment by retrospective review of our clinical experience during January 1, 2003 to December 31 2004.

## Materials and Methods

This was a single-center retrospective study of unresectable HCC who required TACE between January 1, 2004 and December 31, 2005. The medical records of 64 patients were reviewed. Seventeen cases were excluded due to inability to perform chemoembolization after hepatic angiogram or evidence of contraindication for TACE (e.g. complete portal vein thrombosis, Child-Pugh class C, and severe hepatic or renal insufficiency). We recruited 47 cases (88 sessions of successful TACE treatment) to search for evidence of complications in each session, response of treatment, and the survival rate at up to 6 months, 1, 2, and 3 years.

The diagnosis of HCC was made either histological (n= 8), or by hepatic arteriogram and computed tomography (CT) scan combined with serum AFP level (n=39). The American Joint Committee on Cancer (AJCC) and Okuda staging system were used, for tumor staging.

Our inclusion criteria for TACE were Child's A or B class, bilirubin level < 3 mg/dL, prothrombin time ≤ 3 seconds above the control value, a serum creatinine concentration < 2 mg/dL, no total portal vein thrombosis, and no extensive arterio-venous shunting.

TACE procedures were performed by experienced radiologists in a standard fashion. Informed

consent was obtained from every patient for each procedure. After conventional hepatic angiography, a vascular catheter was inserted superselectively into the branch of the hepatic artery that supplied the tumor. The catheter uses were 5 Fr catheter and microcatheters (2.7 Fr or 3 Fr in diameter). Chemoembolization was initiated by infusion of a mixture of iodized oil (Lipiodol; Guerbet, France) and doxorubicin hydrochloride (Adriamycin; Kyowa Hakko Kogyo, Tokyo, Japan) to occlude tumor feeding arteries, followed by administration of absorbable gelatin sponge particles (Gelfoam; Upjohn, Kalamazoo, Mich) 1-2 mm in diameter soaked with 5-10 ml of nonionic contrast medium.

The doses of doxorubicin hydrochloride and iodized oil were 8-40 mg and 3-10 ml, respectively. The doses were given depended on the tumor size, the position of the catheter, the patient's liver function, and the response to previous treatment.

Re-chemoembolization was performed in 23 patients with 4-8 weeks interval between treatment sessions. Just before the next TACE, the liver function and CT of the liver or other imaging studies were checked to assess the response of the tumor and to evaluate the functional reserve of liver using the same criteria mentioned previously. The procedure was not re-performed in the patients who have poor liver function or no obvious tumor vessels. After the treatment, liver function test was periodically checked in patient with severe post-embolization syndrome or signs of hepatic failure. Blood culture was performed in patients with high and sustained fever. Appropriate imaging modalities such as chest radiography, ultrasonography, and CT scan were used for detection of TACE-related complications.

Additional treatments such as Percutaneous Ethanol Injection (PEI) (n=9) and open surgical injection (n=1), were performed after the last TACE. One case underwent right hepatectomy after 2 sessions of TACE. Additional systemic chemotherapy was administered in 2 patients.

Tumor response was assessed objectively by the change in tumor size on US, CT or MR imagings. The reduction in tumor size was measured at the same image level, representing the maximum dimension.[12] The response was determined on follow-up CT scan at 4-6 weeks after last chemoembolization. Tumor response has to be maintained for at least one month. Response criteria, based on the reduction of perpendicular diameter in the tumor are as follows: 1.) A complete response (CR) was total disappearance of tumor; 2.) A partial response (PR) was a reduction in tumor size of more than 50%; 3.) A minimal response (MR) was a reduction of 25-50%; 4.) No change (ND) was a change in tumor size less than ± 25%; 5.) Progressive disease (PD) was an enlargement of more than 25%.[13]

## Results

There were 47 HCC patients (40 males [85%], 7 females [15%], mean age 51 years [range 14-79 years old]), underwent successful TACE. The patient characteristics are shown in Table 1. Forty-two patients (89%) had documented cirrhosis. Thirty-eight patients (81%), and nine patients (19%) had Child A and B cirrhosis, respectively. Twenty-eight patients (59%) were hepatitis B carriers, 8 patients (17%) were hepatitis C carriers, and 39 patients (83%) were chronic alcohol drinkers. Four patients had HCC without documented cirrhosis, hepatitis B or C. Two cases of Child's A class presented with ruptured HCC. Segmentectomy of the liver was

required to stop bleeding prior to TACE. The detail of serum AFP levels, tumor staging, and tumor size is shown in Table 1.

The total number of TACE sessions was 88. The average number of TACE sessions per patient was 1.8, ranged from 1 to 6 sessions. The duration

**Table 1** Baseline characteristics of the patient with hepatocellular carcinoma

| Characteristics | | N=47 |
|---|---|---|
| Demography: | | |
| - Age, mean (range) | | 51 (14-79) |
| - Sex, M:F | | 40 (85%) : 7(15%) |
| Cirrhosis | | 42 (89%) |
| Chronic alcohol drinkers | | 39 (83%) |
| Hepatitis: B | | 28 (59%) |
| C | | 8 (17%) |
| Biochemistry (mean, range) | | |
| - Serum bilirubin (mg/dL) | | 0.96 (0.2-2.6) |
| - Prothrombin time (second) | | 13.2 (10.2-17.6) |
| - Serum albumin (mg/dL) | | 3.4 (2.9-4.7) |
| - Alkaline phosphatase (IU/L) | | 160.5 (70-368) |
| Distribution of serum AFP level (IU/ml) | | |
| < 10 | | 6 (13%) |
| 10 - 100 | | 9 (20%) |
| 101 - 500 | | 5 (10%) |
| 500 - 1000 | | 5 (10%) |
| > 1000 | | 22 (47%) |
| Disease characteristics | | |
| - Tumor size (cm): | < 5 | 7 (15%) |
| | 5 - 10 | 25 (53%) |
| | > 10 | 15 (32%) |
| - AJCC stage: | I | 0 (0%) |
| | II | 3 (6%) |
| | IIIa | 22 (47%) |
| | IIIb | 2 (4%) |
| | IVa | 17 (37%) |
| | IVb | 3 (6%) |
| - Okuda stage: | I | 26 (55%) |
| | II | 20 (44%) |
| | III | 1 (1%) |
| - Child-Pugh class: | A | 38 (81%) |
| | B | 9 (19%) |

of hospitalization was 2 to 21 days. The majority of cases (60 sessions) were discharged from the hospital within 3 days after each procedure. In the patients who were hospitalized longer than 7 days (20 sessions) with long period of fever and suspicious for sepsis syndrome, the final cause of fever was found to be tumor necrosis. Three patients were admitted longer because of deterioration of hepatic function. The other 5 patients can be discharged on the following day after chemoembolization.

The complications are listed in Table 2.

Thrombocytopenia were identified in 10/88 sessions of TACE (11%) and associated with cirrhotic patients whose imaging demonstrated splenomegaly and portal hypertension in alls cases. This could be explained by hypersplenism. None of the cases had severe coagulopathic complication or other rare complications (e.g. bleeding hematoma at punctured site, variceal bleeding, gastrointestinal bleeding from peptic ulcer/gastritis, tumor ruptured, liver abscess, bile duct injury, pulmonary or cerebral embolism, or bile duct injury).

**Table 2** Complications related TACE procedure (n=88)

| Complications | Incidence number (%) |
|---|---|
| Post-TACE syndromes | |
| - Fever | 73 (83%) |
| - Abdominal pain | 33 (37%) |
| - Nausea/Vomiting | 18 (20%) |
| Deterioration of liver function | 3 (3%) |
| - Reversible | 1/3 (1%) |
| - Irreversible with acute hepatic failure | 2/3 (2%) |
| Acute calculous cholecystitis | 1 (1%) |
| Thrombocytopenia | 10 (11%) |

### Post-TACE syndrome

The most frequent complications were fever, abdominal pain, and nausea/vomiting. The mean duration of fever was 2 days (range, 0-17 days). The long duration of fever associated with the initial tumor size, high dosage of Adriamycin, and development of severe hepatic deterioration and hepatic encephalopathy. Nausea/vomiting and abdominal pain were self-limiting in the majority of cases. The remaining could be controlled by the administration of anti-emetics and analgesic drugs. Mean duration time of abdominal pain was 0.8 day (range 0-6 days). Long duration of abdominal pain was 4, 5, and 6 days, associated with the tumor larger than 10 cm accompanying using 5 Fr catheter.

### Deterioration of liver function

Three patients had deterioration of liver function defined as an increased in serum bilirubin concentration (2 mg/dL or higher), newly developed ascites or hepatic encephalopathy. All of them were identified in the first session of TACE. One patient developed within 3 days and spontaneously recovered in 1 week after treatment. Irreversible deterioration with acute liver failure occurred in 2 patients who had pre-existing tumor invasion nearly total occluded the right portal vein. One of them also had acute calculous cholecystitis as a precipitating cause (Table 3).

### Response of treatment

Thirty six patients (76%) were evaluated for responses. Other 11 patients were not analyzed because follow-up CT scan was not available. Six patients (16%) had partial response, 6 (16%) had minimal response, no change in 8 cases (22%).

**Table 3** Characteristics of the patients who had hepatic deterioration.

| Characteristics | Reversible (n=1) | Irreversible (n=2) | |
|---|---|---|---|
| | | 1st patient | 2nd patient |
| Gender : Age | Male : 52 | Male : 50 | Male : 50 |
| Child-Pugh class | A | A | A |
| AJCC staging | 4 | 4 | 4 |
| Tumor location | Segment 2/3 | Segment 8/5 | Segment 6/7 |
| Tumor Size | 15 | 10 | 13 |
| Catheter size | 5 Fr | 3 Fr | 5 Fr |
| Vascular supply | Lt. hepatic a. | Rt. hepatic a. | Rt. hepatic a. |
| Drugs use | | | |
| - Adriamycin | 16 mg | 16 mg | 40 mg |
| - Lipiodol | 6 ml | 6 ml | 10 ml |
| Vascular invasion | None | RPV* | RPV* |
| Precipitating cause | None | None | Acute calculous cholecystitis |
| Survival time | 3 years | 24 days | 23 days of admission without survival record |

* RPV: Right portal vein

**Table 4** Response to TACE (n=36)*

| Tumor size (cm) | CR | PR | MR | NC | PD | Total |
|---|---|---|---|---|---|---|
| < 5 | 0 | 1 | 2 | 2 | 1 | 6 |
| 5-10 | 0 | 5 | 2 | 4 | 7 | 18 |
| > 10 | 0 | 0 | 2 | 2 | 8 | 12 |
| Response | 0 | 6 | 6 | 8 | 16 | 36 |
| Percentage (%) | 0 | 16 | 16 | 22 | 44 | 100 |

* Follow-up CT scan in 11 patients were not available
* CR = complete response, PR = partial response, MR = minimal response, NC = no change, PD = progression of disease

Progressive disease was observed in 16 (44%) cases (Table 4). One patient in PR group is still alive after 3 years and received only 3 sessions of TACE (Fig. 1). One patient in MR group received 3 courses of TACE had a right hepatectomy within 3 months after the last TACE session. The histologic examination demonstrated fibrosis of tumor tissue without residual tumor cells.

### Survival time

The record of survival time was not available in 3 of 47 cases. Survival time of the remaining 44 patients ranged from 24 days to 3 years. The survival outcome related with clinical staging and Child classes is shown in Table 5. The overall survival rate was 61%, 48%, 27%, and 9% of patients after 6 months, 1, 2, and 3 years with mean survival time 13.1 months. Two patients with right main portal vein involvement had survival time approximately 1 month.

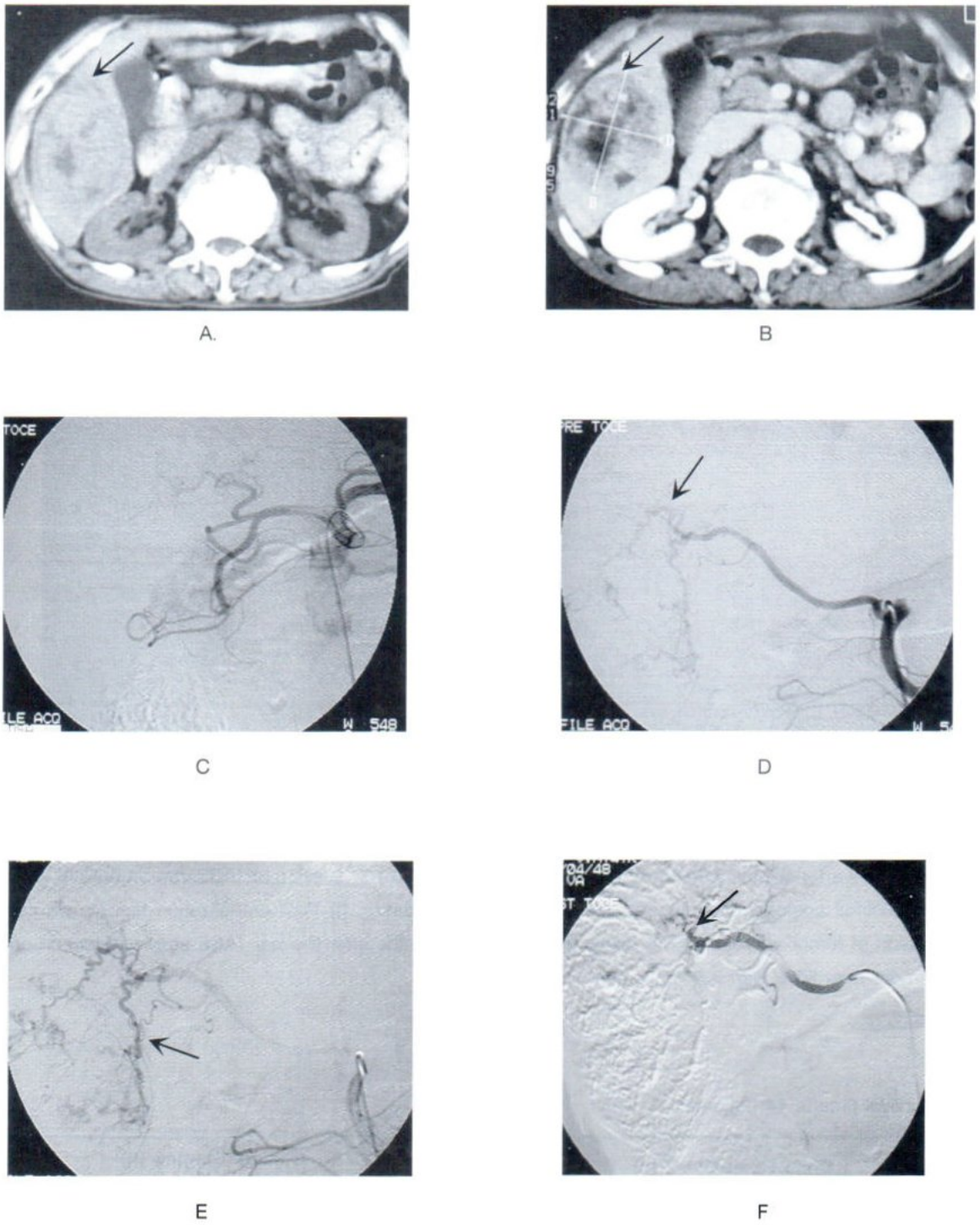


**Fig.1** 74-years-old man with HCC stage III underwent 3 courses of TACE. 1st session of TACE, **(a through f)**. **(a,b)** Initial CT scan shows a 7-cm mixed iso- to hypodense heterogeneously enhancing mass at segment 6 of right lobe liver. **(c,d,e)**. Angiogram shows hypervascularized tumor at right lobe liver (thick arrow) supplied by replaced right hepatic artery from SMA (thin arrow). **(f)**. Post-TACE film shows complete occlusion of tumor vessels (arrow).

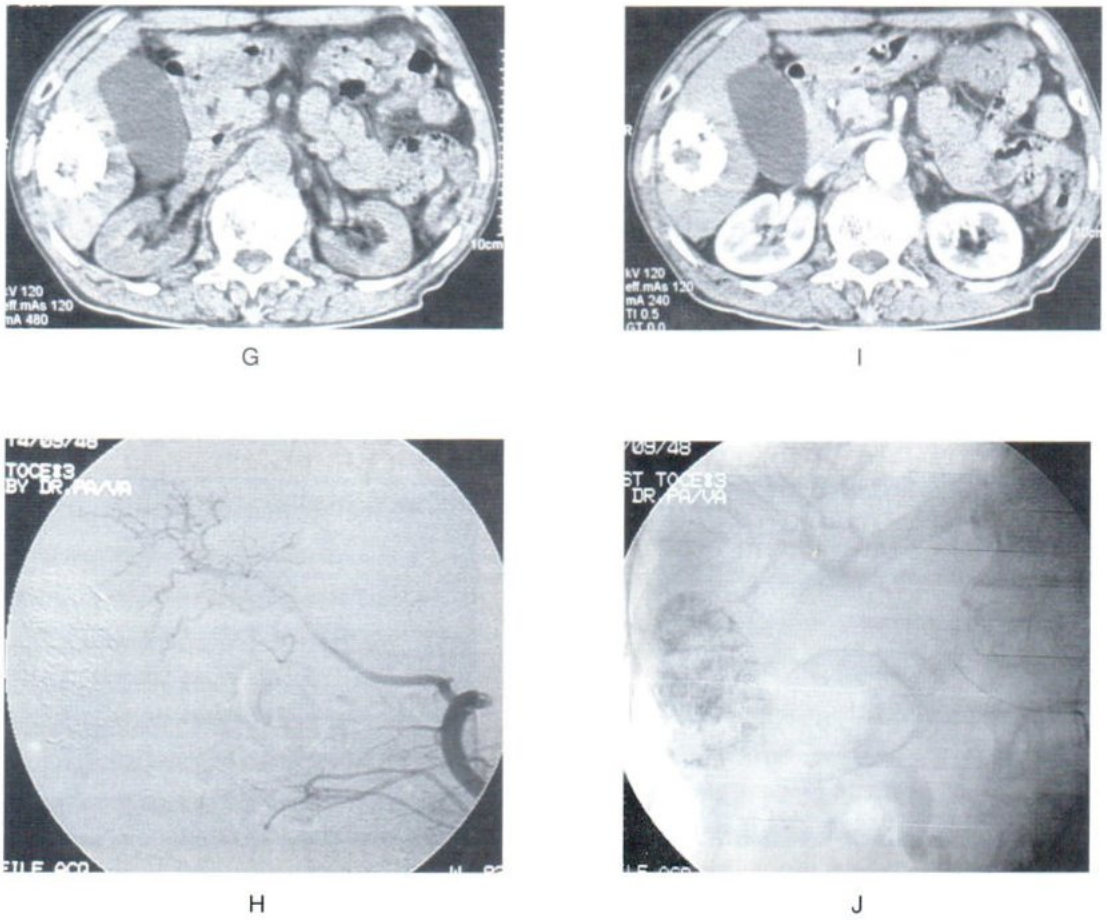

Fig.1 (continued). **(g)** Follow-up CT scan after 2nd TACE, pre and post contrast-enhanced CT show lipiodol staining with minimal arterial enhancement of the HCC at segment 5. **(h)** 3rd session of TACE, pre-embolized angiogram show minimal angiogenic activity at medial aspect of the tumor. **(j)** Post embolization film shows complete occlusion of tumor vessels. **(i)** The follow up CT scan 5-months after the last TACE shows reduction of tumor size more than 50% with > 90% lipiodol staining.

Table 5 Survival time in 44 patients*

| Survive (years) | Child-Pugh Class (n) | | Cases (%) | Clinical Staging (n) | | | | |
|---|---|---|---|---|---|---|---|---|
| | A (36) | B (8) | | II (3) | IIIa (20) | IIIb (2) | IVa (16) | IVb (3) |
| 0.5 | 23 | 4 | 27 (61%) | 3 | 14 | 1 | 9 | 0 |
| 1 | 18 | 3 | 21 (48%) | 3 | 12 | 1 | 5 | 0 |
| 2 | 10 | 3 | 12 (27%) | 3 | 6 | 0 | 3 | 0 |
| 3 | 3 | 1 | 4 (9%) | 2 | 1 | 0 | 1 | 0 |

* Survival record not available in 3 patients

## Discussion

Over the past 20 years, TACE has become the treatment of choice for patients with inoperable HCC. TACE has been shown to improve survival.[1,16] However, this survival benefit may be offset by the worsening of liver function. In this study, the serious complication of TACE was hepatic insufficiency. Portal vein obstruction is a well-known risk factor for hepatic failure and infarction after hepatic artery embolization.[14,15] In our series, 2 patients with nearly total RPV obstruction (Figure 1) had acute hepatic failure after TACE. Therefore, TACE should be cautiously performed with a reduced amount of chemoembolic agents and selective administration of them into tumor feeding arteries. In patients with either right or left major branch of main portal vein obstruction, if there are other predisposing factors to hepatic insufficiency, TACE may be contraindicated because of the risk of irreversible deterioration of the hepatic function. The liver with HCC is frequently compromised by cirrhosis and chronic hepatitis. A safe dose of iodized oil to the compromised liver has not been determined as yet. The total dosage of Lipiodol should be less than 20 ml (0.25-0.3 mL/kg) in order to prevent pulmonary oil embolism.[16] On the basis of our clinical experience, the amount of the iodized oil used is limited to less than 10 ml in all patients of our study.

Most common TACE-related complication in this study was post-embolization syndrome (fever [83%], abdominal pain [38%], and N/V [20%]), similar to those reported in the literature reviews[13,17,19]. Although, it is self-limited or can be managed, it can be considered a major complication of TACE because it prolonged hospitalization and impairs patient compliance with additional repeated treatments. Fever after TACE is mainly due to tumor necrosis. In the clinical setting, it is difficult to differentiate between fever due to tumor necrosis and fever due to secondary infection. In our study, post-embolization syndrome can be predicted on the basis of the size of the tumor to a certain degree. Therefore, unexpectedly high and prolonged fever after TACE in patients with a small tumor size developed sudden onset of high fever with chills, septic complications should be considered. In this study, most of the cases that had longer duration of fever with suspected septic complication had negative aerobic hemoculture and the final diagnosis was fever due to tumor necrosis. Sepsis was documented in only one patient with predisposing factor (acute calculous cholecystitis). Fatal sepsis insults were not found because we used strict sterile technique like other operative procedures. The cause of abdominal pain after TACE is unclear.

Liver function deterioration was found in 3% of total 88 TACE procedures, slightly lower incidence when compared to FAN J, et al.[13] (5%, 4 of 80 patients) and Chung JW, et al.[18] (15%, 54 of 351 cases). Chan OA, et al.[19] reported that 3% of their cases, developed hepatic encephalopathy or hepatic failure. This is close to our study (2%, 2 of 88 TACE sessions). We identified the factors that appear to predispose our patients to developed irreversible acute hepatic failure after TACE, to be a high dosage of Adriamycin 40 mg with evidence of RPV invasion (n=2).

Regarding response to treatment, Fan J, et al.[13] and Chan OA et al.[19] reported that the majority of their patients had partial response (reduction in tumor size more than 50%). In our study, we discovered that the majority of cases had progressive disease which should be due to initial tumor size larger than 10 cm in greatest dimension associated

with advanced tumor staging at the time of presentation.

Survival outcome of patients treated with TACE in this study were 48%, 27%, and 9% of patients at up to 1, 2, and 3 years with mean survival time 13.1 months, shorter time when compared to Llovet et al[2] (survival rates, 82% at 1 year and 63% at 2 years), and Fan J, et al[13] (87%, 46%, and 28% at 1-, 2-, and 3-years respectively). The reason should be due to different study design, patient characteristics, and treatment regimens. Our result was closed to that reported by Huang YH et al.[20] which had survival rates in TACE group at 1 year (42%), 3 years (13%), and median survival 9.2 ± 3 months. Our patient selection may be quite similar.

One of our patients with stage IV HCC caused by hepatitis B virus without evidence of cirrhosis survived more than 3 years. She underwent 2 sessions of TACE. After the 2nd procedure, CT imaging showed reduction in size of tumor from 12 to 9 cm and decreased serum AFP level from 1.8 to 1.11 IU/ml. Then surgical resection (right hepatectomy) was considered and the pathological report revealed no residual tumor with free surgical margin. The long survival time may reflect pre-operative down sizing and down staging by TACE. Another patient, AJCC stage III, the tumor size reduced from 7 to 3 cm after 3 sessions of TACE, survived longer than 3 years (Fig. 1).

The low complications of our procedure should alert the involved clinicians (hepatologists, hepatobiliary surgeons, oncologists, and interventionists) to chose TACE as an alternative treatment modality. The awareness of TACE-related complications should help in better management. However, this study is a retrospective review. There is limitation such as incomplete data collection and small number of patients. Nowadays many other palliative treatments with or without added neo-adjuvant therapy for inoperable HCC patients such as PEI, radiofrequency ablation, or transcatheter arterial embolization with radionuclide labeled iodized oil were used as alternative procedures. Comparative study with each treatment modalities and further prospective randomized trials of sufficient number of patients remain necessary.

## Conclusion

Most complications in our study can be managed. Serious complications, acute liver failure occurred in 2 patients with RPV invasion. Very careful pre-treatment planning should help to solving/reducing the problem. As for the result of treatment, 32% in our patients had partial and minimal tumor response, and the 2- and 3-years survival rate was 27% and 9%, respectively. We believe that we can improve it if the patients come to us in earlier stage.

## Acknowledgement

The authors gratefully acknowledge the efforts of Tula Dhiensiri, MD. for her editorial assistance.

## References

1. Vatanasapt V, Parkin DM, Sripamporn S. Epidemiology of liver cancer in Thailand. In: Vatanasapt V and Sripa B, editors. Liver cancer in Thailand: epidemiology, diagnosis and control. 3rd ed. KhonKaen: Siriphan press; 2000. p. 1-18.
2. Llovet JM, Real MI, Montana X, Planas R, Coll S, Aponte J, et al. Arterial embolisation or chemoembolisation versus symptomatic treatment in patients with unresectable hepatocellular carcinoma: a randomised controlled trial. Lancet2002 May 18;359(9319):1734-9.
3. National Clinical Practice Guidline of hepatocellular carcionoma management, Sep 2005.

4. Franca AVC, Elias J. Junior, Lima BLG, Martinelli ALC, Carrilho FJ. Diagnosis, staging and treatment of hepatocellular carcinoma. Braz J Med Biol Res 2004;37(11): 1689-705.

5. Roche A. Transcatheter arterial chemoembolization of hepatocellular carcinoma. In: Bartolozzi C, Lencioni R, editors. Liver malignancies: diagnostic and interventional radiology. 1st ed. Berlin: Springer; 1999. p. 245-51.

6. Sakamoto I, Aso N, Nagaoki K, Matsuoka Y, Uetani M, Ashizawa K, et al. Complications associated with transcatheter arterial embolization for hepatic tumors. Radiographics1998 May-Jun;18(3):605-19.

7. Yoo KM, Yoo BG, Kim KS, Lee SU, Han BH. Cerebral lipiodol embolization: a case report. Neurology 2004 July 13;63(2):181-3.

8. Kim HK, Chung YH, Song BC, Yang SH, Yoon HK, Yu E, et al. Ischemic bile duct injury as a serious complication after transarterial chemoembolization in patients with hepatocellular carcinoma. J Clin Gastroenterol2001 May-Jun;32(5):423-7.

9. Liu CL, Ngan h, Lo CM, & Fan ST. Ruptured hapatocellular carcinoma as a complication of transarterial oily chemoembolization. Br J Sur 1998 April;85(4):512-4.

10. Hashimoto T, Mitani T, Nakamura H, Hori S, Kozuka T, Kobayashi Y, et al. Fatal septic complication of transcatheter chemoembolization for hepatocellular carcinoma. Cardiovasc Intervent Radiol1993 Sep-Oct;16(5):325-7.

11. Kwok PC, Lam TW, Lam CL, Lai AK, Lo HY, Chan SC. Rare pulmonary complications after transarterial chemoembolisation for hepatocellular carcinoma: two case reports. Hong Kong Med J2003 Dec;9(6):457-60.

12. Yamashita Y, Takahashi M, Koga Y, Saito R, Nanakawa S, Hatanaka Y, et al. Prognostic factors in the treatment of hepatocellular carcinoma with transcatheter arterial embolization and arterial infusion. Cancer1991 Jan 15;67(2):385-91.

13. Fan J, Ten GJ, He SC, Guo JH, Yang DP, Wang GY. Arterial chemoembolization for hepatocellular carcinoma. World J Gastroenterol1998 Feb;4(1):33-7.

14. Yamashita Y, Torashima M, Oguni T, Yamamoto A, Harada M, Miyazaki T, et al. Liver parenchymal changes after transcatheter arterial embolization therapy for hepatoma: CT evaluation. Abdom Imaging1993 Fall;18(4):352-6.

15. Kan Z, Sato M, Ivancev K, Uchida B, Hedgpeth P, Lunderquist A, et al. Distribution and effect of iodized poppyseed oil in the liver after hepatic artery embolization: experimental study in several animal species. Radiology1993 Mar;186(3):861-6.

16. Chung JW, Park JH, Im JG, Han JK, Han MC. Pulmonary oil embolism after transcatheter oily chemoembolization of hepatocellular carcinoma. Radiology1993 Jun;187(3): 689-93.

17. Rose DM, Chapman WC, Brockenbrough AT, Wright JK, Rose AT, Meranze S, et al. Transcatheter arterial chemoembolization as primary treatment for hepatocellular carcinoma. Am J Surg1999 May;177(5):405-10.

18. Chung JW, Park JH, Han JK, Choi BI, Han MH, Lee HS, et al. Hepatic tumors: Predisposing factor for complications of Transcatheter oily chemoembolization. Radiology 1998;198:33-40.

19. Chan AO, Yuen MF, Hui CK, Tso WK, Lai CL. A prospective study regarding the complications of transcatheter intraarterial lipiodol chemoembolization in patients with hepatocellular carcinoma. Cancer2002 Mar 15;94(6): 1747-52.

20. Huang YH, Wu JC, Chen SC, Chen CH, Chiang JH, Huo TI, et al. Survival benefit of transcatheter arterial chemoembolization in patients with hepatocellular carcinoma larger than 10 cm in diameter. Aliment Pharmacol Ther2006 Jan 1;23(1):129-35.

THE ASEAN JOURNAL OF RADIOLOGY 2010; 16(1): 30-34

Original Article

# The Role of Ultrasonography in the Patients with Suspected Acute Appendicitis

**Worawan Chainamnan, MD.**

*Department of Radiology, Taksin Hospital, Bangkok, 10600, Thailand*

## Abstract

**Objective:** To evaluate the usefulness of ultrasonography in the cases of suspected acute appendicitis.

**Materials and Methods:** Sixty-four patients with clinically suspected acute appendicitis in Makarak hospital, Karnchanaburi from June 2006 to July 2008 were retrospectively reviewed for ultrasonographic diagnosis. The sensitivity, specificity, PPV, NPV and accuracy were noted.

**Results:** Nine patients were diagnosed as acute appendicitis but 1 case was false positive. Fifty-five patients were assessed as non appendicitis group but 3 cases were false negative. The specificity and sensitivity were 98% and 73%. The PPV, NPV and accuracy rate were 89%, 95% and 94% respectively

**Conclusions:** Ultrasonography may help in the diagnosis of acute appendicitis and exclude other diseases and decrease unnecessary operation.

## Introduction

Acute appendicitis is one of the most common acute surgical conditions of the abdomen. The diagnosis of appendicitis traditionally has been based on clinical features found primarily in the patient's history and physical examination.[1] However the clinical diagnosis in many patients are difficult to establish. A negative appendectomy rate is about 20-25%.[2,3] In patients with an equivocal diagnosis, imaging techniques such as ultrasonography or computed tomography have a role for improve diagnostic accuracy and patient outcomes.[3,4]

Ultrasonography is a noninvasive, inexpensive and widely available imaging for diagnosis the patients with suspected acute appendicitis. Diagnostic accuracy, reported to range from 71-97% is dependent on operator skill.[4]

The present study aims to evaluate the usefulness of ultrasonography in the cases of suspected appendicitis.

## Materials and Methods

From June 2006 to July 2008, sixty-four consecutive patients with clinically suspected acute appendicitis were admitted to Makarak Hospital, Karnchanaburi and underwent ultrasonography.

The examination was performed by using an ALOKA 3500. A curvilinear 3.5 MHz transducer and high resolution 5-7.5 MHz linear array transducer were used. The scanning was done from right costal margin downwards to right iliac area to demonstrate ascending colon and cecum. The tip of cecum and ileocecal region were concentrated to identify the appendix. The positive criteria for acute appendicitis were a blind-end aperistalsis, noncompressible tubular structure with a laminated wall that arase from the base of the cecum, having an outer appendicial diameter of 6 mm or greater on cross section.[1,5]

All of the patients were retrospectively reviewed the medical records and ultrasonographic reports. The patients with clinically suspected appendicial abscess or phlegmon were not included in this study.

## Results

The retrospective review of 64 patients clinically suspected of acute appendicitis were underwent ultrasonography. There were 16 male (25%) and 48 female (75%) patients, with an age range of 4-88 years (mean, 29 years)

Nine patients were diagnosed by ultrasound to have acute appendicitis, while 55 patients were classified as non appendicial group based on ultrasound.

From table 1, the ultrasonographic finding of nine patients who were diagnosed of acute appendicitis have positive criterion for appendicitis with anteroposterior outer diameter ranged from 7-23 mm (mean, 14 mm). In fig. 1, 2 and 3 all of them were underwent appendectomy and confirmed with histological evaluation. Eight of nine patients were diagnosed of appendicitis (True positive) and 1 (11%) has pathological diagnosis of periappendicitis (False positive).

**Table 1** Correlation between the ultrasonographic results and pathological diagnosis

| | Pathology (+) | Pathology (-) |
|---|---|---|
| Ultrasound (+) | 8 | 1 |
| Ultrasound (-) | 3 | 52 |

Specificity (52/53) x 100% = 98%
Sensitivity (8/11) x 100% = 73%
Accuracy (60/64) x 100% = 94%
Positive predictive value (8/9) x 100% = 89%
Negative predictive value (52/55) x 100% = 95%

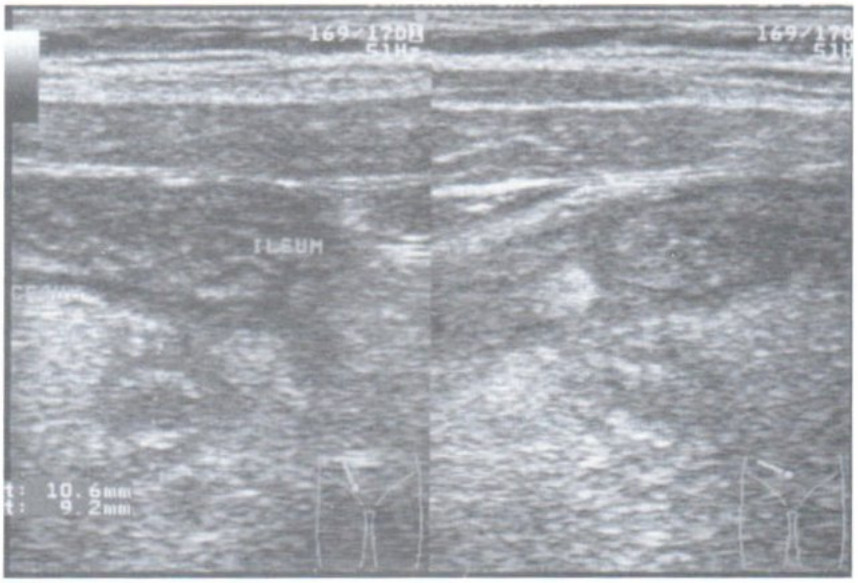


**Fig.1** Acute appendicitis : cross-sectional ultrasound images of RLQ obtained with a linear transducer show a 10.6 mm diameter, blind-ended, nonperistalsis tubular structure with a laminated wall.

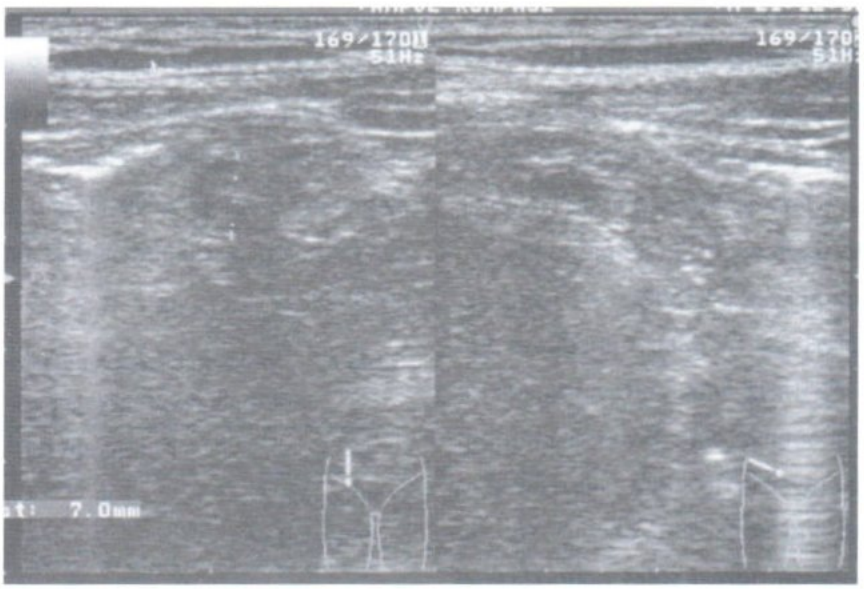


**Fig.2** Transverse and longitudinal ultrasound images at RLQ abdomen show inflamed appendix as a 7.0 mm AP diameter, blind-ended, noncompressible tubular structure.

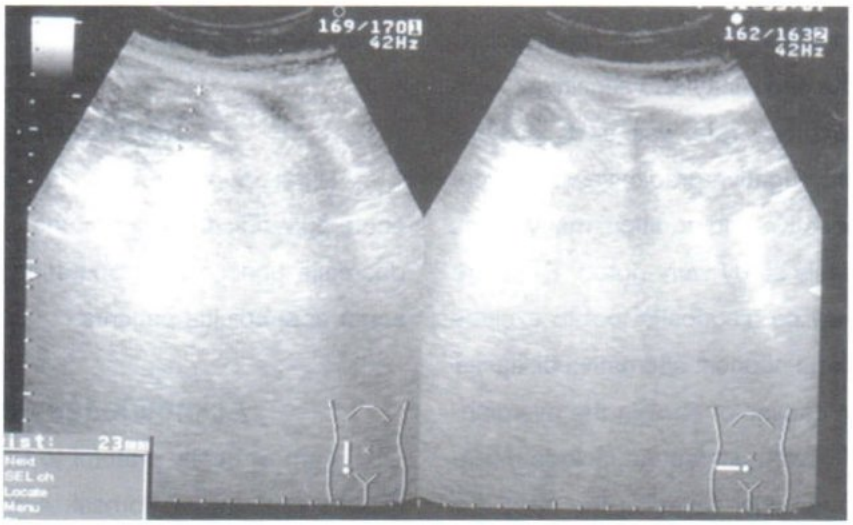


**Fig.3** Ultrasound images in longitudinal and cross-sectional views obtained with a convex transducer of acute appendicitis reveal a 23 mm AP diameter of blind-end aperistalsis, noncompressible tubular structure at right lower quadrant of abdomen

In the 55 patients with negative ultrasonographic findings for appendicitis, three patients were clinically determined to have appendicitis and then underwent surgery with pathological confirmation (False negative). Fifty-two patients had no evidence of appendicitis sign (True negative). In these 52 patients, ultrasound provided alternative diagnosis in 18 patients (gynecological conditions 6 patients, urological diseases 7 patients and hepatobiliary diseases 5 cases). The other 34 patients were clinically diagnosed as having gastrointestinal diseases in 17 patients and nonspecific abdominal pain in 17 patients.

## Discussion

Acute appendicitis is the most common acute surgical condition of the abdomen. The clinical diagnosis of acute appendicitis is based primarily on patient history and on physical examination. In classic presentation, a patient with appendicitis has a typical histological sequence of symptoms (poorly localized periumbilical pain followed by nausea and vomiting, with subsequent migration of pain to the RLQ) and physical findings that vary with time and with the location of the appendix.[6,7] The classic presentation occurs in only 50-60% of patients, and the diagnosis may be missed or delayed when atypical pattern of disease are encountered.[1] The overall diagnostic accuracy of acute appendicitis is about 80% in men and women with approximately 20% false negative appendectomy rate.[1]

In atypical case or equivocal clinical findings, ultrasonography and computed tomography are imaging tools that helps to improve diagnostic accuracy. Ultrasound is available, noninvasive method for diagnosis acute appendicitis. In experience hands, ultrasound has reported specificities of 86-100%, sensitivity of 75-90%, accuracies of 87-96%, positive

predictive values of 91-94% and negative predictive values of 89-97% for diagnosis of acute appendicitis.[1] In present study, the specificity and sensitivity were 98% and 73%, accuracy rate was 94%, positive predictive value and negative predictive value were 89% and 95% respectively. In addition, many cases of true negative in this study were noted. Therefore ultrasonography may be diagnostic tool to exclude acute appendicitis and suggest alternative diseases.

The common causes of error in the overdiagnosis of appendicitis with ultrasound include misinterpretation of the terminal ileum as the appendix and misinterpretation of a normal appendix as an inflamed appendix.[1] However in this study 1 case of false positive had clinical diagnosis of acute right pyelo-nephritis, severe form, with inflammation of paracolic region and periappendicitis. The underdiagnosis of appendicitis is much more difficult to address.[1] Many factors include ultrasonographic machine quality, technique of ultrasound, patient obesity and position of appendix (particularly true pelvic and retrocecal types of appendix). Furthermore, perforation of the appendix may lead to decompression of the appendicial lumen. Two of three cases with false negative in present study, 1 was retrocecal appendicitis and 1 had acute appendicitis with pelvic type.

This study had limitation on number of cases and was performed by one radiologist. However, good accuracy of present study had encountered. Accordingly, ultrasound imaging may help to diagnose acute appendicitis and decrease the negative appendectomy rate.

## Conclusion

Ultrasonography may help in the diagnosis of acute appendicitis and exclude other diseases and decrease unnecessary operation in the suspected acute appendicitis patients.

## Acknowledgements

I am sincerely grateful to Dr.Thanachet Kangsapattarakul and Dr.Pornsak Amornsri, department of surgery, Makarak hospital, for operative and pathological information.

## References

1. Birnbaum BA, Wilson SR. Appendicitis at the Millennium. Radiology 2000;215:337-48.
2. Eriksson S. Acute appendicitis-ways to improve diagnostic accuracy. Eur J surg 1996;162:435-42.
3. John PM. What is the role of ultrasound in evaluating patients with right lower quadrant pain? ASUM ultrasound Bulletin 2004;3:19-21.
4. Jerry LO, Reginald WD, Wendell Y, Jared D. Imaging for suspected appendicitis. Am Fam Physician 2005;71:71-8.
5. Jain RK, Jain M, Rajak CL, Mukherjee S, Bhattacharyya PP, Shah MR. Ind J Radiol Image 2006;16:523-32.
6. Wagner JM, McKinney P, Carpenter JL. Does the patient have appendicitis? JAMA 1996;276:1589-94.
7. Silen W, Fauci AS, Braunwald E, et al. Acute appendicitis. eds. Harrison's principles of internal medicine. 14th ed. New York, NY: McGrawHill, 1998;1658-60.

Original Article

# Patient Skin Dose in Interventional Radiology, TOCE at Songklanagarind Hospital

**Anchali Krisanachinda, Ph.D.**[1]
**Prasert Wattanapongpitak, B.Sc.**[2], **Panomporn Vimuttisuk, B.Sc.**[2]

[1] *Department of Radiology, Faculty of Medicine, Chulalongkorn University*

[2] *Department of Radiology, Faculty of Medicine, Prince of Songklanagarind University*

## Abstract

The purpose of this study is to determine the patient skin dose for Transarterial Oil Chemo Embolization (TOCE) procedure and the factors affecting in this study. Dose Area Product (DAP) meter was used to measure the patient skin dose in terms of Gy.m$^2$. After applying the exposed area on the imaging plate placed on patient's couch, the skin dose, mGy, can be determined. Twenty-nine hepato-cellular carcinoma (HCC) patients underwent TOCE procedure at Songklanakarind Hospital were carried out for interventional radiology procedures in the period of July-September 2008. The average skin dose is 0.428 Gy, the maximum dose is 1.249 Gy and the minimum dose is 0.176 Gy.

As the exposed area on the imaging plate is mostly invariable, the patient skin dose is directly dependent on the DAP readout with the correlation coefficient, $r^2$ of 0.97 while the correlation coefficient with body mass index is 0.102 and the correlation coefficient with the fluoroscopy time is 0.22. The maximum skin dose is lower than the threshold limit of erythema dose of 2 Gy.

## Introduction

The use of ionizing radiation for fluoroscopically guided interventions introduces two principal types of risks during medical care. The first is the stochastic risk of induced neoplasia and the second is deterministic risks for effects in superficial tissues such as the skin or the lens of the eyes. A third stochastic risk associated with ionizing radiation is that of heritable genetic risks passed on to descendants. This risk applies only to patients who will parent future offspring. Therefore, the risk associated with the use of ionizing radiation to treat patients with an urgent demand in medical needs deserve considerations. The aspect of assessing risk of ionizing radiation in relation an individual patient versus the anticipated benefits should be considered.

Since 1990, hundreds of reports on radiation skin injury from fluoroscopic interventions have been published.[1-4] To reduce the likelihood adverse radiation effects, the intervention radiologists must be well trained in the methods to conserve radiation use; the fluoroscopic equipment must be appropriately designed and well maintained for high quality imaging at low radiation output. The purpose of this project is to assess the potential for conserving radiation use by studying circumstances of procedures performed at Songlanakarind Hospital. Therefore, the project was designed to utilize the dosimetry techniques such as dose area product (DAP) to assess patient doses. The ultimate goal is to evaluate the role of different factors in patient dose management.

## Dose Monitoring

Dose-area-product meters are wide-area output detectors that can only assess the average dose over the radiation beam area. Readout is provided in units of $Gy.m^2$. The device provides no assessment of dose to the skin. To obtain an estimate of skin dose, the area of the beam at the skin surface must be known. This should be useful in which the beam seldom changes either in size or in angulations.

## Materials

1. X-ray system. Manufacturer Philips Medical System Model Integress V5000 (Fig 1)
2. DAP Meter Manufacturer PTW Model Pehamed W2 (Fig 2)
3. Imaging plate. Manufacturer Fuji Model ST-VI size 14x17 inch (Fig 3)
4. CR Reader Manufacturer Fuji Model FCR XG 5000
5. Ionization chamber and Electrometer Manufacturer RADCAL Model 9095
6. Workstation Manufacturer Rogan Version 2.0

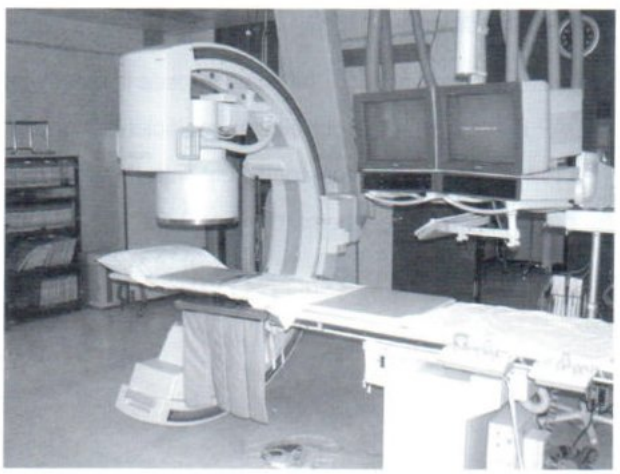

Fig.1 Radiographic Fluoroscopic System for TOCE Procedures

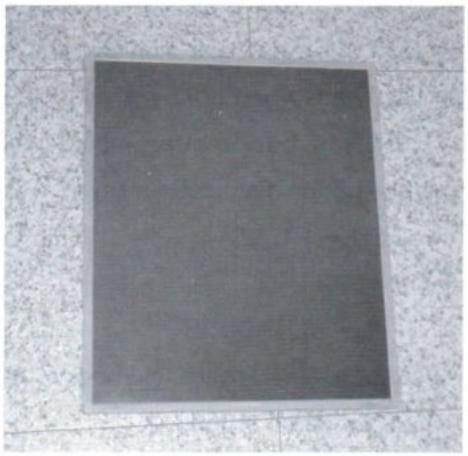

Fig.2 CR Imaging Plate Fuji Model ST-VI

Fig.3 DAP detector and Meter PTW Model Pehamed W 2

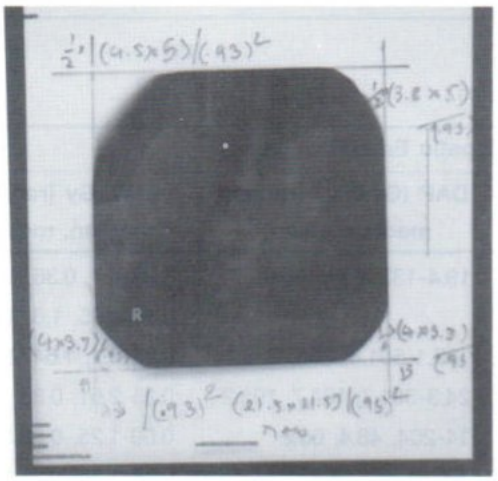

Fig.4 Fluoroscopic Exposed area during TOCE on film

## Methods

1. Perform the quality control of the radiographic-fluoroscopic system using IAEA and AAPM protocols for

- Radiation dose assessment
- Automatic Brightness Control (ABC)
- Maximum dose rate assessment
- Table attenuation determination
- Image size assessment
- Half Value Layer assessment
- Image quality assessment

2. Calibrate DAP with Ionization chamber as in figure 5 to obtain DAP calibration factors.

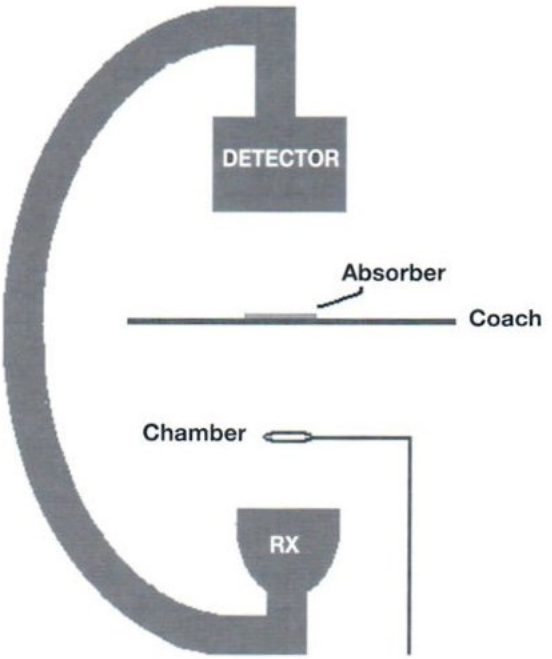


Fig.5 DAP and Ionization Chamber setup to obtain the DAP calibration factor

3. Patient data collection:

- H.N.
- Age, weight, height, sex

4. Patient dose determination

- Place the DAP detector on the x-ray collimator securely.
- Place the imaging plate on the patient's couch and under the patient back at the liver region
- Record the following parameters: kVp, mAs, SID, SSD, fluoroscopic time, DAP cumulative dose, radiologists experience, complexity index.
- Determine the exposed area, $m^2$ from exposed film.
- Calculate the patient entrance skin dose, ESD

$$ESD = f(E) \times BSF \times AK$$

f(E) is the f-factor that converts air-kerma (AK) into absorbed skin dose is usually 1.06 mGy tissue absorbed dose per mGy air-kerma

BSF is backscatter factor which is approximately 1.3 for diagnostic x-rays

$$ESD = 1.4\ AK$$

## Results

1. Patient characteristics. Number of patients is 29 as detail in table 1.
2. Measured and collected items are shown in table 2.
3. Other reports are shown in table 3

**Table 1** Twenty-nine HCC patients who underwent TOCE at Songklanagarind Hospital

| Sex | | Age (years) | | | Weight (kg) | | | Height (cm) | | | BMI ($kg.m^{-2}$) | | |
|---|---|---|---|---|---|---|---|---|---|---|---|---|---|
| Male | Female | Ave | Min | Max | Ave | Min | Max | Ave | Min | Max | Ave | Min | Max |
| 24 | 5 | 62.3 | 39 | 82 | 57.7 | 38 | 73.4 | 165.9 | 151 | 180 | 20.98 | 16.67 | 22.65 |

**Table 2** Parameters collected at the end of TOCE procedures

| Fluoroscopy Time (minutes) | | | DAP ($Gy.cm^2$) | | | Area ($m^2$) | | | ESD (Gy) | | |
|---|---|---|---|---|---|---|---|---|---|---|---|
| Ave | Min | Max | Ave | Min | Max | Ave | Min | Max | Ave | Min | Max |
| 17.91 | 6.5 | 55.4 | 19.60 | 7.67 | 61.32 | 0.05 | 0.04 | 0.07 | 0.428 | 0.176 | 1.249 |

**Table 3** Factors influenced the patient skin dose from other countries.

| Country | Hepatic Embolization | | | |
|---|---|---|---|---|
| | No.of patients | Fluoroscopy Time (min) (range, median, mean) | DAP ($Gy.cm^2$) (range, median, mean) | ESD, Gy (range, median, mean) |
| India | 16 | 2.7-36.5, 20.0, 18.4 | 19.4-133, 63.6, 65.0 | 0.03-0.7, 0.36, 0.34 |
| Japan | 19 | 3.6-62.9, 24.6, 30.4 | - | 0.16-2.95, 1.6, 1.47 |
| Malaysia | 6 | 15.4-59.9, 42,38.3 | 157.1-501.4, 265, 288.1 | 0.68-3.1, 1.64, 1.77 |
| Thailand* | 30 | 2.4-48.0, 9.2, 14.7 | 24.3-381.7, 184.7, 195.2 | 0.25-2.61, 0.88, 1.06 |
| Turkey | 15 | 1.8-12.9, 8.7,7.7 | 14-204, 48.4, 65.2 | 0.09-1.25, 0.32,0.43 |
| This Study | 29 | 6.5-55.4, 16.4, 17.9 | 7.7-61.3, 17.3,19.6 | 0.18-1.25, 0.38,0.43 |

*King Chulalongkorn Memorial Hospital

## Discussion

Data were acquired for a wide variety of hepatic embolization procedures resulted in wide variations in fluoroscopy times, 6.5-55.4 minutes, DAP readout, 7.7-61.6 Gy.cm$^2$ and mean skin dose (MSD), 0.18-1.25 Gy, among twenty-nine patients. While the relationship of DAP to BMI appears to be linear, the data are few and no substantive conclusion should be drawn. There is a mild influence of BMI on skin dose to patients, suggesting that factors other than BMI are more important in predicting the final dose result. The patient with maximum BMI of 26.84 kg/m$^2$ obtained the skin dose of 0.175 Gy while the patient with lowest BMI of 15.22 kg/ m$^2$ obtained the skin dose of 1.248 Gy. None of the data suggest the significant correlation between maximum skin dose and body mass index as in Figure 6. ($R^2$ =-0.1016)

Both ESD and DAP tend to increase with increasing fluoroscopy time in a linear way for hepatic embolization procedures as in figure 8.

Figure 8 demonstrates that the use of DAP to predict skin dose for hepatic procedures must be approached with caution. Generally, a linear relationship between ESD and DAP exist as in figure 7. A consistent behavior in use of beam orientation, geometry, and machine setting is likely to result in tight variation around a linear trend line. Consistency in execution is the key to making DAP a useful tool to estimate skin dose.

### High skin dose

The patient high skin dose during TOCE procedures could be of multiple explanations such as the fluoroscopic time, DAP values, kVp. In this study, the maximum time is 55.4 minutes while other study in Table 3 showed the longest time of 62.9 minutes and the maximum skin dose of 2.95 Gy. The DAP value showed the range of 7.7-61.3 Gy.cm$^2$ which is less than other study ranged up to 501.4

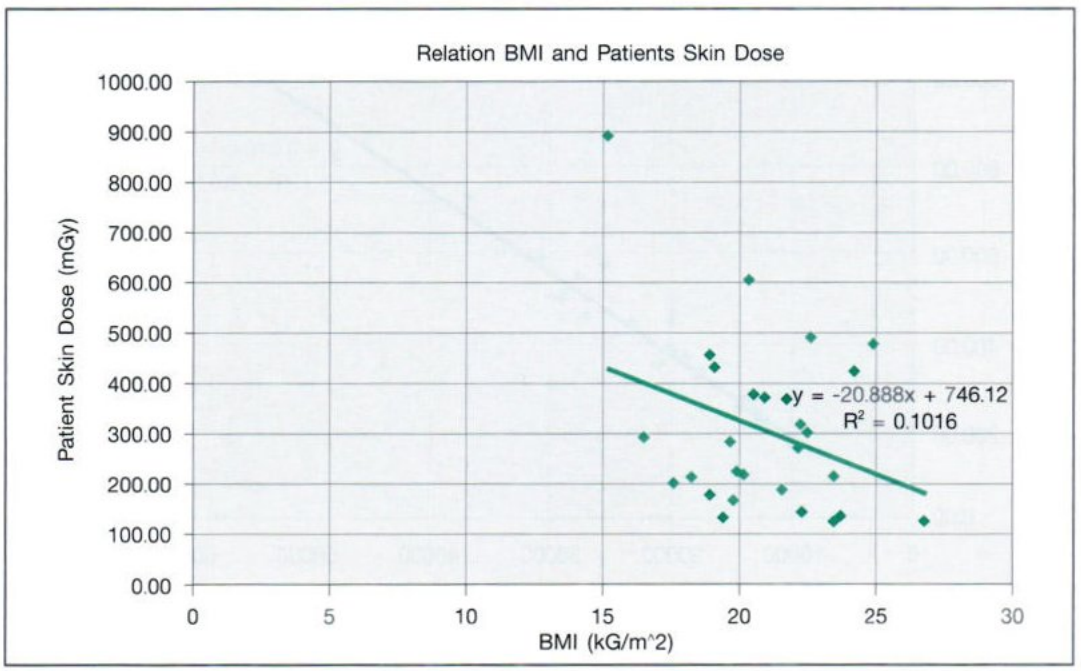


**Fig.6** The poor correlation between the patient skin dose and BMI, body mass index

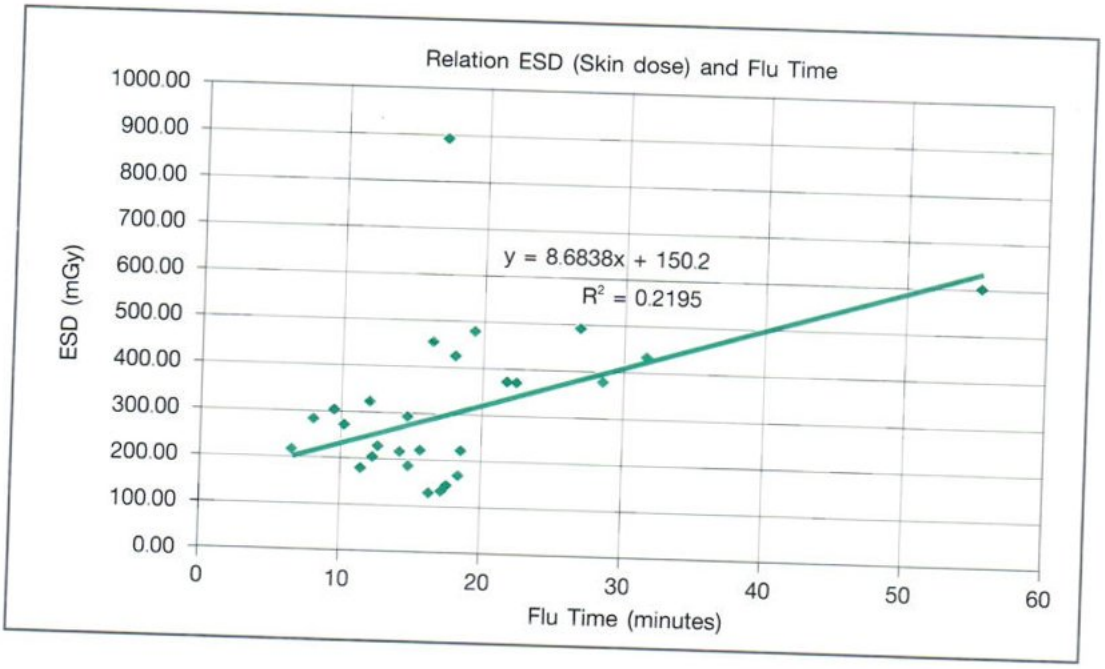


**Fig.7** The linear correlation between the patient skin dose (ESD, mGy) and the fluoroscopic time (minutes)

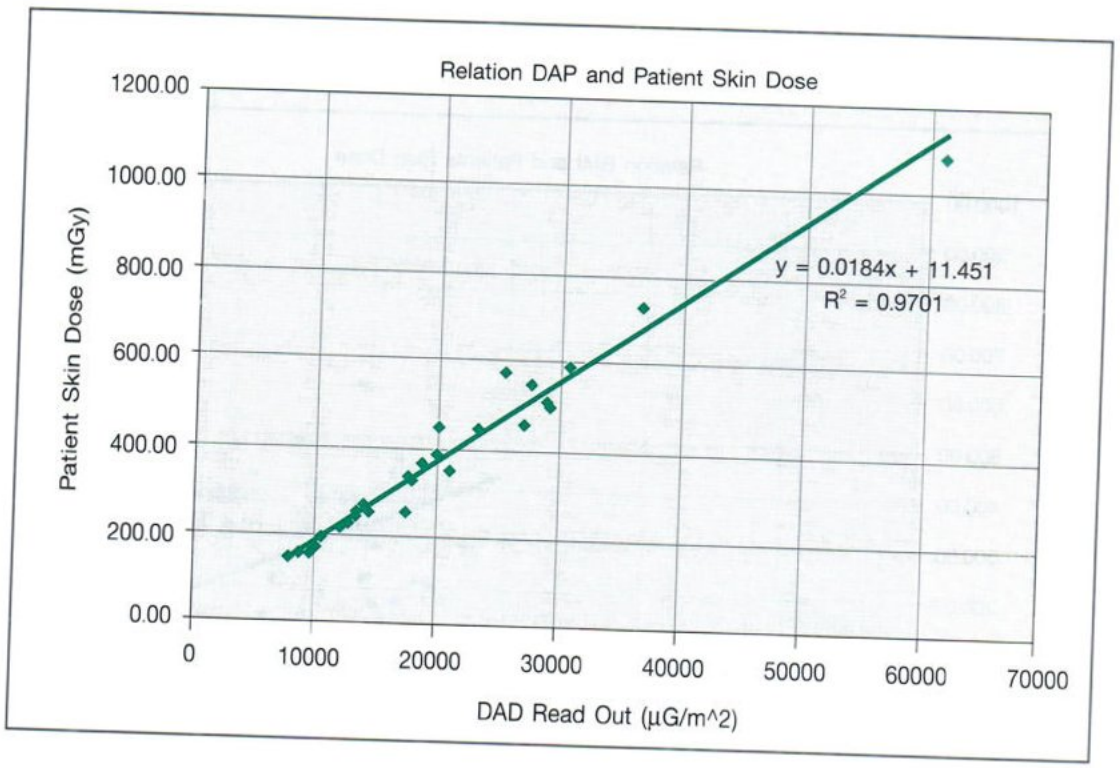


**Fig.8** The linear correlation coefficient between the DAP and ESD of $r^2 = 0.97$

$Gy.cm^2$ causing the skin dose of 3.1 Gy. For maximum kVp, this study used 84 and the average of 75.38 resulting in moderate skin dose compared to the kVp reach above 100 and for high magnification modes for other study. The exposure dose rate could be as high as four times for magnification mode when compared to normal mode. Some physicians did not use collimation very often and this resulted in overlap of fields when the beams were changed to a different orientation. Without overlap, the maximum skin dose would have been much lower. These are likely related to experience and training. The machine pulse rate modes, the automatic exposure rate are parameters influenced the high skin dose if the physicians did not use appropriately.

## Conclusion

Radiation risks. Radiation induced cancer is a long term risk of about one incidence per 1,000 patients receiving DAP of 80 $Gy.cm^2$ at the age of 60. It is about 4 times this amount for the same DAP in a patient of age 10 years. Radiation injury has occurred in patients undergoing complex interventional procedures, many have been severe. A mild radiation injury occurred in the skin of patient during this study. Severe effects are rare in relation to the number of procedures performed.

Dose management. Body mass index is the weak related risk for high skin dose in the interventional procedures. This means that the patient size is far less an important predictor of the dose to be delivered than other factors such as complexity or difficulty of the procedure. A large patient will contribute to the elevation of a high dose delivery during a complex and difficult procedure.

Radiation dose monitoring to patients with sufficient accuracy required the available resources to assure the quality result. However, monitoring patient skin dose to manage near-term adverse effects is important for patient care. Fluoroscopy time is correlated with dose to the patient but is a poor predictor of it because it does not account for the effects of image acquisition modes, different beam geometry and output modes of operation. Table 3 shows DAP readout is more significantly correlated with skin dose than fluoroscopy time. Under careful application and certain circumstances, maximum skin dose may be estimated from DAP. Experience of the interventionist in efficiently completing a procedure is a major factor in dose management. It was demonstrated that significant increases in dose to the patient result from interventionists who are less skilled than others.

Dose monitoring is a valuable tool. It is recommended to each facility establish a dose monitoring methodology suitable for the purpose. Action should be taken as doses exceed certain threshold levels.

## References

1. Koenig TR, Wolff D, Mettler FA, Wagner LK. Skin injuries from fluoroscopically guided procedures: Part 1, Characteristics of radiation injury. AJR Am J Roentgenol 2001: 177;3-11
2. Koenig TR, Mettler FA, Wagner LK. Skin injuries from fluoroscopically guided procedures: Part 2, review of 73 cases and recommendations for minimizing dose delivered to the patient. AJR Am J Roentgenol 2001;177;13-20.
3. Shope TB. Radiation induced skin injuries from fluoroscopy. RadioGraphics 1996;16:1195-9.
4. Vlietstra RE, Wagner LK, Koenig TR, Mettler F. Radiation burns as a severe complication of fluoroscopically guided cardiological interventions. J Intervention Cardio 2004: 17;131-42.

THE ASEAN JOURNAL OF RADIOLOGY 2010; 16(1): 42-51

Original Article

# The Patient Radiation Dose in Whole Abdomen and Thorax Computed Tomography at Songklanagarind Hospital

**Anchali Krisanachinda, MD.[1], Suwimol Jittakul, MD.[2], Uppatham Polpichai, MD.[3], Amporn Funsian, MD.[4]**

[1] *Department of Radiology, Faculty of Medicine, Chulalongkorn University*

[2] *Department of Radiology, Tamod Hospital, Patthalung Province Public Health Office*

[3] *Department of Radiology, Sikarin Hatyai Hospital*

[4] *Department of Radiology, Faculty of Medicine, Prince of Songkla University*

## Abstract

The purpose of this study is to determine the patient radiation dose and the factors affecting in order to develop the potential methods for the radiation dose reduction. The basic population consists of 100 patients who underwent the chest and abdominal computed tomography examinations at Songklanagarind Hospital.

The result shows the average dose length product, DLP, calculated for chest and abdominal CT of 448.10 and 1,192.59 mGy.cm respectively. The average weighted CT Dose Index CTDIw were 8.4 mGy for chest and 11.2 mGy for abdomen. 47 patients or 94 percent for DLP chest CT were lower than the dose reference level of 650 mGy.cm. For abdominal CT, 44 patients or 88 percent of sample population received the radiation dose higher than the dose reference level of 800 mGy.cm. All CTDIw were below the dose reference level of 30 mGy for chest and 35 mGy for routine abdomen.

The major factors affecting the patient radiation dose are the scan techniques such as the tube voltage, tube current, the scan time, the slice thickness, the scan length and the number of the phases or scans. Adaptation of the scan techniques, the reconstruction algorithm and the adjustment of the slice thickness to the appropriate scan length enable the reduction of the patient dose. The result of this study will lead to the awareness of the radiologists and technologists for the proper use of CT especially whole abdomen in young adult and in pediatric studies.

## Introduction

When Godfrey Hounsfield[1] developed the first clinical CT scanner in 1971, a new era of 3D visualization of the human body was initiated. During the 1970s the second, third and fourth generation scanners were developed, but by the end of the 1970s the basic principles of the CT scanner were well established, and the same principles are used in all scanners today. It was not until the late-1990s that rapid development started again. Largely this was the development of multi-row detector scanners and the culmination of efforts to increase the heat capacity or cooling of the x-ray tube. These faster scanning techniques enabled many more patients to be examined by the same number of staff. It also greatly increased the indications for the use of CT, partly because arterial and venous phases could be separated. As well as faster scan times and more clinical indications for the use of CT, the worldwide sale of CT scanners has more than doubled since 1998, and is predicted to continue at the same pace.

In recent years there has been increasing concern over the radiation dose to patients from CT studies.[2-4] The risk of cancer from all diagnostic x-ray procedures has recently been estimated to be between 0.5 and 3% of that for all cancers in developed countries. Although these risks seem relatively high, the current risks must be even higher, as most of the utilization data on diagnostic procedures in this published study was taken from the period 1991-96[6].

Since that time several generations of multi-row detector CT scanners have been introduced, resulting in increased patient throughput and increased indications for CT examinations. Recent papers have estimated that CT examinations now account for nearly 70% of the dose to patients in a tertiary care US hospital.[7] A recent radiation audit in a Canadian hospital provided essentially identical results, showing CT examinations delivering 60% of patient effective radiation dose.[8]

In diagnostic imaging the largest patient doses per examination come from CT and angiographic procedures. In angiography the therapeutic procedures generally give a higher dose to the patient than the diagnostic exams. In recent years, diagnostic angiography has largely been replaced by CT angiography in many radiology departments, possibly further increasing the overall dose to patients.

## Materials

1. Computed Tomography System. Manufacturer Philips Medical System Model Tomoscan AV Serial number K 813952902. (Fig. 1)
2. Ionization chamber and Electrometer Manufacturer RADCAL Model 9095 (Fig. 2)
3. Body CT Phantom diameter 32 cm. with 100 mm. pencil ion chamber (Fig. 3)
4. Fifty patients for whole abdomen scan, fifty patients for whole chest scan.

## Methods

1. Perform the quality control of the CT scanner
2. Determine the exposure dose using AAPM and IAEA protocols for
   - 2.1 CTDI in air
   - 2.2 CTDI in phantom
   - 2.3 The weighted CTDI, CTDIw

Before patient data collection, CTDI measurements were performed using a pencil-shaped ionization chamber with appropriate calibration

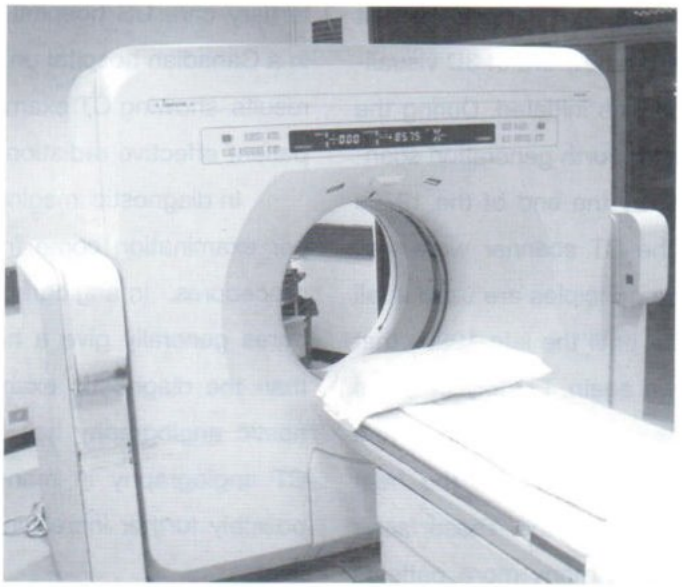

Fig.1 Computed Tomography System. Manufacturer Philips Medical System Model Tomoscan AV Serial number K 813952902.

Fig.2 Ionization chamber and Electrometer Manufacturer RADCAL Model 9095

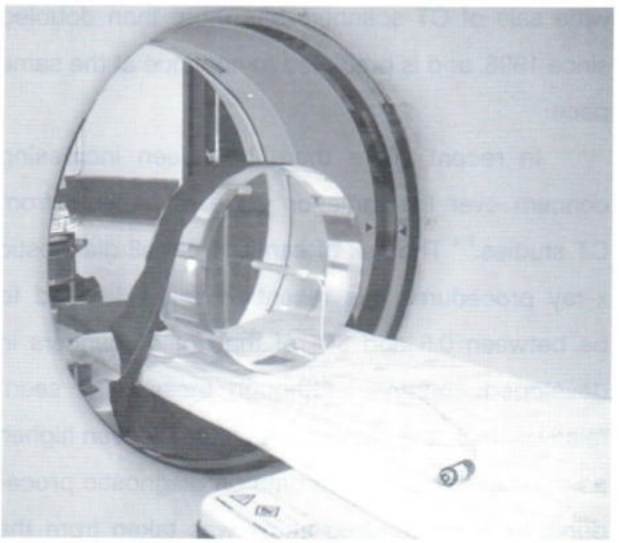

Fig.3 Body CT Phantom diameter 32 cm with 100 mm pencil ion chamber set at the center of the gantry for CTDI measurements.

certificate. The measurements were done in air for simplification purposes, using the following technical parameters: 120 kVp, 5 mm, 100 mAs and 1 pitch. The CTDIair results were compared with the Impact Group results (http://www.impactscan.org/ ) which provides the CT dose information for every CT scanner type and practically every clinical protocol used in routine procedures.

2.4 Dose-Length Product (DLP)

DLP is a dose descriptor that characterizes the exposure of a complete examination and is estimated by the following formula:

$$DLP = CTDI_{wi} * T_i * N_i \quad [1]$$

where $T_i$ is each different slice thickness used in the examination protocol. $N_i$ is the number of $T_i$ slices and CTDIwi is the value of CTDIw of each particular slice thickness $T_i$.

2.5 The Effective Dose (E) mSv

The effective dose is estimated by first estimating the energy imparted to the body region being scanned and then multiplying by the ratio factor for that particular region.

$$E = DLP \cdot f_{mean} \cdot k_{CT} \quad [2]$$

$f_{mean}$ is the average conversion factor for the specified region

$k_{CT}$ is the scanner factor

3. Patient data collection:

3.1. H.N.

3.2. Age, weight, height, gender

4. Patient dosimetric data collection.

4.1. Record the following parameters: kVp, mAs, slice thickness, the ratio of slice width and bed index, SW/BI, scan length, number of phases of study.

4.2. Determine the CTDIw, DLP for the chest and abdominal regions

4.3. Compare the result in 3.2 to the dose reference level, DRL

4.4. Calculate the patient effective dose

## Results

1. The CTDI in air. The 100 mm ionization camber was placed in air at the central point of the gantry. The chamber was exposed 5 times and the average result was recorded in Table 1. The measured CTDI was compared to ImPACT data to obtain the percent error of the measurement. The result is accepted when within 10 percent of the ImPACT. (table 1)

2. The CTDI in phantom. The 100 mm chamber was inserted in the centre position of the body phantom and measure the dose as the result in table 2.

3. The CTDI at four peripheral positions of body phantom were measured as in table 3 and compared to the ImPACT scan value as in Table 4.

**Table 1** The CTDI in air is compared to ImPACT value.

| CTDI in air (mR) | | | | | | Measured CTDI (mGy) | ImPACT CTDI (mGy) | Percent Error |
|---|---|---|---|---|---|---|---|---|
| 1 | 2 | 3 | 4 | 5 | Average | | | |
| 2.14 | 2.19 | 2.18 | 2.13 | 2.18 | 2.16 | 18.92 | 19.3 | 9.8 |

4. The weighted CTDI determination:

$$CTDIw = 1/3\ CTDI(center)+2/3CTDI(peripheral)$$
$$= 6.8\ mGy$$

5. Patient dose determination. The weighted CTDI (mGy) and the DLP (mGy.cm) for 50 patients underwent CT of the chest and 50 CT of the whole abdomen were determined. The result on DLP is displayed as the average, range and compared to the dose reference level (DRL) as in the table 5. The weighted CTDI for chest and whole abdomen are shown in table 6 and compared to the DRL.

The dose length product for both studies exceeds the DRL of 3 from 50 chest and 44 from 50 whole abdomen as details in table 7.

The dose length product is increasing as the increasing number of slices as in table 8 and as the increasing number of phases as in table 9.

The scan technique in this study is as the followings, the range of mAs is 150-200, the slice thickness is 3-7 mm resulting in the DLP exceeds the DLR as in table 10.

**Table 2** The CTDI at the centre of the body phantom of 32 cm. diameter.

| CTDIcerter (mR) | | | | | | Measured CTDI (mGy) | ImPACT CTDI (mGy) | Percent Error |
|---|---|---|---|---|---|---|---|---|
| 1 | 2 | 3 | 4 | 5 | Average | | | |
| 0.46 | 0.45 | 0.44 | 0.45 | 0.44 | 0.45 | 3.94 | 4.3 | 9.16 |

**Table 3** The CTDI at 4 positions peripheral sites on the body phantom of 32 cm diameter.

| | $CTDI_{PERIPHERAL}$ (mR) | | | | | | Measured | | ImPACT | |
|---|---|---|---|---|---|---|---|---|---|---|
| Position | 1 | 2 | 3 | 4 | 5 | Average (mR) | Average (mR) | mGy | mGy | Percent Error |
| Top | 1.04 | 1.04 | 1.03 | 1.03 | 1.02 | 1.03 | | | | |
| Bottom | 0.82 | 0.84 | 0.82 | 0.82 | 0.82 | 0.82 | 0.94 | 8.23 | 9.00 | 9.14 |
| Right | 1.00 | 0.98 | 0.98 | 0.99 | 1.00 | 0.99 | | | | |
| Left | 0.93 | 0.94 | 0.93 | 0.93 | 0.94 | 0.93 | | | | |

**Table 4** ImPACT scan data for Philips Tomoscan Model AV LX SR 7000

| kVp | Sub-group | Scanner | CTDI Head, mGy/100mAs | | | CTDI Body, mGy/100mAs | | | ImPACT Factor | |
|---|---|---|---|---|---|---|---|---|---|---|
| | | | Air | Centre | Perip | Air | Centre | Perip | Head | Body |
| 120 | PH.e.120 | Philips AV, LX, SR7000 | 19.3 | 13.6 | 14.8 | 19.3 | 4.3 | 9.0 | 1.03 | 1.01 |

**Table 5** The Dose Length Product, DLP (mGy.cm) for 50 chest and 50 whole abdomen scans.

| Organ | Range (mGy.cm) | Average (mGy.cm) | DRL (mGy.cm) |
|---|---|---|---|
| Chest | 288.29-709.63 | 448.10 | 650 |
| Whole abdomen | 613.54-1714.94 | 1192.59 | 800 |

**Table 6** The weighted CTDI for this study

| Organ | Average CTDIw (mGy) | DRL CTDIw (mGy) |
|---|---|---|
| Chest | 10.5 | 30 |
| Whole Abdomen | 13.4 | 35 |

**Table 7** Number of patients with DLP, mGy.cm exceeds the dose reference level

| Organ | Number | Percent |
|---|---|---|
| Chest | 3/50 | 6 |
| Whole abdomen | 44/50 | 88 |

**Table 8** The dose length product for whole abdomen and chest CT scans in relative to the number of slices.

| Number of Slices | Whole Abdomen DLP (mGy.cm) | Chest DLP (mGy.cm) |
|---|---|---|
| 39-50 | - | 288.29-369.60 |
| 51-70 | - | 376.99-517.43 |
| 71-90 | 739.20 (75 slices) | 524.74-591.36 |
| 91-120 | 896.60-1183.20 | 672.34-709.63 (96 slices max) |
| 121-209 | 1192.58-1714.94 | - |

**Table 9** The average number of phases and number of slices per phase

| Organ | Average Number of Phases | Number of Slice per Phase |
|---|---|---|
| Chest | 2.2 (1-3 phases) | 28 |
| Abdomen | 2.7 (2-5 phases) | 47 |

**Table 10** The CT scan techniques resulted in the excess DLP in abdomen

| mAs | Slice Thickness (mm) | Number of cases | Percent | Number of cases exceed DRL |
|---|---|---|---|---|
| 150 | 7 | 2 | 4 | 1 |
| 175 | 7 | 11 | 22 | 9 |
| 200 | 7 | 32 | 64 | 31 |
| 150 | 3 | 1 | 2 | 1 |
| 175 | 5 | 1 | 2 | 1 |
| 200 | 5 | 3 | 6 | 2 |

**Table 11** The Effective Dose (E, mSv) for Chest and Whole Abdomen

| Study | $E_{Av}$, mSv | $E_{min}$ mSv | $E_{max}$, mSv |
|---|---|---|---|
| **Chest** | 2.44 | 1.57 | 3.86 |
| **Whole Abdomen** | 6.87 | 3.53 | 9.82 |

In order to compare CT procedures with other types of radiological examinations and to estimate the radiological risk, the effective dose, E (mSv) was calculateded according to Hidajat 1996,[11] as in the equation[2] and the results are shown in table 11.

## Discussion

The EC[9] specify criteria for patient dose for CT examinations and give examples of good imaging technique. The dose that the patient receives in a CT examination is determined by two aspects of the particular scanner - the radiation output characteristics of the scanner and the clinical protocol of how the scanner is used in performing the examination. The first aspect can be determined using the $CTDI_w$ - a weighted measure of the amount of radiation the scanner "uses" per slice. This parameter in turn depends on the kVp, base filtration, shaping filters, slice width and the mAs per slice. The second aspect is essentially determined by the volume scanned. The combination of these two aspects determines the patient dose, which can be specified by effective dose or more simply by DLP.

The specification for CTDIw for the general chest CT is that it should be less than 30 mGy[9] which all CTDIw values in this study were 10.5. The protocol for chest is 120 kVp, 150 mAs and the slice thickness is 7.0 mm for all 50 cases. The average $CTDI_w$ for whole abdomen is 13.4, with minimum and maximum values of 10.5 and 14.0 mGy as in Figure 4. The abdomen protocol is 120 kVp, 150-200 mAs, and 3-7 mm slice thickness. These values are compared to the Dose Reference Level reported from the UK[10] of 35 mGy criteria for CTDIw.

Dose length product is an overall measure of patient dose. The proposed diagnostic reference level for DLP is given as 650 mGy. cm for chest.[9] The average of the reported DLP values was 448.1, with minimum and maximum values of 288.3 and 709.6 mGy.cm as in figure 5. These values are very similar to those reported from the UK.[10]

For the whole abdomen, the average DLP was

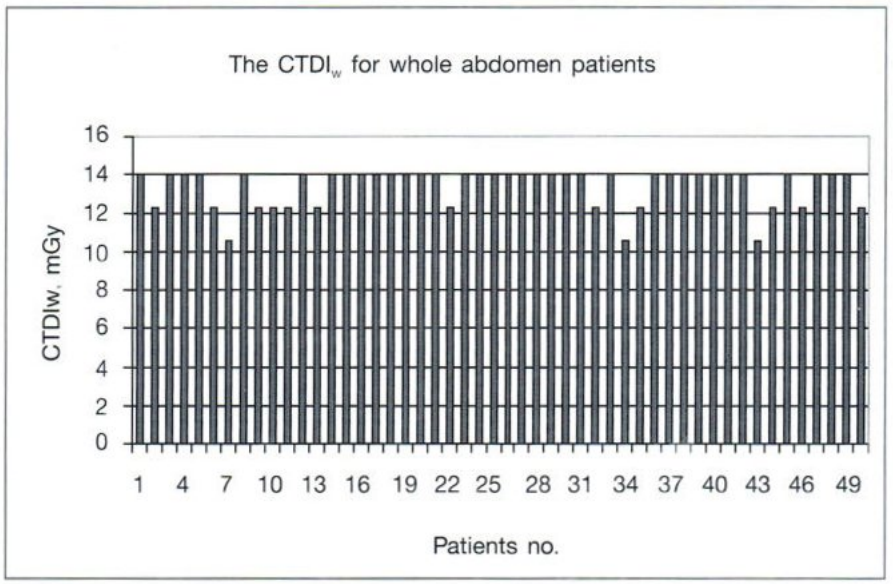


Fig. 4 The weighted CTDI for whole abdomen of 50 patients with DRL of 35 mGy

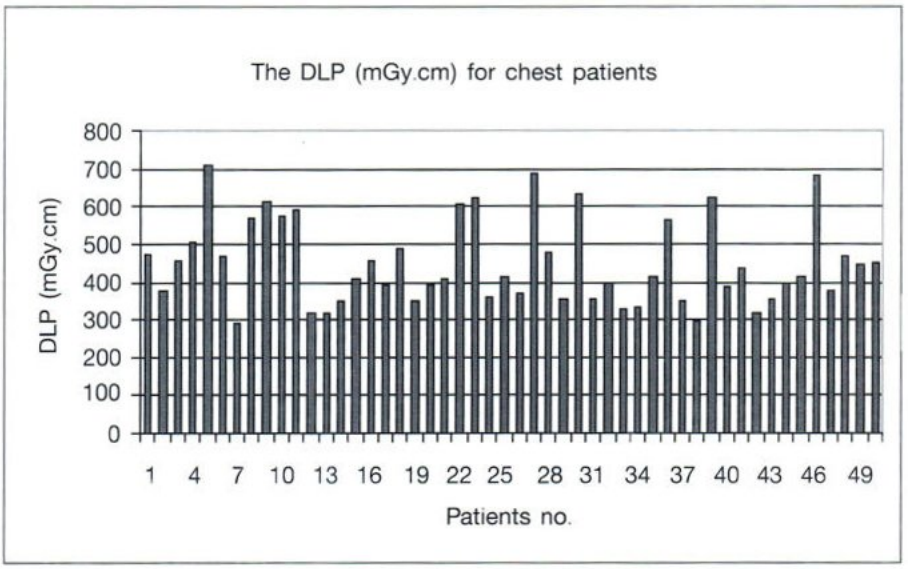


**Fig. 5** DLP for chest patients with Dose Reference Level of 650 mGy.cm

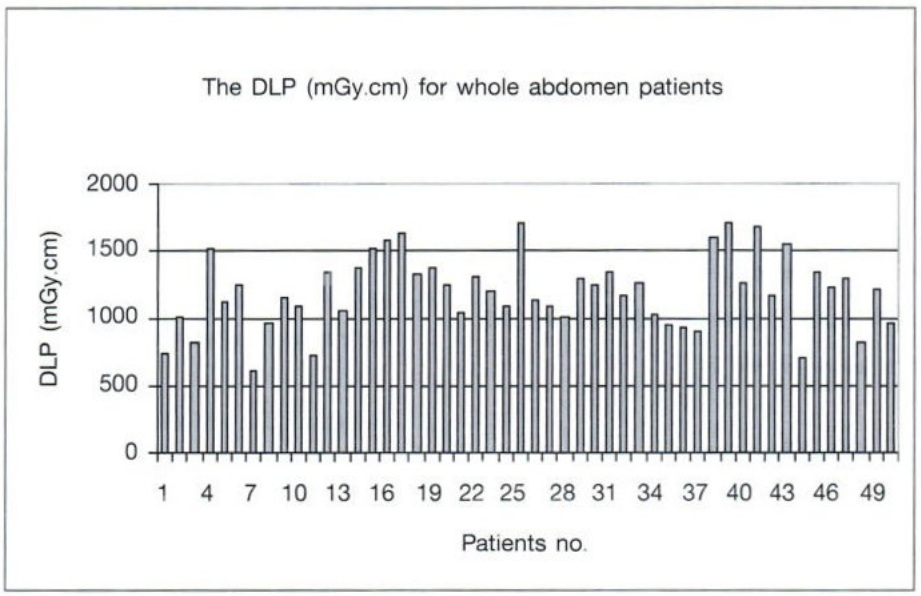


**Fig. 6** The DLP for 50 whole abdomen patients which DRL is 800 mGy.cm

1,192.59 with the range of 613.54 - 1,714.94 mGy.cm as in figure 6. The DRL is 800 mGy.cm

The EC[9] in "examples of good imaging technique" states that the nominal slice width should be in the range 7 to 10 mm, with an inter-slice distance of zero (contiguous slices) or a pitch equal to 1 in the case of spiral scanners. Our technique used slice widths of 7.0 mm for chest CT and 3 to 7 mm for abdomen with one 3 mm, four 5 mm and forty-five 7 mm slice widths respectively.

The scan length for each patient was variable and dependent on the number of phases. For chest,

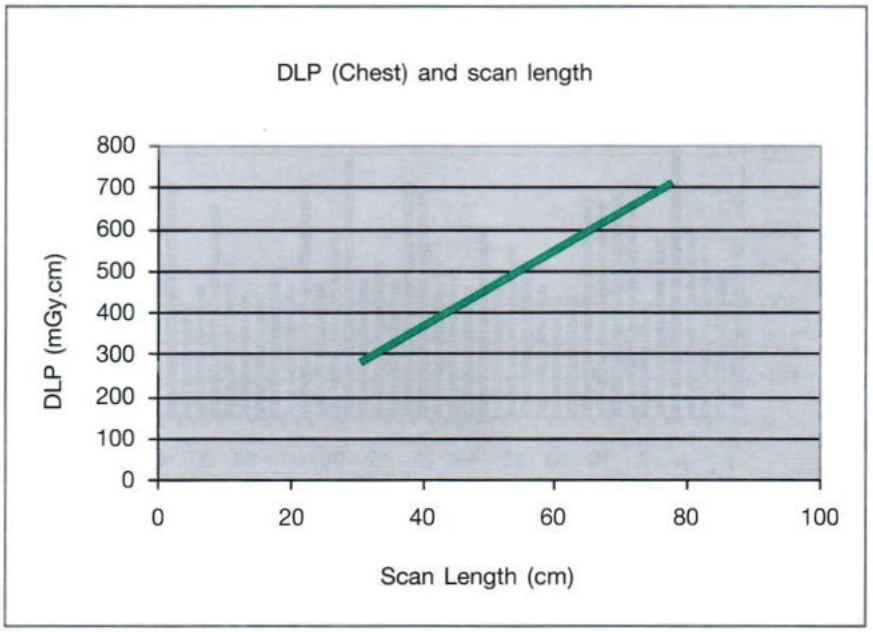


Fig.7 The linear relation of the scan length and DLP in chest CT patients.

the average number of phases was 2.2 and the range was 1-3. For abdomen the average was 2.7 and the range was 2-5 as in Table 11. The DLP was reflected by the scan length for chest. The maximum length of 74.4 cm, 2 phases resulted in DLP of 687.5 mGy.cm as in Figure 7.

## Conclusion

As the number of CT examinations is increasing rapidly, patient dose reduction is a task that needs urgent attention. Appropriate use of reduced dose protocols for common clinical indications requires further investigation. Radiation dose reduction is a key in the pursuit of novel applications of multi-detector CT. Medical personnel involved in radiological imaging should be familiar with the variety of methods and techniques for radiation dose reduction to ensure that radiation exposure is kept as low as reasonably achievable.

## References

1. Hounsfield GN. Computerized transverse axial scanning (tomography): part 1. Description of system. BJR. 1973;46:1016-22.
2. Brenner DJ, Elliston CD. Estimated radiation risks potentially associated with full-body CT screening. Radiology 2004;232:735-8.
3. Nickoloff EL, Alderson PO. Radiation exposure to patients from CT: reality, public perception, and policy. AJR Am J Roentgenol 2001;176:285-7.
4. Rehani MM, Berry M. Radiation doses in computed tomography. The increasing doses of radiation need to be controlled. BMJ 2000;320:593-4.
5. Gonzalez AB, Darby S. Risk of cancer from diagnostic x-rays: estimates for the UK and 14 other countries. Lancet 2004, 363:345-51.
6. United Nations Scientific Committee on the Effects of Atomic Radiation. Sources and effects of ionizing radiation. Report to the General Assembly, with Scientific Annexes. United Nations, New York 2000.
7. Mettler FA Jr, Wiest PW, Locken JA et al CT scanning: patterns of use and dose. J Radiological Protection 2000. 20:353-9.

8. Aldrich JE, Williams J. Change in patient doses from radiological examinations at the Vancouver General Hospital 1991-2002. Canadian Association of Radiology Journal 2005;56:94-9.
9. Office for Official Publications of the European Communities, European Guidelines on Quality Criteria for Computed Tomography, Report EUR 16262, Luxembourg 1999. ISBN 92-828-7478-8.
10. National Radiological Protection Board-R249, Survey of CT Practice in the UK. Part 2: Dosimetric Aspects. Shrimpton P.C. et al 1991. ISBN 0-85951-342-4.
11. Hidajat N, Schroder RJ, Vogel T et al. Effektivitat der Bleiabdeckung zur Dosisreduktion beim Patienten in der Computertomographie. Fortschr. Rontgenstr.1996;165: 462-6.

THE ASEAN JOURNAL OF RADIOLOGY 2010; 16(1): 52-61

Original Article

# Experience of the Commissioning and Implementation the Total Skin Electron Therapy (TSET) at Siriraj Hospital

**Lalida Tuntipumiamorn, MD., Lukkana Apipanyasopon, MD., Piyanan Liammukda, MD., Khammook Krongyuth, MD., Chumpot Kakanaporn, MD., Porntip Iampongpaiboon, MD., Surat Vinijsorn, MD.**

*Division of Radiation Oncology, Department of Radiology, Faculty of Medicine, Siriraj Hospital, Mahidol University, Prannok Rd, Bangkok-10700, THAILAND*

## Abstract

**Objective:** TSET at our institution has been commissioned. Technique and dosimetry were investigated and reported.

**Methods & Materials:** According to the Stanford six-dual field technique, using a high dose rate (888 MU/min) mode 6 MeV electron, at 400 cm SSD, on Varian 23 EX linear accelerator, investigation for the optimal irradiation geometry and TSET dosimetric features were performed.

**Results:** Acceptable field symmetry was obtained at the gantry angle ± 17.5° from 90°. Using a 1 cm perspex scatterer, the electron mean energy was degraded from 6 MeV to 2.1 MeV. Depth of dose maximum was detected at the surface to a depth of 2 mm. with R80 and R50 were at 0.52 and 0.9 cm from the surface, respectively. Absolute dose to water at a calibration point from the dual gantry in the high dose rate mode delivery was 1.367 Gy/1000 MU. The overlap factor (B) in this study was found to be 2.93. Phantom dosimetry revealed the accuracy of delivered dose was within ± 5%. Skin dose distribution was within ± 10%, of the dose at prescription point and the x-ray background dose averaged over a phantom body was 0.58%. Dose homogeneity over the patient's flat surface varied only a few percents. But at the tangential surfaces, the 10-30% difference from the delivered dose were presented.

**Conclusion:** TSET procedure for our first mycosis fungoides patient was successfully commissioned and implemented to the patient. Acceptable dosimetric features with the high dose rate electron mode were achieved. At one year follow-up, a satisfactorily clinical result was detected from the given technique.

## Introduction

It is acknowledged that TSET have been used for both primary and secondary cutaneous malignancies involving large segments of a body such as mycosis fungoides, lymphoma cutis cutaneous lymphoma and Kaposi's sarcoma.[1-2] Various TSET techniques have been developed with an objective to obtain a large electron field to deliver a uniform specified dose over the entire skin surface to a particular depth.[3-5] However, in practice, it is difficult to deliver to the entire skin of a patient with the irregular surface without the overdose and underdose. Moreover, the photon contamination from electron beam may be a source of side effects for the patient. It is strongly recommended that, in each particular TSET technique, the x-ray background magnitude must be known accurately and that an acceptable level averaged over a body volume should be 1% or less of the total mean electron dose at dose maximum.[6] At our institution, based on availability of the standard linear accelerator, the Stanford TSET technique was selected for our first mycosis fungoides patient. With a large SSD, dual angled electron beams and the six patient positions geometry, a thorough commissioning procedure of the proposed TSET technique was carried out and discussed.

## Materials & Methods

With the 23 EX Varian linear accelerator at 400 cm SSD and the collimator size 36x36 $cm^2$, the optimal beam geometry was first investigated. To flatten and degrade the electron energy, a 1 cm thick perspex panel, was placed at 30 cm in front of a 1x1.8 $m^2$ in size wooden board. Vertical profiles in different dual gantry angles varied from $\pm$ 13.5° to 18.5° from a horizontal plane were quickly assessed at equal intervals by using 12 electron diodes. 2D spatial distribution at the angle presented the best field symmetry will be examined using the TLD-100 dosimeters. Appropriate placement for the beam degrader was also investigated at between 30 and 50 cm in front of the treatment plane.

Dosimetric characteristics including central axis depth dose and electron beam output at a calibration point will be carried out with the optimal geometry obtained from the previous step. The electron depth dose was measured to a depth of 10 cm using PTW Markus parallel plate (PP) chamber and solid water phantom. In addition, to investigate the efficiency of the beam degrader, depth dose curves and beam profiles between with and without the scatterer were compared. Possible inaccurate depth dose from a cable effect of PP chamber was reevaluated using TLD-100 chips.[7-8] Electron beam parameters ;depth of dose maximum, R80 and R50, were determined from the measured depth dose curve. Then, the electron mean energy and output determination at the calibration point were carried out according to the code of practice for high energy electron beams from TRS-398.[9]

Total prescription dose, 36 Gy, was planned to deliver in 9 weeks for this patient[10]. A whole skin irradiated with 2 Gy was achieved from 12 treatment fields in six-dual angles and six positions in two days. To calculate the monitor unit per treatment field, the overlap factor (B) was determined from the mean treatment skin dose as described by AAPM Report No.23.[11] In this study we used 72 TLD-100 caps distributed uniformly on the 26 cm in diameter x 35 cm in height polystyrene cylindrical phantom. After irradiating the phantom under a complete cycle from the TEST technique, the mean treatment skin dose along a circumference of the

cylindrical phantom was achieved. The overlap factor (B) was then calculated from the ratio of mean treatment skin dose to the absolute dose at the calibration point (0, 0, 0) received from a single-dual pair irradiation. The number of monitor units to deliver the prescribed dose per field per treatment cycle was obtained from the following equation(1). (Factor 0.5 means at the prescription point, 50% of dose delivered from the beam up and down)

Dose per field = (Prescribed dose x 0.5)/ B
Monitor Unit = Dose per field/Electron beam output .....(1)

To verify the dose distribution, beam calibration accuracy and dose penetration, humanoid phantom dosimetry was performed. Sixty-eight TLD-100 measurement points were chosen as recommended by Antolak JA, et al.[12] We also inserted 41 TLD caps at the various anatomical locations from head to pelvis inside the phantom to evaluate the x-ray background dose receiving from TSET.

Since the surface contour between the humanoid phantom and the actual patient are different, in vivo dosimetry with TLD was performed at the first fraction as a pretreatment quality assurance. Accuracy of the delivered dose, surface dose distribution, dose to critical organs (such as lens) will be assessed. The entire procedure was evaluated. Careful consideration was made by the team to ensure the quality of the treatment before applying to the patient.

## Results

### Optimal Treatment Geometry

Uniform vertical profile assessed from diodes was shown at the gantry angle of 72.5° and 107.5° (±17.5° from 90°). 2D spatial dose distributions at this dual gantry angle were remeasured using numerous of TLD-100 dosimeters. It was found that the field symmetry were observed within ± 5% on the entire length of 180 cm and 40 cm field width as seen in Fig. 1 and 2.

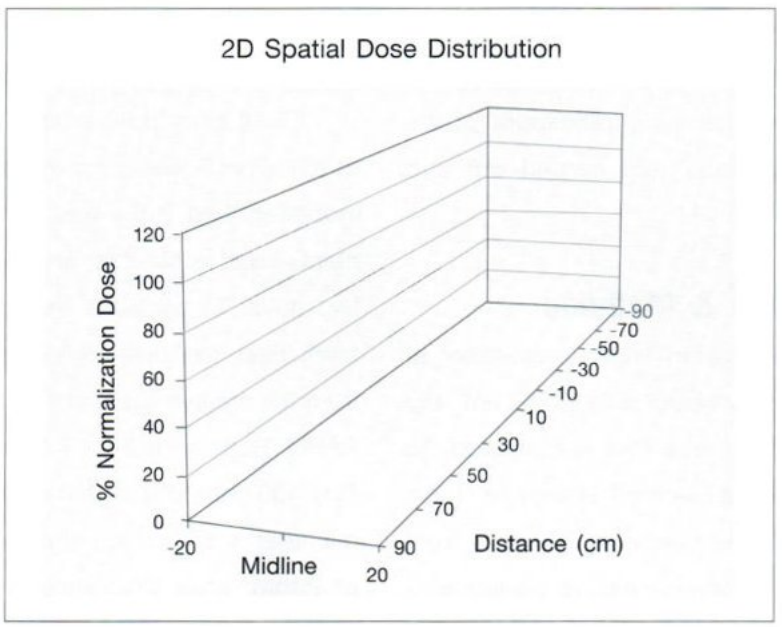


Fig. 1 2D spatial dose distribution at the gantry angles ± 17.5° from 90°

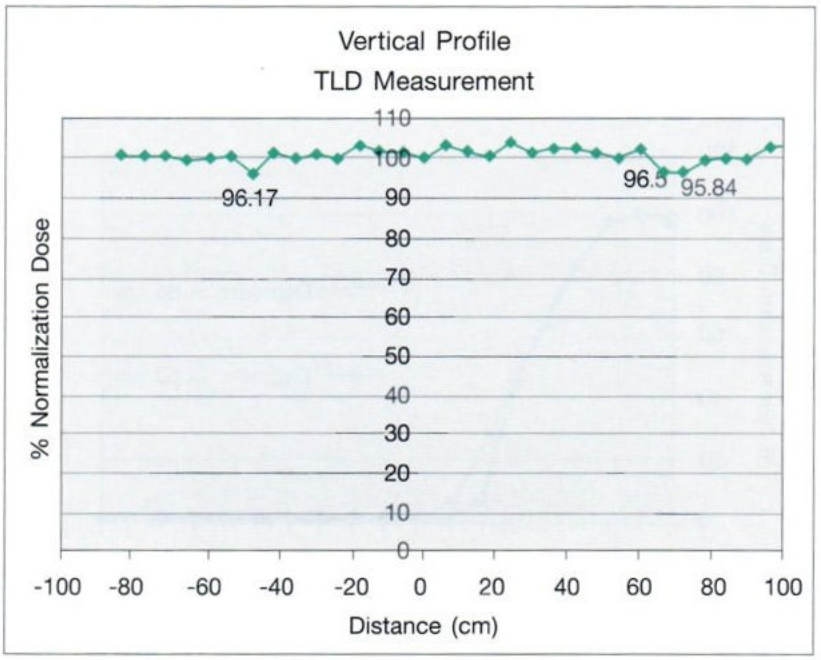


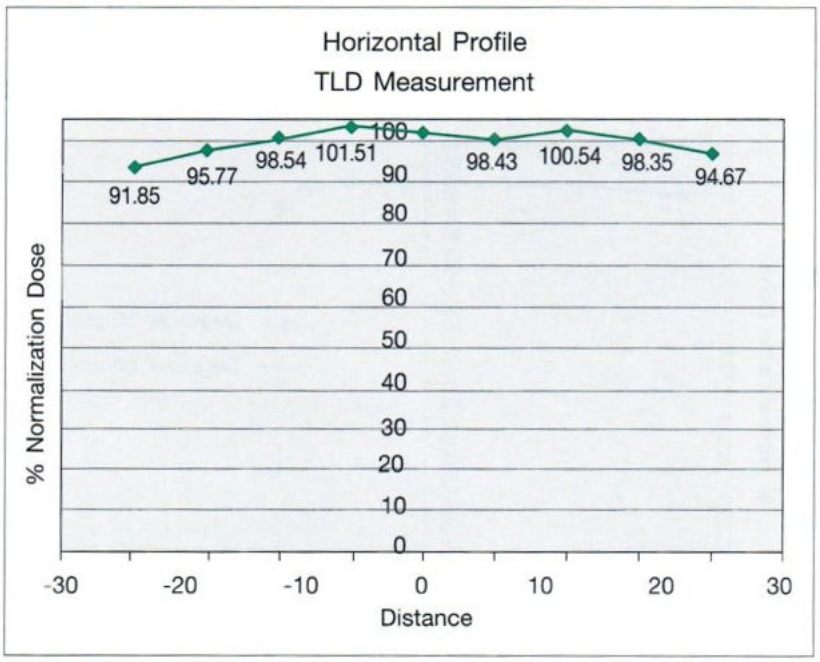


Fig. 2 Satisfactory field symmetry were found within ± 5% on the entire length of 180 cm and 40 cm field width

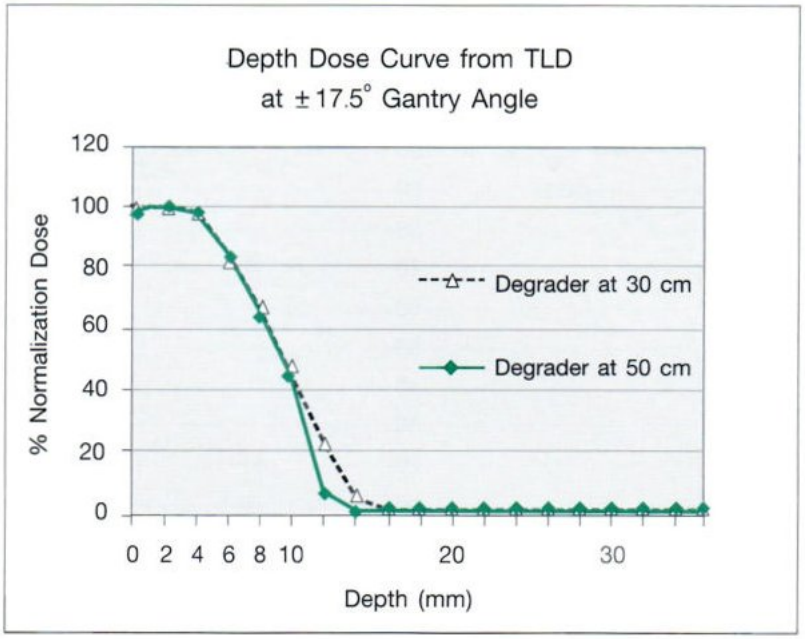


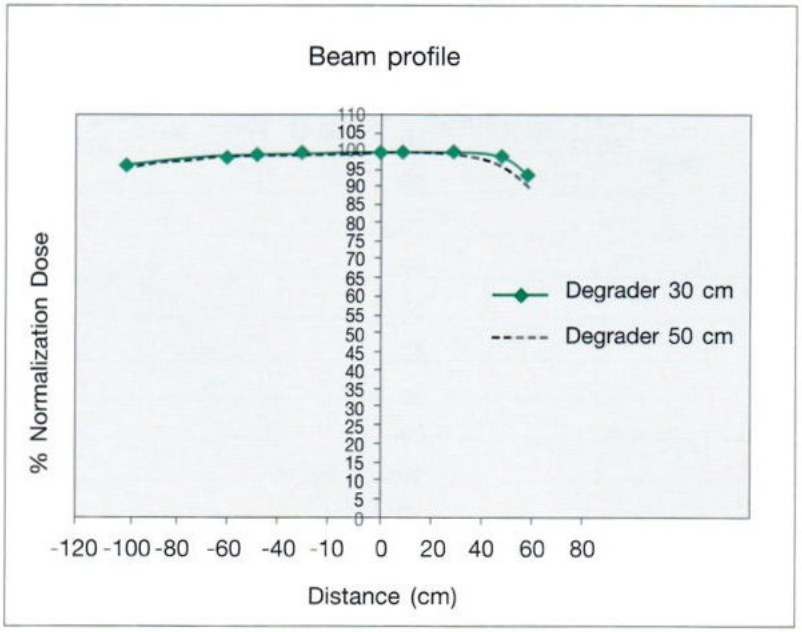


**Fig. 3** Electron profile and depth dose curve at gantry angles ± 17.5° from 90° compared between two different locations of the beam degrader.

Concerning about the location for the beam degrader, no difference of the beam characteristic between the 30 and 50 cm distance in front of the treatment plane were detected as shown in Fig. 3. However, in this study, the 30 cm distance was selected due to a slightly better surface dose.

### TSET Dosimetric Characteristics

It was clearly shown that using the beam degrader, the higher surface dose and shallower depth dose were obtained when compared with the open beam as seen in Fig 4. Depth of dose maximum was presented at the surface to a depth of 2 mm. and beam penetration, R80 and R50, were at 0.52 cm and 0.9 cm below the surface, respectively. The electron mean energy at the treatment SSD was determined to be 2.1 MeV.

Accurate photon contamination dose when assessed with TLDs in humanoid phantom was found to be less than 1%. This result was in contrast to the PP chamber which the cable effect will increase the contaminated dose to the level of 12%.

### Beam Output at a Calibration point

TSET calibrated dose was evaluated at the calibration point located at (0,0,0) as shown in Fig 5. The output was determined by Markus PP chamber in the solid water phantom and was found to be 136.7 cGy /1000 MU from the dual gantry angles.

### The overlap factor (B)

With the 72 TLD measurement points, the result of the mean treatment skin dose from the six-dual fields, 1000 MU irradiation, on the cylindri-

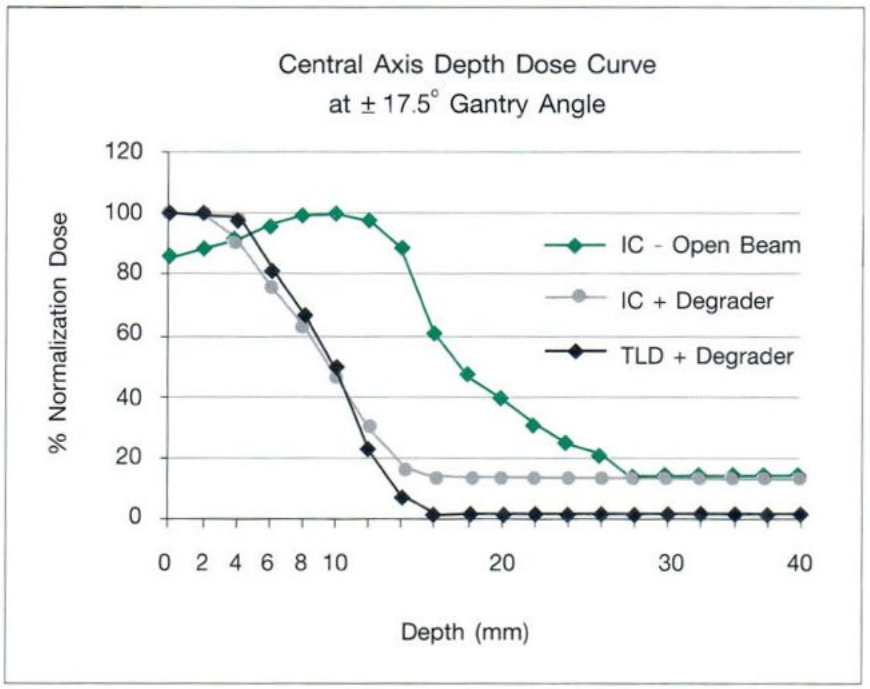


**Fig.4** Central axis depth dose curve compared between the presence and absence of the beam degrader, and between the parallel plate ionization chamber and TLDs.

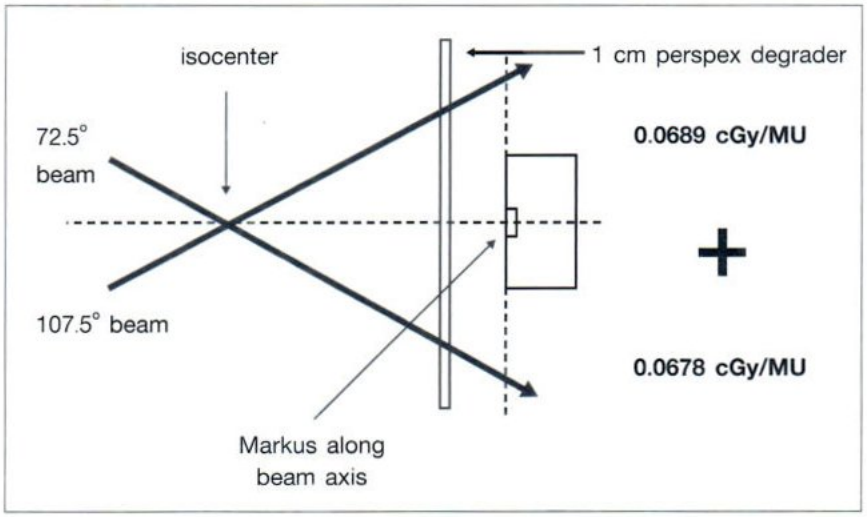


Fig.5 Absorbed dose measurement geometry and dose determination from each dual angle

cal phantom was equal to 383.33 cGy ± 5.54%. With the same geometry and number of MUs, the absolute dose at the calibration point received from a single-dual pair field was 130.83 cGy. Accuracy of the calibrated output was verified by the deviation of the measured dose from the expected dose (136.7cGy) and was about 4.29%. From previous study, typical B factor was reported in the range 2.5 to 3.1[11], and in this investigation was found to be 2.93. With the prescribed dose 2 Gy per cycle (in 2 days) with six dual beams per cycle, monitor units required for 72.50 and 107.50 treatment beam were 495 and 503 MU, respectively.

### Phantom Dosimetry

Dose verification on the rando phantom showed the measured dose at the prescription point was 94.8% of the delivered dose. Acceptable dose uniformity at the entire flat surface of the phantom was achieved as illustrated in Fig 6. Photon contaminated dose, measured from 41 TLD points, was found to be 0.58% of the total prescribed dose.

### In Vivo Patient Dosimetry

Owing to the difference between the humanoid phantom and the actual patient, dose verification on the first treatment fraction was performed. Results of the measured doses at various anatomical locations of the patient is presented in Table 1. Due to the obesity of the patient, some areas expected to be underdosed such as inframammary region, buttock skin fold were added in the experiment.

## Discussion

To provide a large, uniform and low energy electron field, the appropriate material and thickness of the scatterer-degrader was required for the TSET. Selection and placement of the degrader are strongly influenced by the need to minimize the background radiation.[13] Anacak Y, et al has reported

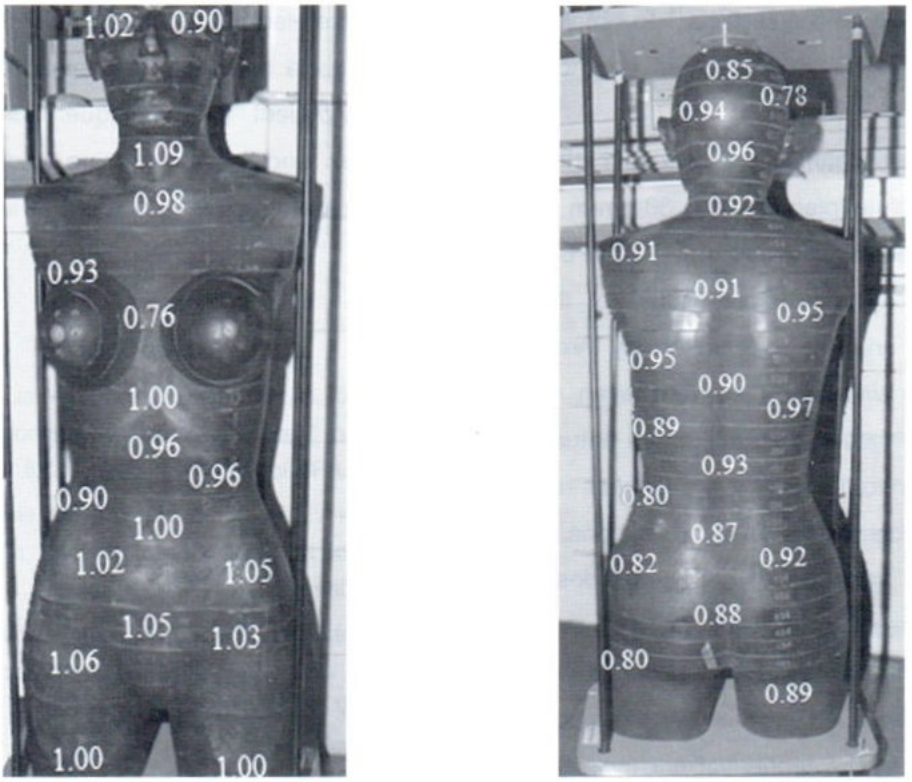


Fig.6 Surface dose distribution on humanoid phantom

Table 1 Patient's surface doses measured on the first fraction of treatment.

| Anatomical Location | % of Prescription Dose | Anatomical Location | % of Prescription Dose |
|---|---|---|---|
| Vertex | 81 | Eyelid (No shielding) | 84 |
| Neck | 89 | Axilla | 76 |
| Shoulder | 78 | Elbow | 86 |
| Breast | 98 | Under breast | 70 |
| Hand | 89 | Finger | 92 |
| Ant Abdomen (prescription point) | 96 | Post Abdomen (prescription point) | 104 |
| Lat Abdomen | 103 | Buttock | 73 |
| Ant Thigh | 89 | Medial Thigh (close to perineum) | 31 |
| Mid dorsal foot | 86 | Toe | 100 |

that, the thicker the beam degrader, the worse the dose homogeneity at the surface.[14] To obtain better dose homogeneity, a thinner beam degrader was suggested.

In this investigation, we used our old 1 cm thick perspex panel placed at the 30 cm in front of the treatment plane as a beam degrader. Both the acceptable background dose (0.58% of the prescription dose) and the dose uniformity throughout the flat surface, within ± 10%, were taken.

About the dose homogeneity on actual TSET patient, dose uniformity within ± 15% was reported to be acceptable by several publications.[15-17] In our study, the variation of measured dose from prescription dose on the flat surface of the body, was within 10%. However, due to the four oblique treatment positions, in addition to, the size of the patient, doses at the tangential and self shielding areas such as shoulder, axilla, elbow, underbreast and buttock, showed a lower dose from 70% to 78% of the prescribed dose. These results were found to be comparable to those of past studies.[14,16] No overdose was seen for thin areas such as hands, fingers and toes, of the body.

For dose to critical organs, such as lens of the eyes, using external wax shields (about 3 cm thickness), the lens dose were reduced from 84% to approximately 10% The data suggested using the internal eye shielding should be more suitable. Underdosed areas including soles of feet and the perineum were considered by the physician to be subject to local boost fields during the TSET was performed.

## Conclusion

TSET for our first mycosis fungoides patient was successfully commissioned and implemented to the patient. Acceptable dosimetry with the high dose rate electron mode was achieved. At one year follow-up, a satisfactorily clinical result was found for this patient. The technique was experienced as complex, and time consuming to develop; rigorous quality assurance was needed as well.

## References

1. Nisce LZ, Chu CHF, Lee SH , et al. Total skin electron beam therapy for cutaneous lymphomas and leukemias. Int J Radio Oncol Biol Phys 1982;8:1587-92.
2. Ravi A , Nisce LZ, Nori D. Total skin electron beam therapy in the management of cutaneous malignancies. Clinics in Dermatology 2001;19:354-6.
3. Tetenes PJ, Goodwin PN. Comparative study of superficial whole-body radiotherapeutic techniques using a 4 MeV nonangulated beam. Radiology 1977;122:219-26.
4. Williams PC, Hunter RD, Jackson SM. Whole body electron therapy in mycosis fungoides - a successful translation technique achieved by modification of an established linear accelerator. Br J Radiol 1979;52:302-7
5. Podgorsak EB, Podgorsak MB. Special Technique in radiotherapys Part B Total skin electron irradiation. In Van Dyk J: The modern technology of radiation oncology. Medical physics publishing , Madison WI, USA, 1999: 663-78.
6. American Association of Physicist in Medicine. Total Skin Electron Therapy, Technique and Dosimetry. AAPM Report No. 23. American Institutes of Physics Inc & New York, USA, 1988
7. Das IJ, Copeland GF, Bushe HS. Spatial distribution of bremstrahlung in a dual electron beam used in total skin treatment: Errors due to ionization chamber cable irradiation. Med Phys 1994;21(110):1733-8.
8. Chen Z, Agostinelli A, Nath R. On the use of unshield cables in ionization chamber dosimetry for total skin electron therapy. Phys Med Biol 1998;43:539-46.
9. International Atomic Energy Agency. Absorbed dose determination in external beam radiotherapy. Technical reports series No. 398 IAEA & Vienna, Austria, 2000.
10. Jones GW, Trados A, Hodson DI, Rosenthal D, Roberts J,

Thorson B. Prognosis with newly diagnosed mycosis fungoides after total skin electron radiation of 30 Gy or 35 Gy. Int J Radiat Oncol Biol Phys 1994;28:839.

11. American Association of Physicist in Medicine. Total Skin Electron Therapy. Technique and Dosimetry. AAPM Report No. 23. American Institutes of Physics Inc & New York, USA 1988:39.
12. Antolak JA, Cundiff JF, Ha CS. Utilization of thermoluminescent dosimetry in total skin electron beam radiotherapy of mycosis fungoides. Int J Radiat Oncol Biol Phys 1998; 40(1):101-8.
13. American Association of Physicist in Medicine. Total Skin Electron Therapy. Technique and Dosimetry. AAPM Report No. 23. American Institutes of Physics Inc & New York, USA 1988:39.
14. Anacak Y, Arigan C, Bar-Deroma R, Tamir A, Kuten A. Total skin electron irradiation: Evaluation of dose uniformity throughout the skin surface. Medical Dosimetry 2003; 28(1):31-4.
15. El-Khatib E, Hussein S, Nikolic M, Voss NJ, Parsons C. Variation of electron beam uniformity with beam angulation and scatter position for total skin irradiation with the Stanford technique. Int J Radiat Oncol Biol Phys 1995; 33:469-74.
16. Weaver RD, Gerbi BJ, Dusenberg KE. Evaluation of dose variation during total skin electron irradiation using thermoluminescent dosimeters. Int J Radiat Oncol Biol Phys 1995;33:475-8.
17. Desai KR, Pezner RD, Lipsett JA, et al. Total skin electron irradiation for mycosis fungoides: Relationship between acute toxicities and measured dose at different anatomic sites. Int J Radiat Oncol Biol Phys 1988;15:641-5.
18. Chen Z, Agostinelli AG, Wilson L, Nath R. Matching the dosimetry characteristics of a dual-field Stanford technique to a customized single-field Stanford technique for total skin electron therapy. Int J Radiat Oncol Biol Phys 2004;59(3):872-85.
19. Peters VG, Jaywant SM. Implementation of total skin electron therapy using an optional high dose rate mode on a conventional linear accelerator. Medical Dosimetry 1995;20(2):99-104.
20. Parida DK, Verma KK, Chander S, Joshi RC, Rath GK. Total skin electron irradiation therapy in mycosis fungoides using high-dose rate mode: Preliminary experience. International Journal of Dermatology 2005;44:828-30.

THE ASEAN JOURNAL OF RADIOLOGY 2010; 16(1): 62-70

Original Article

# Palliative Treatment of Advanced Lung Cancer with Radiotherapy and Thai Herbal Medicine as Supportive Remedy, Analysis of Survival

**Montien Pesee, MD.[1] Wichit Kirdpon, Ph.D[2], Anucha Puapairoj, MD.[3]**
**Sukachart Kirdpon, MD.[4], Pongsiri Prathnadi, MD.[5]**

[1] *Division of Radiotherapy, Department of Radiology, Srinagarind Hospital, Faculty of Medicine, Khon Kaen University, Khon Kaen 40002, Thailand*

[2] *Division of Nuclear Medicine, Department of Radiology, Srinagarind Hospital, Faculty of Medicine, Khon Kaen University, Khon Kaen 40002, Thailand*

[3] *Department of Pathology, Srinagarind Hospital, Faculty of Medicine, Khon Kaen University, Khon Kaen 40002, Thailand*

[4] *Department of Pediatrics, Faculty of Medicine, Khon Kaen University, Khon Kaen 40002, Thailand*

[5] *Department of Surgery, Faculty of Medicine, Chiang Mai University, Chiang Mai 50000, Thailand*

## Abstract

**Objective:** To evaluate the outcome of Thai herbal medicine, Vilac Plus (G716/45) on standard palliative radiotherapy for advanced non small cell lung cancer, stage IIIB-IV compared with historic control from the literature reports.

**Patients and Methods:** Between March 2003-June 2006, thirteen patients of advanced non small cell lung cancer, stage IIIB -IV with poor performance status were treated by palliative radiotherapy in adjuvant with the Thai herbal tonic solution (Vilac PlusG716/45) as supportive remedy. This study was performed at Radiotherapy Division, Department of Radiology, Faculty of Medicine, KhonKaen University, KhonKaen 40002, Thailand. The results were analysed in the aspect of clinical benefit rate of survived patients more than 15 months, median survival time and overall survival rates. The survival curve was estimated by the Kaplan-Meier method.

**Results:** Thirteen patients (8 male, 5 female) of advanced non small cell lung cancer with poor performance status (Eastern Co-operative Oncology Group 2-3), stage IIIB 11 cases, stage IV 2 cases were treated by palliative radiotherapy in adjuvant with the Thai herbal tonic solution (Vilac Plus G716/45) as supportive remedy. Median age was 66 years (range 44.4 -83 years). The pathological reports were classified to be squamous cell carcinoma (5 cases), adenocarcinoma (2 cases), bronchioalveolar carcinoma (1 case), mixed squamous and adenocarcinoma (1 case). There were 30.77% (4/13 cases) of clinically advanced lung cancer by evidenced of computed tomography chest scan / chest X-ray. The clinical benefit rate of survived patients more than 15 months was 84.62%. The median survival time was 28 months (range14-74 months).The overall 1, 2, 3, 4 and 5 survival year rates were 100%, 53.85%, 30.77%, 23. 08% and 15.38% respectively.

**Conclusion:** This pilot study was limitation in the aspect of a small number of patients, but all cases were in advanced stages of diseases with poor performance status. The results of this study were promising in the aspect of improving overall survival rates and cost effectiveness. The treatment of cancer patients has many interrelated and confounding factors that have to be sorted out so further research will be necessary.

**Key words:** advanced lung cancer, palliative radiotherapy, Thai herbal medicine

## Introduction

In advanced lung cancer, palliative radiotherapy alone or in combination with the appropriated combination of chemotherapeutic agents are the available methods of treatment with not fully satisfactory results.[1-21] The disadvantage side effects are not only poor quality of life but also very expensive chemotherapeutic agents. The other modality may be using oral epidermal growth factor recepter (EGFR) inhibitors which have demonstrated antitumor activity in advanced non small cell lung cancer (NSCLC) without serious side effects.[17] Both of these agents are very expensive, therefore can not be accessible by the low socioeconomic group of patients.

The reports of antioxidants combined with therapeutic modalities reveal enhancing the therapeutic effects of chemotherapy and/or radiotherapy, decrease side effects, protect normal tissues and also increase survival.[22] Most of the studies demonstrate the evidences of synergistic effect of antioxidants and radiotherapy and decrease adverse effect of the therapy.[23]

Based on this rationale, the Thai herbal medicine was used as another choice for supportive to the standard palliative radiotherapy in this study. The Thai herbal medicine (Vilac PlusG716/45) was proven to have no acute oral toxicity in animal study.[24] No traces of prednisolone and dexametasone were detected.[25] An In Vitro study, the Vilac Plus (G716/45) presented an important antioxidant capacity.[26] The recipe of the ingredients of the Thai herbal tonic solution consisting of three edible herbs, the whole part of mushroom namely *Ganoderma Lucidum*, *Houttuynia Cordata Thunb* (leaves) and the roots of *Boesenbergia Pandurata Holtt* (Kra chai), all of them have found to be an effective anti-tumor promoting agents.[27,28]

We therefore conducted a follow-up study to determine whether the survival rates of palliative treatment in advanced NSCLC by using palliative radiotherapy and the Thai herbal medicine as supportive remedy.[29,30]

## Objective

To evaluate the outcome of Thai herbal medicine, Vilac Plus (G716/45) on standard palliative radiotherapy for advanced NSCLC, stage IIIB-IV compared with historic control from the literature reports.

## Patients and methods

This study was performed at radiotherapy division, department of radiology, Faculty of Medicine, Khon Kaen University, Khon Kaen 40002, Thailand. Between March 2003 to June 2005, thirteen patients of advanced NSCLC stage IIIB-IV according to TNM staging[31] with poor performance status were treated by palliative radiotherapy (tumor doses range 20-60Gy/2-6 weeks) in adjuvant with the Thai herbal tonic solution (Vilac Plus G716/45) daily dose 15-30 cc. orally three time after meal as a supportive remedy.[30] Staging procedures were performed by chest oncologist/expert opinions using history, physical examination, routine laboratory evaluations, chest X-ray, bronchoscopic examination included cytology/ biopsy, chest computed tomography scan and bone scan. Inclusion criteria were: (1) advanced stage lung cancer; (2) superior vena cava obstruction; (3) metastatic lung cancer; (4) poor performance status; (5) minimal response of the tumor to standard radiotherapy 30-40 Gy/3-4 weeks; (6) the informed consent has been signed by the patients. Exclusion criteria was the patients to be refuse on this treatment modality.

The results were analyzed in the aspect of clinical benefit rate of survived patients more than 15 months, median survival time and overall 1, 2, 3, 4, and 5 year survival rates. The survival curve was estimated by the Kaplan-Meier method. The procedure of this project has been approved by the Committee of Khon Kaen University Human Ethics (HE 480745).

## Radiotherapy Technique[30]

### Results

Thirteen patients (8 male, 5 female) of advanced NSCLC, stage IIIB 11 cases,stage IV 2 cases with poor performance status (ECOG2-3) were treated by palliative radiotherapy in adjuvant with the Thai herbal tonic solution (Vilac Plus G716/45). The median age was 66 years (range 44.4 -83 years). The pathological reports were classified to be squamous cell carcinoma (5 cases), adenocarcinoma (2 cases), bronchioalveolar carcinoma (1 case), mixed squamous and adenocarcinoma (1 case). There were 30.77% (4/13 cases) of clinically advanced lung cancer by evidenced of computed tomography chest scan /chest X-ray according to poor performance of the patients. (Table 1).

The clinical benefit rate of the survived patients more than 15 months was 84.62%. The survival analysis (Kaplan-Meier survival estimate) revealed median survival time of 28 months (range 14-74 months). It was noted that improving survival

Table 1 Patient characteristics[30]

| Patient characteristics | Cases (%) |
|---|---|
| **Gender** | |
| Female | 5 (38.46%) |
| Male8 (61.54%) | |
| **Age in years** | |
| Median (range) | 66 (44.4-83) |
| **Stage of disease** | |
| Stage III B | 11 (84.62%) |
| Stage IV, 1 case, T4N3M1 (bone metastasis), | 2 (15.38%) |
| 1 case, T3N3M1 (contralateral lung metastasis) | |
| Median survival time (range) in months | 28 (14-74) |
| **Pathology** | |
| SCC | 5 (38.46%) |
| Adenocarcinoma | 2 (15.38%) |
| Mixed Adeno CA. + SCC. | 1 (7.69%) |
| Bronchoalveolar CA | 1 (7.69%) |
| Clinically advanced lung cancer stage IIIB | 4 (30.77%) |
| - superior vena cava obstruction (1 case) | |
| - patients refused to perform biopsy (2 cases) | |
| - bronchoscopy revealed brochogenic mass obstruction but biopsy showed negative of malignancy (1 case). | |

time of 59 months in 1 case of metastatic squamous cell carcinoma with superior vena cava syndrome was detected while a case of NSCLC stage III B, poor performance status (ECOG2-3), adenocarcinoma poorly differentiated are still alive of 74 months after diagnosis.

The overall 1, 2, 3, 4, and 5 year survival rates were 100%, 53.85%, 30.77%, 23.08% and 15.38% respectively (Table 2 and Fig 1). There were 2/13 cases of stage IIIB NSCLC survived more than 5 years (1 case of stage IIIB, T3 N2-3 M0, ECOG2-3, adenocarcinoma poorly differentiated while 1 case of clinically stage IIIB lung cancer by expert opinions).

**Table 2** The overall 1, 2, 3, 4 and 5 year survival rates (Kaplan-Meier survival estimate)

| Follow up time (year) | Overall survival rates (%) | 95% Cont. Int. |
|---|---|---|
| 1 | 100 | 0.2-0.8 |
| 2 | 53.85 | 0.2-0.4 |
| 3 | 30.77 | 0.1-0.6 |
| 4 | 23.08 | 0.1-0.5 |
| 5 | 15.38 | 0.02-0.4 |

## Discussion

Advanced NSCLC patients with poor performance status should generally not be recommended chemotherapy because these patients tend to experience increase toxicity, decrease survival without clinical benefit.[1] The treatment with chemotherapy reveals median survival times approximately 4.2-15 months.[1-21] The most common site of relapes is in the brain. The median survival times of superior vena cava (SVC) syndrome is approximately 1.2 months -15 months.[19] Treatments of advanced NSCLC by using 3D conformal radiotherapy reveale median survival time of 15.8 months, 1, 2, 3, 4 and 5 year survival rates are 61%, 35%, 23%, 19% and

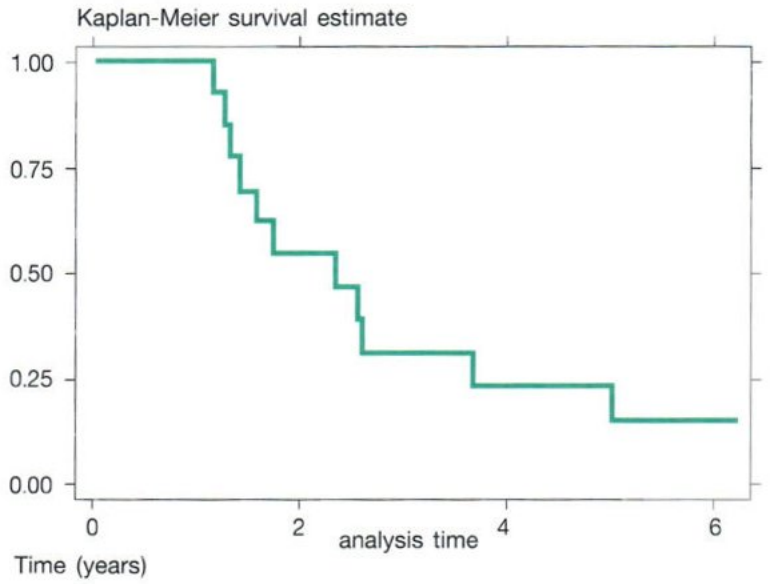


**Fig.1** The overall survival curve of advanced NSCLC treated with palliative radiotherapy and Thai herbal medicine as supportive remedy.

17% respectively.[18] The median survival times of palliative radiotherapy for NSCLC are approximately 7-9 months.The 1,2 year survival rates are 9-28%, 6-18% respectively.[1-21] There are evidences of radiation esophagitis and radiation myelitis of 17Gy in 2 fractions and 39 Gy in 13 fractions.[1] There is no significant survival difference between brachytherpy combined with external irradiation versus external radiation alone.[1]

The enhancing effect of Thai herbal medicine (Vilac Plus G716/45) on radiotherapy to prolong the survival of these patients was very impressive. Our study revealed 84.62% of the clinical benefit rate of the survived patients more than 15 months. The median survival time was 28 months (range 14-74 months) compared with 7 months (range 10-15 months) from historic control.[1-21] The overall 1, 2, 3, 4 and 5 year survival rates were 100%, 53.85%, 30.77%, 23.08%, and 15.38% respectively compared with 1, 2, and 3 year survival rates of 9-40%, 4.1-18% and 3.3% respectively from historic control.[1-21] It was noted that improving survival time of 59 months in 1 case of metastatic squamous cell carcinoma with superior vena cava syndrome was detected while a case of stage III B, adenocarcinoma poorly differentiated, ECOG2-3 are still alive of 74 months after diagnosis. The clinical outcomes were shown higher survival rates than historic control suggested to be synergistic results of Thai herbal medicine (Vilac Plus G716/45) on radiotherapy.

The enhancing effect of Vilac Plus® on radiotherapy to prolong the survival of these patients can be explained under the principle of antioxidants by anti-tumor effect and normal tissue protection. The Vilac Plus® tonic revealed antioxidant potency[26] which being concurrently bioavailable in the subcellular level. The hypothesis of radical-scavenging activity of the tonic against excess free radicals of the radiotherapy may be explained by specific protection on DNA damage of normal cells. This is the key and crucial evidence for scientific explanation upon the mechanism and pharmacological action of our clinical studies, therefore further research deep in detail will be needed.

The ingredients of the Vilac Plus® tonic consisting of anti-tumor mushroom, LingZhi *(Ganoderma lucidum), Houttuynia cordata, Thunb* and *Boesenbergia pandurata Holtt* (Krachai) were demonstrated. The tonic preparation accomplished by fermentation by using *Lactobacillus casei spp.* (Genebank Reg. No. AF 320255) and *Lactobacillus plantarum spp.* (Genebank Reg. No. AF 320256). The promising supportive adjuvants actions contributed from each composition of the 4 ingredients in Vilac Plus® including the microorganism used in the fermentation proceedings that should be recognized as the "probiotics" which is one key component in the biotechnology procedure of production. The herbal ingredients are world recognition mushroom, Ling Zhi (*Ganoderma lucidum*) or Reishi, where it has been mentioned as sacred mushroom which has been found the 119 different terpinoids, about 80 of which biologically active.[32-33] The role to be the supportive action in cancer treatment is immunomodulation anticancer by protection DNA damage of normal cell through its powerful antioxidant mechanism and inhibition of tumor necrosis factor (TNF). There are a number of reports that have mentioned the benefit on various cancers.[34,35]

The other herbs are the edible plants, *Houttuynia cordata Thunb*[37-38] and the root of *Boesenbergia Pandurata Holtt* (Krachai).[35] The role to contribute as supportive remedy of phytosterols in addition to their characteristic is one of the essen-

tial antiproliferative of cancer cells such as flavonoids and volatile oil which the strongest one that present this action is linolool.[36] The co-operative actions of these herbs are reported to be the "interferon-inducing herb" that may contribute some important role to play on antitumor-antiviral activity through the "interferon" molecule.[37-38]

The probiotics/ antioxidants action on role of cancer therapy could be summarized as follows.

1. The antioxidants combined with therapeutic modalities reveal enhancing the therapeutic effects of chemotherapy and/or radiotherapy, decrease side effects, protect normal tissues and also increase survival.[22-23]

2. The antioxidants mechanism by inhibiting the activation of mitogen activated protein kinase pathway, cell proliferation and phosphorylation of p53 have been reported.[39]

3. Antitumor and antimetastatic effects by induction or stimulation the synthesis of several cytokines have been known to be the immunomodulating factor. The small molecular weight cytokines such as IFN-gamma, IL-1 beta and TNF alpha being one of the enhancement transfer factor to work effectively has been reported.[41]

4. Immunomodulation enhancement through probiotics that resulting in the delayed or inhibit the process of distance metastases in various cell type of cancers and delayed process of cancer recurrences have been reported.[40,42]

5. The clinical reports of probiotics in adjuvant with radiotherapy demonstrate an enhancing tumor regression, prolonged survival and relapse-free survival compared with radiotherapy alone.[42]

The clinical trails of Vilac Plus® in the study as an supportive adjuvant to radiation therapy on lung cancers shown this potentiative and synergistic effect due to powerful antioxidant and probiotics properties with improving survival times and survival rates were noted.The cost effectiveness is another considerable issue compared with chemotherapeutic agents and oral epidermal growth factor recepter (EGFR) inhibitors of lung cancer treatments.

Potential advantages of integrating complementary therapies into cancer care, future areas of research will be included improving access for patients, improving symptom control for patients, improving patient well-being, enhancing patient satisfaction, and cost effectiveness.[43]

## Conclusion

This pilot study was limitation in the aspect of a small number of patients, but all cases were in advanced stages of NSCLC with poor performance status.The results of this study was promising in the aspect of improving survival rates and cost effectiveness. The treatment of cancer patients has many interrelated and confounding factors that have to be sorted out so further research will be necessary. This modality is being investigated as part of the cost effectiveness complementary therapies in advanced NSCLC care for developing countries.

The value could be expressed as follows:

1. Improving the 1, 2, and 3 year survival rates of 100%, 53.85%, and 30.77% respectively compared with 1, 2, and 3 year survival rates of 9-40%, 4.1-18% and 3.3% respectively from historic control.[1-21]

2. Improving the median survival time of 28 months (range 14-74 months) compared with 7 months (range 10-15 months) from historic control.[1-21]

3. Improving the clinical benefit rate of 84.62%

for survived patients more than 15 months was detected.

## Acknowledgements

We would like to express our deep appreciation to Associate Professor Nittaya Chamadol, Head, Department of Radiology, Associated Professor Vorachai Tungvorapongchai, Mr. Khajornkiat Srichachet of assisting on manuscript editing, Department of Radiology, Mr. Supot Kamsa-ard, Cancer unit and our colleagues, Associate Professor Apinun Aramrat, Professor Maitree Suthajit Assistant Professor Dusadee Musikapodoke. Appreciations acknowledgement for kind contribution from Lanna Probiotic Company Limited, Thailand, particulary Mr. Suriya Vichitchot who provided the herbal tonic products for clinical trial.

## References

1. Bonfill X. Lung cancer. In: Text book of evidence-based oncology. Williams C, ed. London: BMJ publishing Books 2003;203-23.
2. Whelen S, Smith TJ. Lung cancer. In: Handbook of advanced cancer care. Fisch M, Bruera E, eds. UK: Cambridge university press 2003;137-49.
3. Srisam-ang K,Podhipak A, Narksawat K, et al. Survival of patients with advanced non-small-cell lung cancer at Ubon ratchathani cancer center,Thailand.Southeast Asean J Trop Med Public Health.2005;36(4):994-1006.
4. M. Lyikesici, P. Yumuk, F. Dane, et al. Outcome of patients with stage III and IV non-small cell lung cancer in Marmara university Hospital, Istanbul, Turkey. Lung Cancer official Scientific Publication of the international association for the study of lung cancer. Abstracts of the 11th World Conference on Lung Cancer 3-6 July 2005. Barcelona, Spain 2005;49(2):5249.
5. R Huber, M. Schmidt, A Borgmeier, et al. Weekly docetaxel and vinorelbine as second-line therapy in advanced non-small cell lung cancer. Lung Cancer official Scientific Publication of the international association for the study of lung cancer. Abstracts of the 11th World Conference on Lung Cancer 3-6 July 2005. Barcelona, Spain 2005; 49(2):S248.
6. S. Hasturk, N. hatabay, F Ece, et al. Gemcitabine, vinorelbine and cisplatin combination chemotherapy in advanced non-small cell lung cancer. Lung Cancer official Scientific Publication of the international association for the study of lung cancer, Abstracts of the 11th World Conference on Lung Cancer 3-6 July 2005. Barcelona, Spain 2005; 49(2):S247.
7. M. Zimmermann, F. Luthi, A. Zouhair, et al. Gefitinib (Iressa) as first- line therapy in advanced non-small lung cancer. Lung cancer official scientific publication of the international association for the study of lung cancer Abstracts of the 11th World Conference on Lung Cancer 3-6 July 2005. Barcelona, Spain 2005;49(2):S276.
8. Wake B, Taylor R, Sandercock J. Hyperfractionated/accelerated radiotherapy regimens for the treatment of non-small cell lung cancer. A systematic review of clinical and cost-effectiveness. West Midlands Health Technology Assessment Collaboration (WMHTAC); 2002 (DPHE Report No.35): 65. Search date 2001; primary sources Medline, Embase, it, Cochrane Library, reference lists, contact with experts in the field and Internet searches.
9. Hansen O, Paarup H, Sorensen P, et al. Curative radiotherapy of local advanced non-small-cell lung cancer. Eight years of experience from Odense. Ugeskr Laeger 2005 Sep 12;167(37):3497-502.
10. Non-Small Cell Lung Cancer Collaborative Group. Chemotherapy for non-small cell lung cancer. In: The Cochrane Library, Issue 3, 2004. Chichester, UK: John Wiley & Sons, Ltd. Search date 1991; Primary sources Medline; Cancerlit; hand searches of meetings abstracts, bibliographies of books, and specialist journals; consultation of trials registers of National Cancer Institute; UK Coordinating Committee for Cancer Research; the Union Internationale Contre le Cancer; and discussion with trialists.
11. Saunders M, Dische S, Barrett A, et al. Continuous, hyperfractionated, accelerated radiotherapy (CHART) versus conventional radiotherapy in non-small cell lung cancer: mature data from the randomised multicentre trial. CHART Steering committee. Radiother Oncol 1999; 52:137-48.
12. Sause W, Kolesar P, Taylor S, et al. Final results of phase III trial in regionally advanced unresectable non-small cell lung cancer: Radiation Therapy Oncology Group, Eastern

Cooperative Oncology Group, and Southwest Oncology Group. Chest 2000;117:358-64.

13. Jeremic B, Shibamoto Y, Acimov L, et al. Randomized trial of hyperfractionated radiation therapy with or without concurrent chemotherapy for stage III non-small cell lung cancer. J Clin Oncol 1995;13:452-8.
14 Ball D, Bishop J, Smith J, et al. A randomised phase III study of accelerated or standard fraction radiotherapy with or without concurrent carboplatin in inoperable non-small cell lung cancer : final report of an Australian multicentre trial. Radiother Oncol 1999;52:129-36.
15. Kawahara M, Kubota K, Furuse K. [Radiotherapy and chemotherapy for locally advanced non-small-cell lung cancer: report of a clinical trial and review of the literature. South Osaka Lung Cancer Chemotherapy Study Group]. Nihon Kyobu Shikkan Gakkai Zasshi 1993;31 Suppl:212-7.
16. Mirimanoff RO. Concurrent chemotherapy (CT) and radiotherapy (RT) in locally advanced non-small cell lung cancer (NSCLC): a review. Lung Cancer 1994; 11 Suppl 3:S79-99.
17. Silvestri GA, Rivera MP. Targeted therapy for the treatment of advanced non-small cell lung cancer: a review of the epidermal growth factor receptor antagonists. Chest 2005;128:3975-84.
18. Zwitter M. Comments on treatment strategy for locally advanced non-small cell lung cancer. Lung Cancer 2002; 38 Suppl 3:S33-5.
19. Chen JC, Bongard F, Klein SR. A contemporary perspective on superior vena cava syndrome. Am J Surg 1990; 160:207-11.
20. Emami B, Munzenrider JE, Lee DJ, Rene JB. Radical radiation therapy of advanced lung cancer: evaluation of prognostic factors and results of continuous and split course treatment. Cancer 1979;44:446-56.
21. Maddox AM, Valdivieso M, Lukeman J, Smith TL, Barkley HE, Samuels ML, et al. Superior vena cava obstruction in small cell bronchogenic carcinoma. Clinical parameters and survival. Cancer 1983;52:2165-72.
22. Simone CB 2nd, Simone NL, Simone V, Simone CB. Antioxidants and other nutrients do not interfere with chemotherapy or radiation therapy and can increase kill and increase survival, part 1.Altern Ther Health Med 2007; 13(1):22-8.
23. Moss RW. Do antioxidants interfere with radiation therapy for cancer. Integr Cancer Ther 2007;6(3):281-92.
24. Suntorntanasat T, Banchonglikitkul C, Klungsupaya P, et al. Acute oral toxicity test Herbal tonic solution (G716/45) Thailand Institute of Scientific and Technological Research. (Written personal communications) September 2003;1-8.
25. Amadi Pirasahid P, Suntorntanasat T. Analytical report on Herbal tonic solution (G716/45) Thailand Institute of Scientific and Technological Research. (Written personal communications) July 2004;1-3.
26. Durand Phillippe,Prost Michel. In Vitro study of Vilac Plus analysis. Kirial International laboratories Spiral, (Written personal communications) 3 rue des Mardors 21560 COUTERNON, France (Written personal communications). July 2006;1-4.
27. Lee S-S, Wei Y-H, Chen C-F, et al. Anti-tumor effects of polysaccharides of Ganoderma lucidum. Proc Int Symposium Ganoderma Sci, Auckland, 27-29 April, 2001; 1-6
28. Murakami A, Jiwajinda S, Koshimizu k, et al. Screening for in vitro anti-tumor promoting activities of edible plant from Thailand.Cancer Letters 1995;95:139-14.
29. Pesee M, Prathnadi P,Kirdporn S, et al. Palliative treatment of late stages of cancer with radiotherapy and Thai herbal medicine as supportive remedy (primary report of 4 cases). The asean journal of radiology ,Bangkok, Thailand 2003;9(3):195-208.
30. Pesee M, Prathnadi P,Kirdporn S, et al. Palliative treatment of advanced lung cancer with radiotherapy and Thai herbal medicine as supportive remedy. The asean journal of radiology, Bangkok, Thailand 2006;12(3): 149-76.
31. Greene FL, Compton CC, Fritz AG, et al, eds. AJCC Cancer staging Atlas. Springer, New York 2006, 167-76.
32. Kim HW,Kim BK. Biomedicinal triterpenoids of Ganoderma lucidum (Aphyllophoromycetideae). Int J of Med Mushroom 1999;1:121-38.
33. Van der Hem LG, Ling Zhi-8. Studies of a new immuno modulating agent. Trasplantation 1995;60:438-43.
34. Wang SY. Anti-tumor effect of Ganoderma Lucidum is mediated by cytokines released from activated macrophages and T-lymphocytes. Int J Cancer 1997;70: 699-705.

35. Murakami A, Kondo A, Nakamura Y, et al. Possible anti-tumor Promoting and identification of Active Constituent Cardomoin of Boesenbergia Pandurata. Biosci Biotech Biochem 1993;57(11):1971-3.

36. Cherng JM, Shieh DE, Chiang W, et al. Chemopreventive effects of minor dietary constitutents in common foods on human cancer cells. Bioscience, Biotechnology and Biochemistry 2007;71(6):1500-4.

37. Morita N, Hayashi K, Fujita A, et al. Extraction of antiviral substances from Houttuynia cordata Thunb. Chemical abstract 1995;123:93249j.

38. Hayashi K, Kamiya M, Hayashi T. Virucidal effects of the steam distillate from Houttuynia cordata and its components on HSV-1, influenza virus and HIV. Plant Med 1995; 61(3):237-41.

39. Kim Y, Chongviriyaphan N, Liu C, Russell RM, Wang XD. Combined antioxidant (beta-carotene, alpha-tocopherol and ascorbic acid) supplementation increases the levels of lung retinoic acid and inhibits the activation of mitogen-activated protein kinase in the ferret lung cancer model. Carcinogenesis 2006;27:1410-9.

40. Matsuzaki T. Immunomodulation by trestment with Lactobacillus casei strain shirota. Int J Food Microbiol 1998;41(2):133-40.

41. Salminen S, Isolauri E, Salminen E. Probiotics and stabilization of the gut mucosal barrier. Asia Pacific J Clin Nutr 1996;5(1):53-6.

42. Okawa T, Niibe H, Arai T, et al. Effect of LC 9018 combined with radiation therapy on carcinoma of the uterine cervix. A phase III, multicenter, randomized, controlled study. Cancer 1993;72(6):1949-54.

43. Barnett M. Overview of complementary therapies in cancer care. IN: Textbook of Integrated Cancer Care. Holistic, complementary, and Creative approaches. Barraclough J, ed. NewYork: Oxford University Press 2001;1-17.

THE ASEAN JOURNAL OF RADIOLOGY 2010; 16(1): 79-84 71

Original Article

# Hepatobiliary Abnormalities in Pediatric and Adolescent Hemoglobin Ebeta-thalassemia Detected by Ultrasonography

**Eimorn Mairiang, MD.[1], Charoon Jetsrisuparb, MD.[2], Arunee Jetsrisuparb, MD.[2]**
**Sumitr Sutra, MD.[2], Anothai Trevanich, MD.[3]**

*[1] Department of Radiology Faculty of Medicine.*
*[2] Department of Pediatrics Faculty of Medicine*
*[3] Department of Statistics, Faculty of Sciences*
*Khon Kaen University, Khon Kaen 40002, Thailand*

## Abstract

**Background/Aims;**

1. To detect hepatobiliary abnormalities in hemoglobin Ebeta-thalassemia pediatric and adolescent patients by ultrasonography
2. To identify correlation between ultrasonographic findings, serum ferritin and liver function test

**Material and method:** Abdominal ultrasonography serum ferritin and liver function test were performed in 64 DNA analysis proven hemoglobin Ebeta-thalassemia pediatric and adolescent patients, age ranging between 5-18 years (mean 14.1 years). Ultrasonographic parameters include: gallbladder length, width, cross section, gallstone, height of left lobe of the liver, diameter of the aorta, liver parenchymal echoes, cranio-caudal length of spleen, and splenic echoes. Liver function test includes; cholesterol, total protein, albumin, globulin, total bilirubin, direct bilirubin, alanine aminotransferase (ALT), aspartate aminotransferase (AST) and alkaline phosphatase (AP).

**Result:** Statistical analysis, using factor analysis and discriminant analysis, showed negative correlation between serum ferritin and age of the patients. Gallbladder sludge and stone correlated with splenic length and cross section of the gallbladder. Splenic parenchyma abnormality correlated with height of left lobe of the liver/aorta diameter, total protein albumin and AP and length of spleen/aorta.

**Conclusion:** Gallbladder hypomotility may contribute to stone formation. Total protein albumin and AP showed correlation with hepatobiliary abnormalities detected by ultrasonography. Negative correlation of serum ferritin and patient's age may be due to increased iron absorption from gastrointestinal tract in younger age.

**Keywords:** hemoglobin Ebeta-thalassemia, hepatobiliary abnormalities, liver function test, ultrasonography, gallstone

## Introduction

Thalassemia is a class of genetic disease of abnormal globin chain synthesis and remain a significant health problem in several regions of the world. The incidence is highest in Southeast Asia, the Middle east and Africa. Clinical manifestations result from the decrease or absent production of normal globin chain of hemoglobin.[1] Thalassemia is classified according to deficient globin chain. Main subtypes are alpha and beta thalassemia. Hemoglobin Ebeta-thalassemia is an important cause of childhood chronic disease in Southeast Asia. The patients are generally classified as having thalassemia intermedia because they have inherited a beta-thalassemia allele and hemoglobin E, which acts as a mild beta$^{+}$-thalassemia. However, a remarkable variability in the clinical expression, ranging from a mild form of thalassemia intermedia to transfusion-dependent conditions, is observed.[2] Iron overload occurs without exception in hemoglobin Ebeta-tha-lassemia.[3-5] Excessive iron accumulates because of blood transfusion and enhanced gastrointestinal absorption. Liver fibrosis from iron overload is common whereas ascites and other signs of cirrhosis are rare.[6-7]

Gallstone is also known to have high incidence in hemolytic disease.[8] Liver biopsy is an invasive and high risk procedure for children. Ultrasonography has made the study of liver and biliary tract easier and is wildly available in all hospitals. Ultrasonography may be used to identify hepatobiliary abnormalities that might reduce liver biopsy and reduce cost of unnecessary liver function test in routine follow up of the patients.

## Method

### Patients

This study is a part of prospective study of illness in hemoglobin Ebeta-thalassemia patients. Sixty-four hemoglobin Ebeta-thalassemic pediatric and adolescent patients diagnosed by DNA analysis, age ranging between 5-18 years (mean 14.1 years), were enrolled in the study. They had received regular leukocyte-poor packed red cell transfusion 10 ml/Kg every time at 3-4 weeks interval. Their pre-transfusion hemoglobin was < 9 g/dL. This allows thalassemia patients to have normal growth and suppress over-erythropoiesis.[9] Desferrioxamine (Desferal$^{R}$) was given by their parents at home (20-40 mg/Kg/d using subcutaneous infusion in 8-10 hr, 2-7 times/wk, depending on the level of serum ferritin). Informed sign consent was obtained from the parents of each subject before ultrasonography. The study was approved by the Ethics Committee of Khon Kaen University (HE451032). The study was performed during March 2003 to June 2004.

### Ultrasonography

Abdominal ultrasonography was performed after at least 4 hours fasting. We used a full size high resolution machine, Acuson model Aspen, with a 4 MHz convex array probe. The maximum height of left lobe of the liver above the abdominal aorta was determined. The diameter of aorta below left lobe of the liver was recorded in order to use as an internal reference for other parameters. The maximum gall bladder length width and cross section were measured after locating the largest images in all planes of view. Cranio-caudal length of spleen,

parenchymal echoes of liver and spleen were also recorded. During the investigation, the radiologist was unaware of the serum ferritin or liver function test results of the subjects. The sonographic criteria to use in diagnosis of hepatobiliary status are listed in table 1.

### Biochemical study

Serum ferriitin and liver function test were performed in each subject the same day as ultrasonography. The liver function test includes cholesterol, total protein, albumin, globulin, total bilirubin, direct bilirubin, ALT, AST, AP. The mean values are listed in table 2.

### Statistical Analysis

Factor analysis and discriminant analysis were performed. The number of factors was determined on the basis of eigen values (ie, >1.0)

## Result

### Patient characteristics

There were 3 cases of gallbladder sludge (4.69%), 5 cases of gallstones (7.82%) and 24 previous splenectomy patients (37.50%).

Factor analysis showed negative correlation between serum ferritin and age of the patients. Discriminant analysis showed standardized Canonical-function Coefficients as:

Gallbladder abnormality = .712 cross section of gall bladder ± .675 splenic length

Splenic parenchyma abnormality = -.449 left lobe of the liver/aorta - 1.023 total protein + 1.157 albumin -0.94 AP +1.129 splenic length/ aorta ($p<0.01$)

**Table 2** Mean values of hemoglobin, serum ferritin and liver function test

| | Mean value | normal value |
|---|---|---|
| Hemoglobin | 7.31 | 12 g/dL |
| Ferritin | 2063.64 | 12-122 ng/ml |
| Cholesterol | 98.11 | 127-262 mg/dL |
| Total protein | 7.62 | 6.5-8.8 g/dL |
| Albumin | 4.14 | 3.8-5.4 g/dL |
| Globulin | 3.56 | 2.6-3.4 g/dL |
| Total bilirubin | 1.67 | 0.25-1.50 mg/dL |
| Direct bilirubin | 0.34 | 0-0.5 mg/dL |
| ALT | 47.96 | 4-36 U/L |
| AST | 53 | 12-32 U/L |
| AP | 142.93 | 42-121 U/L |
| Volume of transfusion | 90.69 ml/Kg/yr | |

**Table 1** Diagnostic criteria for ultrasonography

| | |
|---|---|
| Gall bladder abnormality | normal (0) minimal sludge* (1) obvious sludge (2) gall stone (3) |
| Liver parenchyma | normal (0) slightly increased as compared to kidney (1) markedly increased as compared to kidney (2) |
| Splenic parenchyma abnormality | normal (0) slightly increased as compared to kidney (1) markedly increased as compared to kidney (2) previous splenectomy (3) |

Scores were given for statistical analysis

* Sludge is defined as low intensity gravity dependent echoes within the gallbladder with a fluid-fluid level

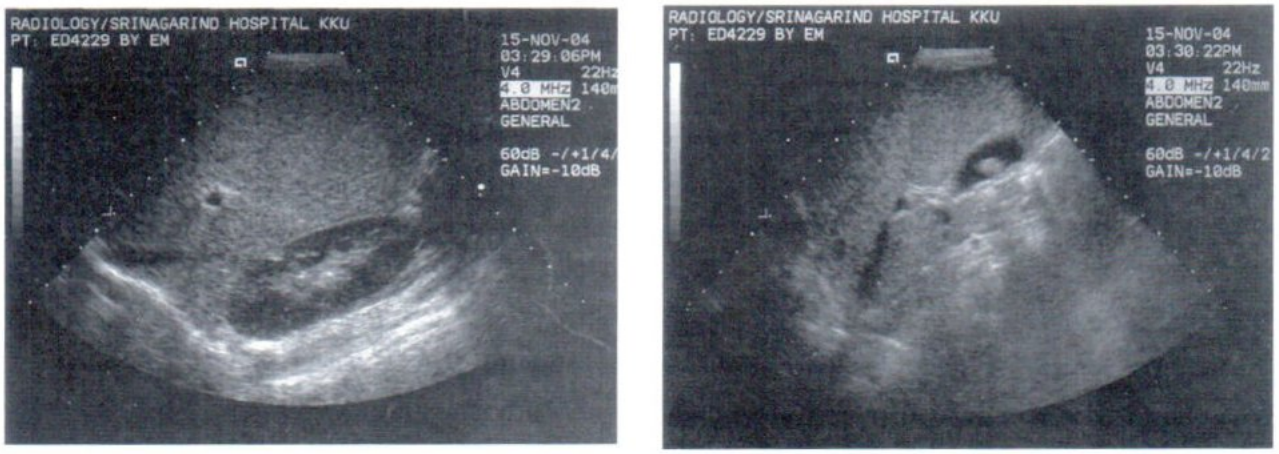


A B

**Fig.1** Ultrasonography (US) of a typical case of thalassemia. A) US shows diffusely and homogeneously increased liver parenchyma. B) US shows a gallstone.

Where: Cumulative percentage = 69.3
Canonical Correlation = .498
Wilks lambda = .719

## Discussion

In children and young adult with thalassemia major, liver disease remains a common cause of morbidity and mortality. The major factor in the generation of liver damage is iron overload. The iron loading in thalassemia depends on both volume of blood transfused and the amount accumulated from gastrointestinal absorption.[10] In beta-thalassemia intermedia, some patients do not require frequent transfusion but progressive iron overload occurs due to increased intestinal absorption.[11] Our patients who had serum ferritin more than 1,000 ng/ml had received iron chelator still had high serum ferritin level.

In this study we present complication of hemoglobin Ebeta-thalassemia in Northeast Thailand. We identified the correlation between ultrasonographic findings, serum ferritin, and liver function test. It is well recognized that level of serum ferritin is poorly correlated with hepatic iron content.[12] Ferritin is an iron storage protein complex found principally in the intestinal mucosa, spleen and liver that functions as the primary form of the iron storage in the body. In assessment of iron overload it can be misleading. There are many inflammatory conditions that can elevate the serum ferritin including viral hepatitis, fatty liver and arthritis.[13] This study showed that serum ferritin did not correlate with liver or splenic parenchyma abnormality detected by ultrasonography. Serum ferritin showed negative correlation with patient's age. This could be explained that in younger age the iron absorption is faster than adult. Animal model showed increased iron absorption in younger animal com-pared to the older group.[14]

Gallbladder abnormality, sludge and stones

correlated with cross section of the gallbladder and splenic length. There are 3 factors that may involve in gallstone formation: cholesterol supersaturation, accelerated nucleation, and gallbladder hypomotility.[15-16] Our patients did not have significant high cholesterol or bilirubin level. Statistical analysis did not show correlation between gallbladder abnormality and serum cholesterol or bilirubin either. Hypomotility or stasis of the gall bladder may play an important role in Ebeta-thalassemia patients. As indicated by correlation with cross section of the gallbladder, bile flow in static gallbladder stagnates and renders biliary sludge formation. Bililary sludge can be an antecedent to gallstones. The abnormal erythrocytes of thalassemia in the circulation are taken up by liver and spleen with ensuing enormous hepatosplenomegaly. Hepatosplenomegaly may cause stasis of the blood circulation (congestion) of the gallbladder resulting in hypomotility. Our study also showed correlation of splenic length with gallbladder abnormality. Splenic parenchyma abnormality correlates with liver size, total protein, albumin and AP. As mentioned previously, both liver and spleen take up abnormal erythrocystes, thus splenic parenchyma abnormality relates with liver size. protein albumin and AP are the component of liver function test that could be used as indicators for severity of the disease. With progressive parenchymal liver disease, albumin synthetic capacity decreases. Although, serum albumin concentration reflects a variety of extrahepatic factors, including nutritional and volume status, vascular integrity, catabolism, hormonal factors and loss in the urine and stool.[17] The patients in this study did not have other diseases. The correlation of total protein and albumin with splenic parenchyma abnormality should be due to corresponding chronic liver impairment.

AP comprises a group of enzymes present in a variety of tissues, including liver, bone, intestine, kidney, placenta, leukocytes and various neoplasms. AP production tends to increase in tissue undergoing metabolic stimulation. Bone and liver are the major sources of serum AP. Thalassemia affects both bone and liver of the patients. Increased AP in thalassemia patients should reflect both bone and liver impairment.

## Conclusion

Serum ferritin did not correlate with liver or splenic parenchyma abnormality. It showed negative correlation with age of the patient, which could be due to increased iron absorption in younger age.

Gallbladder hypomotility might contribute to the formation of sludge and gallstone in Ebeta-thalassemia patients. Gall bladder sludge, gall stone, size of liver, size of spleen total protein albumin and AP can be used as indicators for severity of the disease. Blood chemistry components other than total protein albumin and AP of the liver function test may be skipped from the routine follow up of the patients.

## References

1. Weatherall DJ. Pathophysiology of thalassemia. Bailliers Clin Haematol 1998;11:127-46.
2. Fucharoen S, Winichagoon P. Thalassemia in Southeast Asia: Problem and strategy for prevention and control. Southeast Asian J Trop Med Public Health 1992;23: 647-55.
3. Brittenham G, Pootrakul P, Finch CA, et al. Iron overload in HbE β-thalassemia: magnetic measurement of hepatic iron store (abstract). Blood 1986;68:72.
4. Pootrakul P, Huebers HA, Finch CA, Pippard MJ, Cazzola M: Iron metabolism in thalassemia. Birth Defects 1988;23: 3-8.

5. Pootrakul P, Kitcharoen K, Yamsukon P, et al. The effect of erythroid hyperplasia on iron balance. Blood 1988; 71:1124-9.
6. Thakerngpol K, Sonakul D, Fucharoen S, Vathanapas V, Stinimankan T: Histochemical study of liver tissue from thalassemic patients. Birth defects 1988;23:199-206.
7. Thakerngpol K, Sonokul D, Fucharoen S, et al. Electron microscopic study of liver tissue from 30 thalassemic patients. Birth defects 1988;23:199-206.
8. Dewey KW, Grossman H, Canale VC. Cholelithiasis in thalassemia major. Radiology 1970;96:385.
9. Cazzola M, Borgna-Pignatti C, Locatelli F, Ponchio L, Beguin Y, De Stefano P. A moderate transfusion regimen may reduce iron loading in beta-thalassemia major without producing excessive expansion of erythropoiesis. Transfusion 1997;37(2):135-40.
10. Weatherall DJ, Clegg JB. The thalassemia syndrome. 4th edition, London: Blackwell Science Ltd. 2001. P.311.
11. Cossu P, Toccafondi C, Vardue F, et al. Iron overload and desterrioxamine chelation beta-thalassemia intermedia. Eur J Pediatr 1981;137:267-71.
12. Cunningham MJ, Macklin EA, Neufeld EJ, Cohen AR. Complication of beta-thalassemia major in North America. Blood 2004;104:34-9.
13. Wong K, Adams PC. The diversity of liver diseases associated with and elevated serum ferritin. Can J Gastro 2007;20:467-70.
14. Gardenghi S, Marongiu M, Ramos P, et al. Ineffective erythropoiesis in β-thalassemia is characterized by increased iron absorption mediated by down-regulation of hepcidin and up-regulation by ferroportin. Blood 2007; 109(11):5027-35.
15. Sedaghat A, Grundy SM: Cholesterol crystals and the formation of cholesterol gallstones. N Engl J Med 1980; 302:1274.
16. Holan KR, Holzbach RT, Hermann RE, et al. Nucleation time: A key factor in the pathogenesis of cholesterol gallstone disease. Gastroenterology 1979;77:611.
17. Timothy J, Davern and Bruce F Schrschmidt. Biochemical liver tests. In: Feldman M, Freidman L, Sleisenger MH, editors. Gastrointestinal and Liver Disease, Vol.2. Philadelphia: Saunders, 2002. p. 1230-1.

THE ASEAN JOURNAL OF RADIOLOGY 2010; 16(1): 77-84 77

Original Article

# Malignant Cranial Dural Arteriovenous Fistula with Symptom Aggravated by Spontaneous Venous Thrombosis

**Kittisak Unsrisong, MD.[1,2], Komsun Limsopatham, MD.[2], Sirintara Singhara Na Ayudya (Pongpech), MD.[2]**

[1]*Department of Radiology Maharaj Nakorn Chiang Mai Hospital, Chiang Mai University, Chiang Mai, Thailand*

[2]*Interventional Neuroradiology Unit, Department of Radiology Ramathibodi Hospital, Mahidol University, Bangkok, Thailand*

## Introduction

Intracranial dural arteriovenous fistulae (DAVF) is a disease with a variety of presenting symptoms, depending on the shunt location and venous drainage route, and multiple treatment strategies such as transcatheter embolization, surgical clipping, radiation therapy.[1,2] The disease is considered an acquired disease initiated by thrombosis of the intracranial venous system mostly the dural sinuses and later on developed arteriovenous fistulae at the level of the dural mater. Spontaneous regression of the DAVF has been widely reported, which is likely caused by thrombosis of the sinus or fistula.[3] Spontaneous thrombosis of the venous outlet route can occur before closure of the fistula and causes worsening of the patient's symptom, such instance frequently occurred with the cavernous DAVF with spontaneous thrombosis of the superior ophthalmic veins (SOV). Up to date, spontaneous thrombosis of the cerebral veins in cases of cranial malignant DAVF has rarely been reported as well as the role of anticoagulant as an additional treatment.

## Purpose

To report two cases of malignant intracranial DAVF whose symptoms worsen by spontaneous thrombosis of the CVR.

## Method

We reported two cases of malignant cranial DAVF with spontaneous thrombosis of the cerebral vein presented at our institute during April 2009 to June 2009 (1 male 22-year-old; 1 female 62-year-old), in terms of presenting symptoms, imaging features, therapeutic methods, and clinical outcomes.

## Illustrative cases

**Patient 1:** A 22-year-old man presented with headache and repeated seizure for 2 months. He suddenly developed deteriorated conscious level and was sent to our hospital. The initial blood workup which included CBC, electrolytes, renal function and coagulogram were normal. The brain CT scan showed multiple dilated and tortuous hyperdense supratentorial veins which suggestive evidence of

DAVF with CVR. The patient's symptoms were suspected due to intolerance of the brain to chronic venous congestion from the CVR. Cerebral angiogram showed DAVF at the middle 1/3 of the superior sagittal sinus (SSS) with arterial supply from bilateral middle meningeal arteries, transosseous branches of both superficial temporal arteries, and pial supply from the cortical branches of both ACAs. There were CVR into both cerebral hemispheres superficial cortical veins and occlusion of the anterior 1/3 of the SSS and right transverse sinus. Transarterial embolization with n-butyl-2-cyanoacrylate (NBCA) was done with significant reduction of the shunt flow and CVR. Three days post embolization, there was no significant improvement of the patient's conscious level. The patient's history, brain CT scan, angiograms, and the follow up brain MRI (figure 1 and 2) were then reviewed and found that massive thrombosis of the deep venous system was missed diagnosed initially and worsening of the patient's neurologic symptoms were likely to be aggravated by thrombosis of the deep cerebral veins. Low molecular weight heparin was given with improvement of the patient's neurological status.

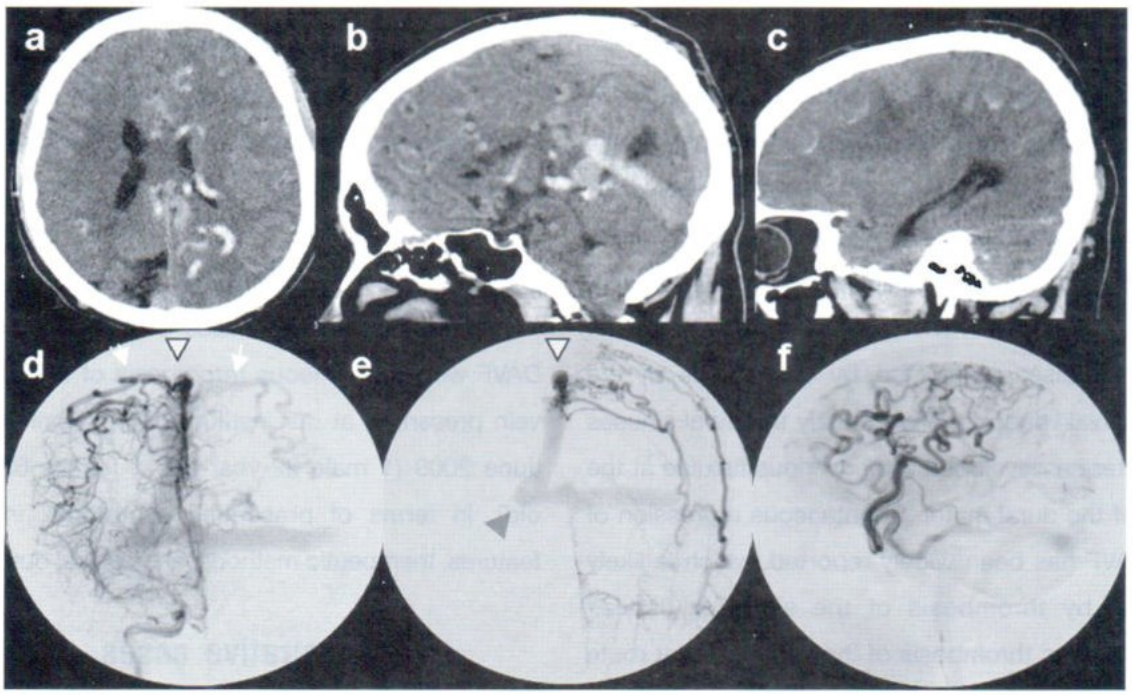


**Fig.1** Non contrast brain CT scan axial (a) mid-sagittal (b), right parasagittal views (c) showed multiple hyperdense vessels at the midline and left parasagittal region with hyperdensities within the Galenic vein and straight sinus. Tonsilar brain herniation was evident in the mid sagittal veiw. Patchy hypodensities were seen at the right cerebrum white matter as well as curvilinear subcortical calcifications, a finding of chronic venous congestion. Right ICA angiogram late arterial phase (c) and left external carotid angiogram (d) AP view showed DAVF at the middle 1/3 of the SSS (arrow heads) with occlusion of the right transverse sinus (read arrow) and bilateral CVR (yellow arrows). Left ICA angiogram lateral view capillary phase (f) showed the appearance and drainage route of the left-sided CVR.

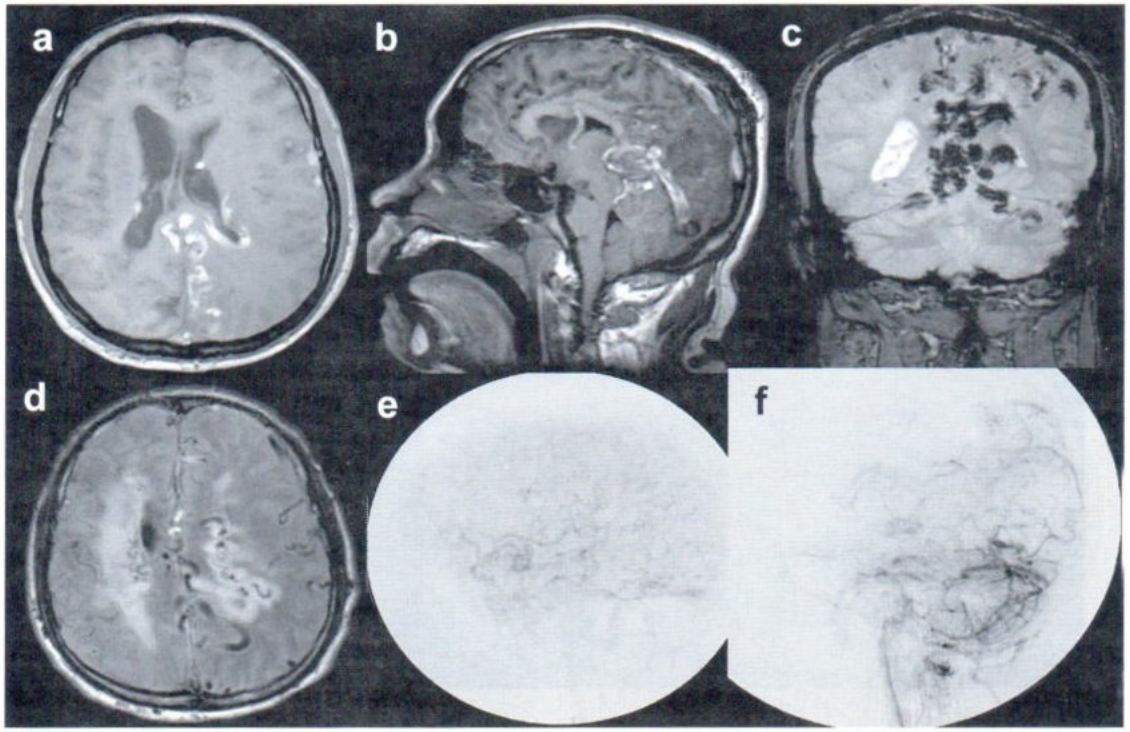


**Fig.2** Post embolization MRI noncontrast axial TIWI (a), sagittal T1WI (b), and coronal GRE T2* showed massive thrombosis of the cerebral veins and deep venous system evident by T1 hyperintense signal within the vessel lumens and hypointense signal blooming on GRE T2*. Axial FLAIR (d) showed extensive T2 hyperintense signal at both cerebral hemispheres white matter. Retrospective reviewed of the late venous phase right ICA (e) and vertebral (f) lateral view angiograms showed cerebral venous congestion and no visualization of the deep venous system, confirming evidence of venous thrombosis preembolization.

**Patient 2:** A 62-year-old female presented with acute onset of nausea and vomiting and deteriorated conscious level later on. The brain CT scan showed an acute intracerebral hematoma (ICH) at the perinsular region of the right frontal lobe, enlarged bilateral cavernous sinuses and superior ophthalmic veins (SOV), and dilatation of the cortical veins at the right frontal and temporal lobes. Cavernous DAVF with CVR was suspected and the bleeding was thought due to hemorrhagic venous infarction from the CVR. Urgent cerebral angiogram showed DAVF at both cavernous sinuses with venous reflux into both superior ophthalmic veins (SOV) and CVR into the right superficial middle cerebral vein. Transvenous coil embolization was done with complete obliteration of the CVR and nearly complete obliteration of bilateral cavernous DAVF flow. Three days post embolization, the patient neurologic symptom worsen by developed grade IV left-sided weakness. Follow up brain CT and MRI showed worsening of the hemorrhagic venous infarction and thrombosis of two right intrasylvian veins. Retrospective reviewed of the initial brain CT scan showed that thromboses of the right intrasylvian veins were already evident and miss diagnosed. Low molecular weight heparin (LMWH) was given with

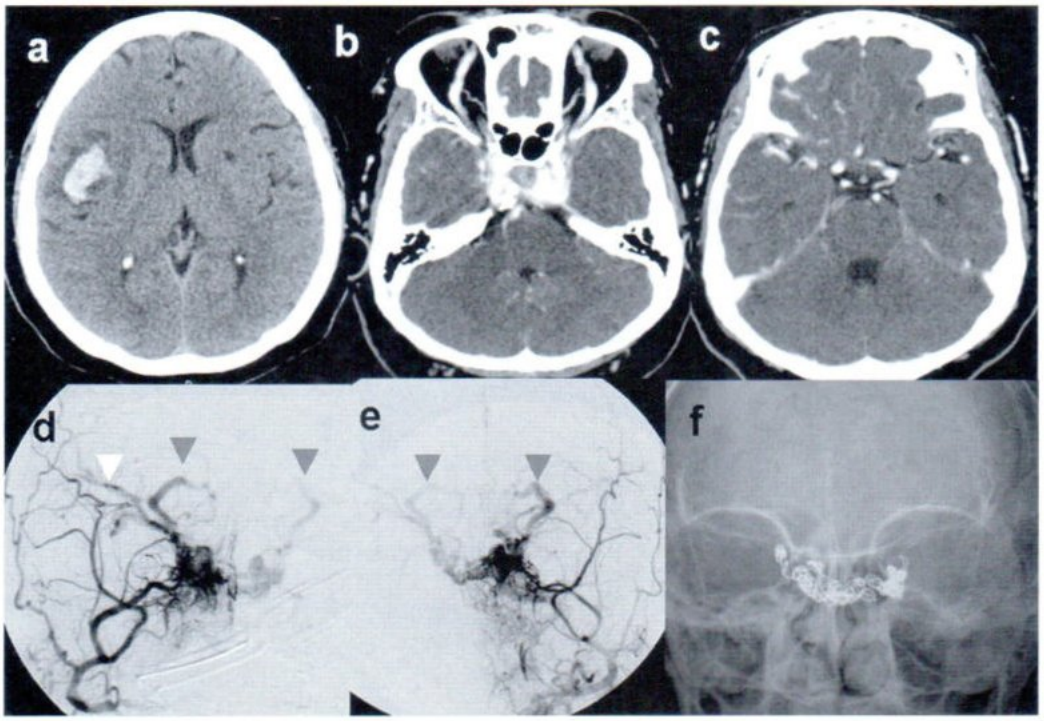


Fig.3 Noncontrast brain CT (a) showed an acute ICH at the right frontal lobe periinsular region and an old lacune at the left lentiforn nucleus. Contrast enhanced CT showed (b,c) showed enlargement of both cavernous sinuses, SOVs, and too much enhanced vessels at the right frontal and temporal lobes) (red arrows). Right external carotid (d) and left external carotid (e) angiograms AP view showed DAVF at both cavernous sinuses with venous reflux into the SOVs (green arrows), right middle cerebral vein (yellow arrow), and also the intercavernus sinus. Skull film AP veiw (f) showed the position of the transvenous embolized coils.

improvement of patient's neurodeficit and venous infarction on follow MRI.

## Discussion

The association of venous thrombosis and cranial DAVF has been well known, mostly by the postulation that venous thrombosis occurs initially and then develop DAVF later on which could be seen by sequential follow up imaging. Recent studies have shown the evidence of thrombophilic abnormalities in patients with DAVF such as a higher level of D-dimer (a biological marker of endogenous fibrinolysis) and mutation of the prothrombin gene (G20210A).[4,5]

Cranial DAVFs with cortical venous reflux (CVR) are considered aggressive lesions. Aggressive symptoms include neurologic dysfunction related to intracranial hemorrhage or venous hypertension such as progressive dementia, seizures, and cerebellar symptoms. Thrombosis or partial thrombosis of the dural sinus with DAVF can often be demonstrated either by noninvasive vascular imaging or conventional angiography. However, symptomatic thrombosis of the cerebral vein in case of malignant cranial DAVF has rarely been reported. Demonstrable of intraluminal thrombus within the cerebral veins and continuous worsening of our two patient's neurologic symptoms despite disconnection of the

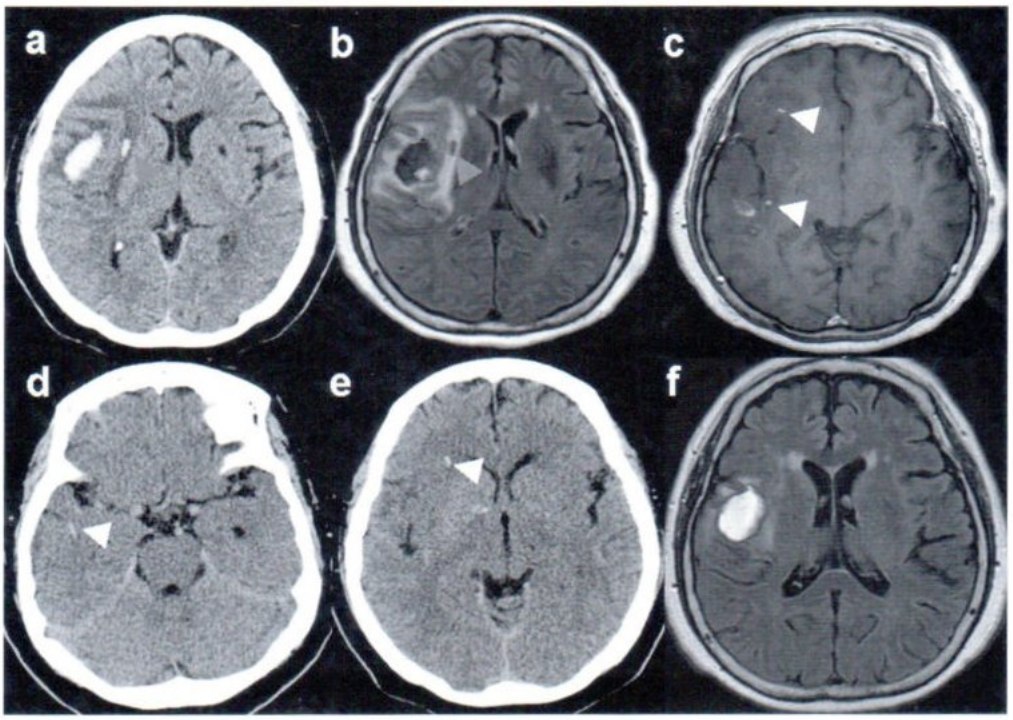


**Fig.4** Noncontrast brain CT (a), MRI FLAIR sequence (b) showed expansion of the perihematoma brain swelling and a new small acute hemorrhage at the right external capsule (red arrows). MRI T1WI (c) showed two hyperintense thrombosed intrasylvian veins which was neglect on the initial brain CT (yellow arrows) (d, e). One month follow up MRI FLAIR sequence (f) after treatment with LMWH showed marked regression of the T2 hyperintense brain swelling and stable in size of the previous hematoma.

CVR by transcatheter embolization are the two main reasons for our postulation that thrombosis of the cerebral vein is actually the responsible cause for worsening of the patient's neurologic symptom and not by brain congestion from the CVR.

Anticoagulant was given as treating cerebral venoocclusive disease in both cases with continuous improvement of their symptoms on follow up. The role of anticoagulant in cranial DAVF has not been established. By our best searching of the medical data base, there are only a few reports of the usefulness of anticoagulant in cranial DAVF.[6,7] Therefore, thoroughly evaluation of the CT or MR images for evidence venous thrombosis in case of malignant cranial DAVF should always be performed because embolization alone may not improve the patient's symptom.

## Conclusion

Associated cerebral venous thrombosis should be carefully searched in patient with malignant DAVF in pre-embolization stage, as even successful embolization alone may not improve clinical symptoms, and anticoagulant may play a major role as the parallel treatment to embolization.

## References

1. Hiro K, Yuzo H, Mika O, Shuichi T, Yoshiko S, Shunro M. Treatment of Intracranial Dural Arteriovenous Fistulas: Current Strategies Based on Location and Hemodynamics, and Alternative Techniques of Transcatheter Embolization. Radiographics November 2004;24:1637-53.
2. Geibprasert S, Pereira V, Krings T, Jiarakongmun P, Toulgoat F, Pongpech S, et al. Dural arteriovenous shunts: a new classification of craniospinal epidural venous anatomical bases and clinical correlations. Stroke 2008; 39:2783-94.
3. Luciani A, Houdart E, Mounayer C, Saint Maurice JP, Merland JJ. Spontaneous closure of dural arteriovenous fistulas: report of three cases and review of the literature. AJNR Am J Neuroradiol 2001;22:992-6.
4. Gerlach R, Boehm-Weigert M, Berkefeld J, Duis J, Raabe A, Seifert V, Marquardt G.Thrombophilic risk factors in patients with cranial and spinal dural arteriovenous fistulae. Neurosurgery. 2008 Oct;63(4):693-98; discussion 698-9.
5. Izumi T, Miyachi S, Hattori K, Iizuka H, Nakane Y, Yoshida J. Thrombophilic abnormalities among patients with cranial dural arteriovenous fistulas. Neurosurgery. 2007 Aug;61(2):262-8; discussion 268-9.
6. Yousry TA, Kühne I, Straube A, Brückmann H. An unusual combination of carotid artery-cavernous sinus fistula and sinus thrombosis. Successful therapy with anticoagulation. Nervenarzt. 1997 Feb;68(2):135-8. German.
7. Tateshima S, Akiyama M, Hasegawa Y, Abe T. Paradoxical Worsening of Cavernous Sinus Dural Arteriovenous Fistula: Case Report with Serial Angiograms. No Shinkei Geka. 2005 Sep;33(9):911-7.

# Instructions for Authors

1. The Asean Journal of Radiology publishes the papers on Radiological Sciences, such as research work, reviews articles case reports, innovations in medical Sciences related to all branches of Radiology, and letters to the editor. The aforementioned materials can be written in English only.
2. The authors have to submit 2 copies of the manuscript and a CD :to Assoc. Prof. Sirintara Singhara Na Ayudya, Department of Radiology, Faculty of medicine, Ramathibodi hospital 270, Rama VI Road, Toong Phayathai, Ratchathewi, Bangkok, 10400. Tel 02-2011259#110, Fax 02-2011297, E-mail Sirintarapongpech2@hotmail.com
3. The original copy to be submitted must be typed in a double space on one of the page 8.5"x11" (A4) paper.
4. The format of the article must include:
   a. Title page and address of the author (s)
   b. Abstract (Objective, Methods, Results and conclusion)
   c. Introduction
   d. Material and Method
   e. Results and discussion
   f. Acknowledgment (if any)
   g. References (Follow the Vancouver style)
5. We will provide 5 copies of reprints for the author (s) an article for publication in the Asean Journal.
6. The illustrations and table must be clearly prepared with legends in English as they are the art works to be reproduced
7. The authors are responsible for the contents of the article as to its facts and findings.
8. Ethics

Paper reporting studies which might be interpreted as human experimentation (e.g. controlled trials) should conform to the standards of the Declaration of Hilsinki (see British Medical Journal 1964:2:177) and should indicate that, approval that such studies may proceed, has been granted by the local or hospital Ethics Committee.

When reporting experiments on animal indicate whether the institution's or the National Research Council's guide for, or any national law on, the care and use of laboratory animals was followed.

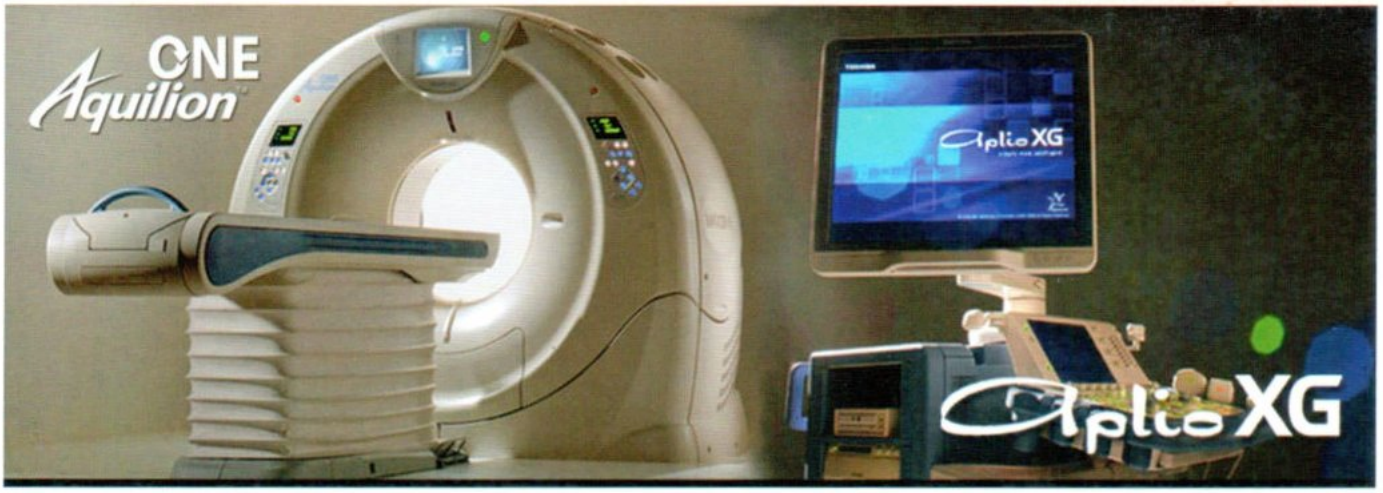


# The World's First Dynamic Volume CT

## 640 Slices 4 Dimensions CT scanner

### ONE Rotation

The wide coverage provided by the 160 mm-wide Area Detector enables scanning of the heart or brain within one rotation,eliminating the need for helical scanning.

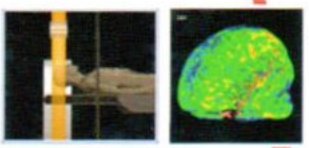

Whole brain Perfusion

An entire organ can be captured at one time, resulting in multiplanar and 3D images demonstrating perfect continuity along the Z-axis.In addition, ultrafast scan times allow the contrast medium dose and exposure dose to be reduced.

### ONE Phase

The entire heart can be captured in as little as one rotation for coronary analysis, or over a single heartbeat to include complete functional diagnosis.

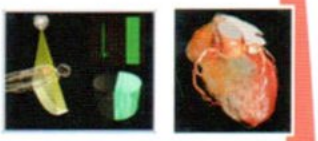

Whole heart image

Each reconstructed 3D volume represents exactly the same phase the cardiac cycle, providing incredible motion-free images of the coronary arteries with homogenous contrast enhancement.

### ONE Volume

The ability to acquire the entire brain with one volume scan opens the door to new diagnostic possibilities.

Whole body image

The Neuro ONE protocol allows acquisition of multiple low-dose volume scans of the entire brain during contrast infusion to provide whole brain perfusion and whole brain dynamic vascular analysis in one examination. Dynamic volumetric acquisition protocols can also be used to review moving joint structures in 3D, providing new clinical applications for orthopedic imaging.

**24 - Hour Service Call Center**
**Tel. +66(0)2935-6667-8**

# Ultrasound System

## Precision

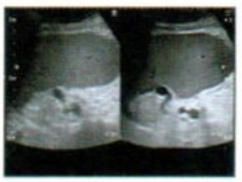

Precision Imaging technology increases productivity and diagnostic confidence by providing more detailed ultrasound images.

As a multi-resolution signal processing technology, it not only evaluates images line-by-line, but also includes information from adjacent lines to enhance the amount of information obtained.

Clinical Benefit ::

- Enhances subtle tissue differences
- Creates a more sharp and homogeneous image
- Improves spatial and contrast resolution.

## Elastography

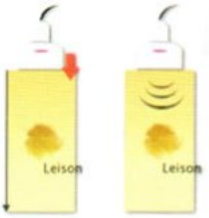


Gentle compression of breast tissue with transducer

Tissue velocity across entire image automatically recorded using Doppler technique

Full raw data acquisition integration of velocity data to give displacement and comparison across all frames to yield strain information

Comparison of lesion and normal breast tissue

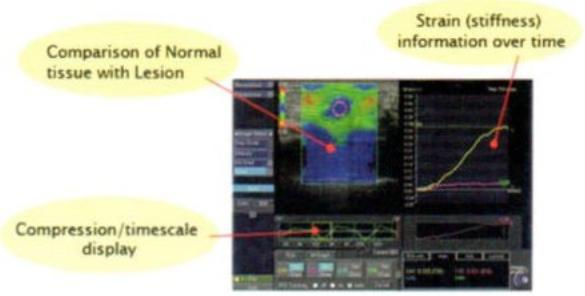


**CMC Biotech CO., LTD.**
364 Muban Town-in-Town, Soi Ladphrao 94, Ladphrao Road,Wangthonglang, Bangkok 10310
Head Quarter: Tel. +66(0)2530-4995 Fax. +66(0)2935-6527
Central Branch: Tel. +66(0)2934-5884-5 Fax. +66(0)2934-5882
Northern Branch: Tel. +66(0)5328-3261 Fax. +66(0)5320-4463
North Eastern Branch: Tel. +66(0(4334-1642 Fax. +66(0)4334-1643
Sounthern Branch: Tel. +66(0)7442-9803 Fax. +66(0)7442-9804

**TOSHIBA**
**Leading Innovation** >>>